Minisatellites in Meiosis: Crossover Regulation and Stability of Repetitive DNA

A DISSERTATION
SUBMITTED TO THE FACULTY OF THE GRADUATE SCHOOL
OF THE UNIVERSITY OF MINNESOTA
BY

Andrea Ruth LeClere

IN PARTIAL FULFILLMENT OF THE REQUIREMENTS
FOR THE DEGREE OF
DOCTOR OF PHILOSOPHY

Dr. David Kirkpatrick
Adviser

April 2012

Acknowledgements

I want to especially thank David for his guidance and support throughout these past six years. I am thankful to have worked with such a brilliant and kind advisor while attaining my Ph.D.

Also thanks to:

- All of my family for keeping me grounded and constantly laughing.
- Past and present members of the Kirkpatrick lab: Melanie Legrande, Katy Kelly-Sustacek, Peter Jauert and Bonnie Alver.
- My thesis examination committee: Anja Bielinsky, Duncan Clarke, Paul Siliciano and David Zarkower for all their guidance and helpful suggestions.
- Duncan Clarke and Anja Bielinsky for great rotations during my first year.
- Jeff Simon and David Zarkower for a great teaching assistant experience.
- Sue Knoblauch for all her help and invaluable expertise with the program.
- All 6th floor MCB yeast labs for sharing reagents and media, and providing a friendly and intelligent atmosphere to work in.
- Marc McClellan for always being helpful and willing to share his knowledge of various techniques and equipment.
- Members of the Yeast Journal Club for helpful suggestions and discussions.

Dedication

This dissertation is dedicated to Robert Becker, who first sparked my interest in science during high school and whose enthusiasm and encouragement has lasted me these past 10 years and onward. Woof!

Table of Contents

List of Tables

List of Figures

Chapter 1: Introduction

Chapter 2: The Role of *CSM3*, *MRC1*, and *TOF1* in Minisatellite Stability and Large Loop DNA Repair During Meiosis in Yeast

Chapter 3: Minisatellite-Stimulated Meiotic Recombination in *MSH4* and *MSH5* Mutants in *Saccharomyces cerevisiae*

Chapter 4: Discussion and Future Directions

Materials and Methods

Chapter 1

Introduction

The Cell Cycle and Mitosis

The propagation of life depends on the ability of cells to divide and create more cells. Progression through the cell cycle, culminating in a cell division, is important to the life of all organisms. The division of a unicellular organism, such as the baker's yeast *Saccharomyces cerevisiae*, produces two entirely new organisms. On a larger scale, cell division enables multicellular organisms to develop from a single cell. For a sexually reproducing species such as mammals and yeast *S. cerevisiae*, a specialized cell division called meiosis enables reproduction.

Cell division, or mitotic (M) phase, is a process that produces two genetically identical daughter cells from a progenitor cell. M phase alternates with a much longer stage of the cell cycle known as interphase, which alternates phases of growth (G_1 and G_2) with DNA replication (S) and prepares cells for division during M phase (Figure 1). M phase is comprised of two distinct stages: mitosis, or division of the nucleus, which is followed quickly by cytokinesis, or division of the cytoplasm and its components. While numerous molecular and cellular events occur throughout the cell leading up to and during M phase, the events pertaining to the chromosomes will be focused on here.

M phase is a complex and multistep process that involves packaging and distributing the chromosomes into two identical sets to form two new nuclei (Figure 2). As each chromosome is unique in both its size as well as genetic content, it is crucial that each daughter cell receives a complete copy of every chromosome. Cells begin mitosis with a replicated genome, so that every chromosome consists of two sister chromatids, which are identical DNA molecules that are attached at the centromere and along their

arms (Tanaka et al. 2000, Tanaka et al. 1999, Anderson et al. 2002, Ball Jr. and Yokomori 2001, Haering et al. 2002). The events of mitosis are broken down into stages: prophase, prometaphase, metaphase, anaphase and telophase. During prophase the chromosomes, which are loosely bundled during interphase, condense into tightly compact structures (Anderson et al. 2002, Ball Jr. and Yokomori 2001, Blow and Tanaka 2005). In higher eukaryotes, the nuclear membrane disintegrates during prometaphase, allowing mitotic spindles access to the chromosomes (De Souza and Osmani 2007, Kutay and Hetzer 2008, Hetzer 2010). In several lower eukaryotes, including *S. cerevisiae*, the nuclear membrane remains intact and mitotic spindles originate from spindle pole bodies (SPBs) that are embedded in the nuclear membrane (Peterson and Ris 1976, Snyder 1994, De Souza and Osmani 2007, Iouk et al. 2002). Sister chromatids attach to mitotic spindles from opposite poles, and the tension between the two poles causes chromosomes to align on the metaphase plate, an imaginary plane that is equidistant from the poles (He et al. 2001, Pearson et al. 2001, Pereira and Schiebel 2001, Blow and Tanaka 2005). Anaphase quickly commences with the separation of the sister chromatids; each sister chromatid is now its own chromosome, and move towards opposite poles (Pearson et al. 2001, Pereira and Schiebel 2001, Blow and Tanaka 2005). During telophase the two poles of the cell have a complete and identical set of chromosomes, forming two new distinct nuclei. In species where the nuclear membrane was fragmented, a new nuclear membrane forms around each new nucleus (De Souza and Osmani 2007, Kutay and Hetzer 2008, Hetzer 2010). Following cytokinesis, two daughter cells exist each with a complete and identical copy of the progenitor cell genome.

Meiosis is a Reductive Cell Division

Cell division via mitosis accounts for the development of a multi-cellular organism from a single cell and for the generation of new organisms for species that reproduce asexually. However, species such as metazoans that reproduce sexually encounter a unique problem. Eukaryotes have a distinct number of chromosomes in the nucleus of every cell, with a few exceptions. For example, the majority of human cells have forty-six chromosomes in their nucleus. Like many eukaryotes, humans are obligate diploids, carrying two copies of every chromosome per cell. These chromosome pairs are called homologous chromosomes. If humans and other diploid species were to produce their reproductive cells, called gametes (the sperm and ovum) or spores, via mitosis these cells would be diploid like their progenitor cells. Upon fertilization the chromosome number of forty-six would double to ninety-two, and each subsequent generation would double the number of chromosomes again. To circumvent this problem, sexually reproducing species generate haploid gametes (1n, where n represents how many copies of each chromosome the cell contains) from diploid progenitor cells (2n) by a reductive cell division called meiosis (Yanowitz 2010, Page and Hawley 2003, Roeder 1997, Marston and Amon 2004).

Meiosis is distinctly different from mitosis in that a single round of DNA replication is followed by two consecutive cell divisions, called meiosis I and meiosis II (Figure 2) (Marston and Amon 2004, Roeder 1997). Instead of producing two daughter cells identical in genomic content to that of the progenitor cell, meiosis produces four daughter cells with half the genomic content of the progenitor cell (Roeder 1997, Page

and Hawley 2003, Hunter 2006, Marston and Amon 2004). For example, human gametes contain one copy of each chromosome instead of two, for a total number of twenty-three chromosomes. The events of meiosis resemble the stages of mitosis and can be broken down into similar phases: prophase I, metaphase I, anaphase I, and telophase I refer to the nuclear events of meiosis I, while prophase II, metaphase II, anaphase II and telophase II refer to the nuclear events of meiosis II. The key differences between mitosis and meiosis occur prior to and during the first cell division, during meiosis I (Figure 2).

Similar to mitotic prophase, during meiotic prophase I each chromosome consists of two sister chromatids, one being the duplicated copy of the other. Unlike mitotic prophase, chromosomes interact and pair with their homolog. Each homolog exchanges DNA with its partner, forming a physical bridge that connects the homologs together, called a chiasma (Figure 2) (Page and Hawley 2003, Roeder 1997, Hunter 2006, Lynn, Soucek and Borner 2007). Chiasmata (plural) formation does not occur during mitosis or meiosis II, because chromosomes do not pair with their homolog.

During anaphase I and telophase I, each chromosome is separated from its homolog and pulled to opposite poles. This is a unique type of chromosome segregation that distinguishes meiosis I from mitosis and meiosis II, because the sister chromatids remain attached and move as a single unit to their respective pole (Figure 2) (Roeder 1997, Page and Hawley 2003, Marston and Amon 2004). After cell division each daughter cell has a complete haploid set of chromosomes. These cells do not undergo another round of replication prior to the second meiotic division (Marston and Amon 2004).

The second meiotic division, or meiosis II, closely resembles a mitotic division (Marston and Amon 2004). Chromosomes line up independently on the metaphase plate, and during anaphase II the sister chromatids separate and move to opposite poles of the cell. Following cytokinesis, a total of four daughter cells are present each with half the number of chromosomes of the original progenitor cell (Figure 2). Upon fertilization, each gamete contributes their genomic content to the fertilized cell, restoring the genomic content to the diploid number.

Meiotic Recombination

The segregation of homologous chromosomes poses a unique problem to cells undergoing a meiotic division in that the homologs must be physically connected in order to successfully align on the metaphase I plate. Cells accomplish this feat through a series of dynamic and complex events in which homologs exchange strands of DNA, a process known as meiotic recombination, and form a bridge that physically connects the homologs to each other (Figure 3) (Page and Hawley 2003, Roeder 1997, Hunter 2006, Lynn et al. 2007, Yanowitz 2010). The molecular events involved in the exchange of DNA have been the focus of several research groups for many decades now. In the last twenty years several key features and intermediates of meiotic recombination have been determined, confirming and improving upon the canonical double-strand break repair (DSBR) model first proposed by Szostak et al. (Szostak et al. 1983).

Meiotic recombination is initiated by the formation of a programmed double-strand break (DSB) catalyzed by the highly conserved Spo11 protein (Keeney, Giroux

and Kleckner 1997, Keeney 2001). Spo11p is the DNA cleaving unit of a large protein complex comprised of at least ten other proteins, including Mre11/Rad50/Xrs2 (MRX), all of which are necessary for meiotic DSB formation (Keeney et al. 1997, Keeney 2001, Diaz et al. 2002, Johzuka and Ogawa 1995, Borde et al. 2004, Borde 2007, Jiao, Salem and Malone 2003). The MRX complex plays several roles in DSB repair, including the signaling of DSB formation by locally activating Tel1/Mec1 (Usui, Ogawa and Petrini 2001, Borde 2007), and removing Spo11p (Keeney 2001, Moreau, Ferguson and Symington 1999, Milman, Higuchi and Smith 2009), which becomes covalently attached to the DNA ends during DSB formation as a result of the transesterification reaction (Keeney et al. 1997, Keeney 2001). Additionally, the MRX complex, along with the nucleases *EXO1, CTP1* and *DNA2*, process the blunt DSB ends by resecting the 5' strands several hundred basepairs and leaving a pair of 3' single-strand overhanging ends (Hodgson et al. 2011, Garcia et al. 2011, Zakharyevich et al. 2010, Milman et al. 2009, Nicolette et al. 2010).

At this stage, repair of the DSB can be accomplished using either the homolog or the sister chromatid as template. During mitotic growth, the sister chromatid is the preferred template for DSB repair (Kadyk and Hartwell 1992, Lao and Hunter 2010). However, during meiosis recombination must occur between homologs and not sister chromatids for homologs to successfully pair and form chiasmata. To accomplish this, cells undergoing meiosis establish an inter-homolog bias of DSB repair (Schwacha and Kleckner 1994, Lao and Hunter 2010, Xu, Weiner and Kleckner 1997). How cells establish this bias is still mechanistically unclear, but research has shown that the process

involves the meiosis-specific chromosome axial proteins Hop1p and Red1p (Carballo et al. 2008, Niu et al. 2005), signaling between the meiosis-specific effector kinase Mek1p and the DNA damage sensor kinases Mec1p/Tel1p (Carballo et al. 2008, Wu, Ho and Burgess 2010, Callender and Hollingsworth 2010, Hollingsworth 2010, Niu et al. 2007), as well as factors involved in strand exchange Dmc1p and Rad51p (Shinohara et al. 1997, Shinohara and Shinohara 2004). Together these elements function to promote DSB repair via inter-homolog recombination.

During inter-homolog recombination, the RecA homologs Dmc1p and Rad51p are loaded onto 3' ssDNA and facilitate strand exchange (Bishop et al. 1992, Sehorn et al. 2004, Shinohara, Ogawa and Ogawa 1992, Shinohara and Shinohara 2004, Neale and Keeney 2006, Kagawa and Kurumizaka 2010). Research has shown that Rad51p and Dmc1p load onto opposite ends of the DSB (Shinohara et al. 2000), leading to the hypothesis that the asymmetric loading of these proteins is responsible for the asymmetric behavior of DSB-ends such that only one of the 3' strands invades the duplex DNA of its homolog (Shinohara and Shinohara 2004, Neale and Keeney 2006, Sehorn et al. 2004, Bishop et al. 1992, Shinohara et al. 1992, Sheridan and Bishop 2006, Shinohara et al. 1997). Strand invasion leads to the formation of heteroduplex DNA, a hybrid DNA duplex composed of strands from two different homologs (Figure 3) (White, Lusnak and Fogel 1985, Nag, White and Petes 1989, Nag and Petes 1993). The 3' end primes DNA synthesis, which repairs the gap formed by the DSB and further drives strand invasion and strand displacement (Figure 3) (Roeder 1997, Hunter 2006). At this point the recombination intermediate is processed down one of two pathways: the noncrossover or

the crossover pathway. In the noncrossover pathway, also known as the synthesis-dependent strand-annealing (SDSA) pathway, the invading strand is released after enough DNA synthesis to repair the DSB (McMahill, Sham and Bishop 2007, Borner, Kleckner and Hunter 2004). In the crossover (CO) pathway, the invading strand is stabilized and the second end is captured leading to the formation of a double Holliday junction, which can then be resolved as a crossover (Roeder 1997, Hunter 2006, Lynn et al. 2007). While both pathways are important for homology search and genetic diversity (McMahill et al. 2007, Page and Hawley 2003, Yanowitz 2010), it is the CO pathway alone that ensures each homolog pair segregates properly during the first meiotic division (Hunter 2006, Lynn et al. 2007, Martinez-Perez and Colaiacovo 2009, Page and Hawley 2003, Storlazzi et al. 2010). Because of this, crossovers are tightly regulated to ensure that every chromosome pair receives a crossover (Shinohara et al. 2008, Lao and Hunter 2010, Hollingsworth 2010, Youds and Boulton 2011, Kaback et al. 1999).

Crossovers Are Regulated by the ZMM Genes

Prior to the first meiotic division, each chromosome is physically linked to its homolog by chiasmata, which are the physical manifestation of the crossover pathway (Hunter 2006, Lynn et al. 2007, Martinez-Perez and Colaiacovo 2009). In the absence of crossovers, homologs frequently mis-segregate, yielding aneuploid gametes that lead to conditions such as Down syndrome and infertility in humans (Page and Hawley 2003, Hassold, Hall and Hunt 2007). Therefore, in most organisms recombination is tightly regulated to ensure that each chromosome pair sustains at least one crossover, called the

obligate crossover (Kaback et al. 1999, Martini et al. 2006, Shinohara et al. 2008, Martinez-Perez and Colaiacovo 2009). Meiotic crossovers are further regulated such that two crossovers rarely occur close together, a phenomenon known as crossover interference (Bishop and Zickler 2004, Martinez-Perez and Colaiacovo 2009, Berchowitz and Copenhaver 2010, Youds and Boulton 2011). Crossover interference decreases with distance along a chromosome and varies between chromosomes, with larger chromosomes displaying stronger interference than smaller chromosomes (Kaback et al. 1999). By preventing excess crossovers on large chromosomes, interference ensures that crossovers, which are limited to an average of 90 per meiosis in yeast (Mancera et al. 2008), are well-distributed, and that every chromosome pair receives an obligate crossover (Hunter 2006, Kaback et al. 1999, Lynn et al. 2007, Martini et al. 2006, Shinohara et al. 2008).

Several meiosis-specific factors promote crossover formation, including the ZMM (Zip/Msh/Mer) genes (Lynn et al. 2007). *MSH4* and *MSH5*, two ZMM genes that are homologs of the bacterial MutS mismatch repair gene but have no role in mitotic mismatch repair (Kirkpatrick 1999, Lynn et al. 2007), are required for wild-type levels of meiotic crossing over (Ross-Macdonald and Roeder 1994, Hollingsworth, Ponte and Halsey 1995, Novak, Ross-Macdonald and Roeder 2001). Msh4p and Msh5p directly interact to form a heterodimer that recognizes Holliday junctions and clamps around recombining homolog arms, holding them in close proximity and ultimately stabilizing the crossover intermediate (Pochart, Woltering and Hollingsworth 1997, Zalevsky et al. 1999, Snowden et al. 2004, Snowden et al. 2008). Yeast strains bearing mutations in

either *MSH4* or *MSH5* exhibit a significant reduction in crossing over and a subsequent loss of spore viability due to increased meiosis I chromosome nondisjunction (Kirkpatrick 1999, Ross-Macdonald and Roeder 1994, Hollingsworth et al. 1995, Novak et al. 2001, Lynn et al. 2007). Both *MSH4* and *MSH5* have been shown to function in chromosome pairing and synapsis in mammals, and deleting either gene causes sterility in male and female mice (Bocker et al. 1999, Neyton et al. 2004, Snowden et al. 2004, Snowden et al. 2008, de Vries et al. 1999, Kneitz et al. 2000, Edelmann et al. 1999).

A Second Class of Crossovers

Research in *S. cerevisiae* has identified the existence of two genetically separable crossover pathways: 1) the Class I pathway is dependent on the ZMM genes and is subject to crossover interference, and 2) the Class II pathway is dependent on *MUS81* and *MMS4* and does not exhibit interference (de los Santos et al. 2001, de los Santos et al. 2003, Whitby 2005, Hollingsworth and Brill 2004, Lynn et al. 2007). Mus81p is related to the XPF (xeroderma pigmentation group F) family of endonucleases and forms a complex with Mms4p (Interthal and Heyer 2000, Boddy et al. 2001); the *MMS4* homolog in fission yeast *Schizosaccharomyces pombe* and mammals is called *EME1* (Ciccia, Constantinou and West 2003, Boddy et al. 2001). The mechanism by which *MUS81/MMS4* generate crossovers is still unclear. Research has shown that Mus81p exhibits robust cleavage of a variety of structures, especially D-loops and nicked Holliday junctions, but has very little double Holliday junction activity (Kaliraman et al. 2001, Ehmsen and Heyer 2008, de los Santos et al. 2003, Gaillard et al. 2003, Ciccia et

al. 2003). On the basis of this research, it is hypothesized that Mus81p/Mms4p act early in the recombination pathway and cleave intermediates that exist after strand invasion but prior to double-Holliday junction formation (Whitby 2005, Hollingsworth and Brill 2004, de los Santos et al. 2003, Gaskell et al. 2007).

The importance of the *MUS81/MMS4* pathway varies among eukaryotes. The fission yeast *S. pombe* relies entirely on the *MUS81/MMS4* pathway to generate crossovers (Osman et al. 2003, Smith et al. 2003, Boddy et al. 2001). In contrast, *Caenorhabditis elegans* appears to rely exclusively on the ZMM pathway, as deleting *MSH-4* or *MSH-5* eliminates all crossovers (Zalevsky et al. 1999, Kelly et al. 2000). Likewise, mice bearing *MUS81* knockouts have been shown to be fertile (McPherson et al. 2004), while *MSH4* or *MSH5* knockouts are sterile (de Vries et al. 1999, Kneitz et al. 2000, Edelmann et al. 1999). In *S. cerevisiae* the *MUS81/MMS4* pathway accounts for only a minor set of crossovers and is largely considered a backup to the ZMM pathway (de los Santos et al. 2001, de los Santos et al. 2003, Hollingsworth and Brill 2004).

Because *MUS81* and *MMS4/EME1* also play a role in replication fork recovery (Kaliraman et al. 2001, Regairaz et al. 2011, Ciccia et al. 2003, Whitby, Osman and Dixon 2003, Doe et al. 2002, Bastin-Shanower et al. 2003, Osman and Whitby 2007), *S. cerevisiae* strains bearing *MUS81* or *MMS4* mutants often fail to progress through meiosis and sporulation is either eliminated or significantly reduced in various strain backgrounds (Interthal and Heyer 2000, de los Santos et al. 2001, de los Santos et al. 2003).

Large Loop Formation and Repair During Meiotic Recombination

During recombination, if a difference exists in the DNA sequences that make up the heteroduplex, a mismatch or a loop will form that is a substrate for repair (Figure 4) (Kirkpatrick 1999, Kearney et al. 2001, Jensen, Jauert and Kirkpatrick 2005). In yeast *Saccharomyces cerevisiae*, there are several possible fates for a loop-generating mismatch after formation (Figure 4). Depending on which strand initiates repair, repair of the loop can either restore normal Mendelian segregation or generate a gene conversion (GC) (Kirkpatrick 1999). If the loop is not detected or repaired, one of the four spores will receive the duplex DNA molecule containing the mismatch (Kirkpatrick and Petes 1997, Kirkpatrick 1999, Kearney et al. 2001, Jensen et al. 2005). When this spore undergoes mitosis, the two strands comprising the mismatched region will each serve as a template during DNA replication, producing daughter cells with different copies of the mismatched region. The result will be a spore colony with a sectored phenotype that can easily be detected if the mismatched region is within an auxotrophic marker; this type of segregation is known as a post-meiotic segregation (PMS) (Kirkpatrick and Petes 1997, Kearney et al. 2001, Jensen et al. 2005). The efficiency with which a mismatch is detected and repaired during meiotic recombination is reflected in the percent of GC and PMS tetrads (Kirkpatrick and Petes 1997, Jensen et al. 2005, Kearney et al. 2001).

In the AS4/AS13 *Saccharomyces cerevisiae* strain background used in this study, the *HIS4* locus exhibits a very high level of recombination activity during meiosis (Nag et al. 1989, Nag and Petes 1993, White, Dominska and Petes 1993, Kirkpatrick and Petes 1997, Kirkpatrick et al. 1999, Kearney et al. 2001, Jauert et al. 2002, Detloff, White and

Petes 1992). This hotspot of recombination activity leads to a high level of mismatch formation in diploids heterozygous for *HIS4* alleles (Kearney et al. 2001, Jensen et al. 2005). Research using strains that are heterozygous for *his4-lopd*, a 26 bp non-palindromic insertion in *HIS4*, has shown that at least two pathways function to repair large loop mismatches during meiosis (Kirkpatrick and Petes 1997, Kearney et al. 2001). The first large loop repair (LLR) pathway, consisting of *RAD1*, *RAD10*, *MSH2*, and *MSH3*, can repair loops no less than 16 bp and up to 5.6 kb in size (Kirkpatrick and Petes 1997, Kearney et al. 2001, Jensen et al. 2005). Although no genes have been identified, studies indicate that a second *RAD1*-independent large loop repair pathway exists, as significant large loop repair is still seen when the *RAD1*-dependent LLR pathway is eliminated (Kirkpatrick and Petes 1997, Kearney et al. 2001). One of the goals of our lab has been to identify other genes involved in meiotic large loop repair. This is especially important for characterizing the meiotic stability of repetitive DNA sequences such as minisatellite DNA.

Minisatellite DNA

Minisatellites are a type of repetitive DNA composed of tandem direct repeats of a consensus sequence that is locus specific, varying between 15 and 100 bp in length (Jeffreys, Wilson and Thein 1985, Jeffreys et al. 1991, Krontiris 1995, Bois 2003). Minisatellites are found throughout mammalian, and most eukaryotic, genomes (Bois 2003, Richard, Kerrest and Dujon 2008), and are often situated upstream or downstream of genes (Cohen, Walter and Levinson 1987, Bell, Selby and Rutter 1982, Virtaneva et al.

1997, Adamson et al. 2007), as well as within introns or exons (Kirkbride et al. 2001, Jeong et al. 2007, Smalley et al. 1998). It is estimated that roughly thousands of minisatellites exist within the human genome (Richard et al. 2008), while a much smaller estimate is given for *S. cerevisiae*, less than 100 (Richard et al. 2008, Marinangeli et al. 2004).

Minisatellites are often polymorphic (hence the alternative name Variable Number of Tandem Repeats) and have proven useful for mapping and DNA fingerprinting (Wyman and White 1980, Jeffreys et al. 1985, Jeffreys et al. 1991, Larson et al. 1999, Cooper and Schmidtke 1984, Bois 2003). Additionally, many studies have linked minisatellite polymorphisms to various human diseases including asthma and lung disease (Guo et al. 2011, Kirkbride et al. 2001), inherited myoclonus epilepsy (Virtaneva et al. 1997, Lalioti et al. 1997, Larson et al. 1999), attention deficit hyperactivity disorder (Smalley et al. 1998, Faraone et al. 2001, Li et al. 2006, Langley et al. 2009), type-1 diabetes mellitus (Adamson et al. 2007, Kennedy, German and Rutter 1995, Bennett et al. 1995, Bell et al. 1982), and many types of human cancers (Kwon et al. 2010, Jeong et al. 2007, Yoon et al. 2010, Wang et al. 2003, Van Gils et al. 2002, Ding et al. 1999, Krontiris et al. 1993a). Clearly, understanding the molecular pathways that regulate minisatellite stability will have an impact on our understanding of the contribution of minisatellites to several important human diseases.

Minisatellites are generally stable during mitotic growth but frequently alter during meiosis, and recombination based alterations have long been confirmed to be a major driving force of minisatellite polymorphisms (Kasperczyk, DiMartino and

Krontiris 1990, Jeffreys et al. 1994, Jeffreys, Neil and Neumann 1998b, Bishop, Louis and Borts 2000, He, Cederberg and Rannug 2002, Jauert et al. 2002, Jauert and Kirkpatrick 2005, Bois 2003, Smith 1976). In humans, it has been noted that minisatellites frequently exhibit germline instability, and that alterations predominantly occur at one end of the minisatellite, with little or no events toward the other end (Jeffreys et al. 1991, Jeffreys et al. 1994, Jeffreys et al. 1998b, Bois 2003), reminiscent of the gradients of meiotic gene conversions (Hunter 2006). One study reported a minisatellite-associated recombination hotspot identified in human sperm (Jeffreys, Murray and Neumann 1998a). Other studies have shown that alterations of human minisatellites occur during meiosis when inserted in yeast and require meiotic DSB formation (Debrauwere et al. 1999, Appelgren, Cederberg and Rannug 1997, He et al. 2002, Appelgren, Cederberg and Rannug 1999, Jauert et al. 2002). While it is known that meiotic recombination is the driving force behind minisatellite alterations, the molecular mechanism of minisatellite alterations and the meiotic factors that influence minisatellite stability remain to be fully elucidated. This has largely been the focus of the Kirkpatrick lab using the minisatellite associated with the human *HRAS1* gene (Jauert et al. 2002, Jauert and Kirkpatrick 2005, LeClere, Jauert and Kirkpatrick *submitted,* LeClere et al. *unpublished*).

The *HRAS1* Minisatellite

The *HRAS1* gene is a member of a highly conserved family of *Ras* genes encoding membrane-bound proteins with weak GTPase activity that, in their GTP-bound

state, can activate many signal transduction pathways (Cohen et al. 1987, Campbell et al. 1998, Parikh, Subrahmanyam and Ren 2007). The human *HRAS1* gene was identified in a study that cloned human genomic DNA sequences that hybridized to the transforming coding region of the Harvey rat sarcoma onco-virus (Chang et al. 1982). During this study, it was noted that the human *HRAS1* gene represented an excellent candidate gene whose "level of expression might play an important role in the pathogenesis of some non-virally induced tumors" (Chang et al. 1982). Since then, mutations that cause overexpression of the *HRAS1* gene or over-activation of the gene product have been isolated in several different human cancers (Zhang et al. 2011, Pelaez et al. 2010, Rossell et al. 1999, Conway et al. 1996, Nishio et al. 1992, Hiwasa et al. 1992, Krontiris 1985), and have been shown to morphologically transform normal cells into cells capable of cancerous growth (Lee, Ahn and Eum 2009, Yeh et al. 2009).

In an effort to identify sequences capable of regulating the expression of the *HRAS1* proto-oncogene, it was noted that a repetitive sequence located 3' of *HRAS1* influenced gene expression (Cohen et al. 1987). This repetitive region of DNA, known as the *HRAS1* minisatellite, is highly polymorphic in the human population, and is capable of enhancing the expression of the *HRAS1* proto-oncogene (Cohen et al. 1987, Green and Krontiris 1993, Krontiris 1995). The *HRAS1* minisatellite is composed of tandem direct repeats of a 28 bp sequence motif that can vary at the 7^{th} (can be a guanine or a cytosine) or the 15^{th} basepair (can also be a guanine or a cytosine), resulting in four different types of the repetitive sequence motif (Figure 5). Four common *HRAS1* minisatellite alleles have been identified in the human population, designated *A1* (1 kb), *A2* (1.45 kb), *A3*

(2.05 kb), and *A4* (2.5 kb) (Krontiris 1985, Krontiris et al. 1987), but several hundred uncommon and rare alleles have been identified as well (Krontiris 1985, Krontiris et al. 1987, Krontiris et al. 1993a, Conway et al. 1996, Weston and Godbold 1997, Tamimi et al. 2003, Zhang et al. 2011, Rossell et al. 1999). It is widely believed that each of the uncommon and rare alleles is a derivative of the common allele nearest in length that has undergone a naturally occurring minisatellite length alteration during meiosis (Kasperczyk et al. 1990). Many of these rare *HRAS1* minisatellite alleles have been associated with various human cancers, including cancer of the breast, colon, lungs, bladder, ovaries, and brain (Krontiris et al. 1993a, Krontiris et al. 1985, Rossell et al. 1999, Weitzel et al. 2000, Vega 2001, Tamimi et al. 2003, Zhang et al. 2011).

A meta-analysis conducted in 1997 reported a >2 fold increased risk for breast cancer among patients carrying rare *HRAS1* minisatellite alleles (Weston and Godbold 1997). A second case-control study analyzing 717 breast cancer cases and 798 controls reported a significant breast cancer risk for rare alleles derived from the two largest common alleles, *A3* and *A4* (Tamimi et al. 2003). More recently, a meta-analysis involving 1296 breast cancer cases and 2800 controls reported a significantly high frequency of rare *HRAS1* minisatellite alleles in breast cancer cases (Zhang et al. 2011).

Although the exact mechanism by which rare alleles contribute to cancer risk remains to be elucidated, it is hypothesized to be the result of varying enhancer activity between different minisatellite alleles (Green and Krontiris 1993, Trepicchio and Krontiris 1992). *HRAS1* minisatellite alleles have been shown to bind members of the *rel*/NF-kB family of transcription factors (Trepicchio and Krontiris 1992). Because

altered minisatellite alleles contribute to several human cancers, uncovering the mechanism that generates minisatellite alterations is important for understanding the heritable risk of cancer and other minisatellite associated diseases, and is the focus of the Kirkpatrick lab.

A Minisatellite Model in Yeast

The budding yeast *Saccharomyces cerevisiae* is a fantastic system for researching meiotic events and has several advantages over mammalian systems. *S. cerevisiae* is one of the few species in which meiosis can be induced and the four haploid products can be accounted for and analyzed via tetrad dissection. In *S. cerevisiae* there are an abundance of auxotrophic markers whose phenotypes can be easily scored, such as *HIS4*. Meiotic recombination is a pathway that is evolutionarily conserved among eukaryotes (Hunter 2006, Lynn et al. 2007); information gained from yeast is applicable to mammals. *Saccharomyces cerevisiae* is thus a powerful system to study meiotic factors that control minisatellite stability.

To further characterize minisatellite DNA during meiosis, the Kirkpatrick lab introduced the human *HRAS1-A1* allele into the *HIS4* locus of *S. cerevisiae*. The *HIS4* locus was chosen because it exhibits an unusually high level of meiotic recombination activity in the AS4/AS13 strain background, and has been used extensively in elucidating the recombination molecular pathway (Detloff, Sieber and Petes 1991, Detloff et al. 1992, Nag et al. 1989, Nag and Petes 1993, White et al. 1985, White et al. 1993, Kirkpatrick 1999, Kearney et al. 2001, Fan, Xu and Petes 1995).

Key to the Kirkpatrick lab's yeast system is the *his4*-Δ*52* allele. The *his4*-Δ*52* allele is a mutation in which 171 bp of promoter sequence upstream of *HIS4* have been deleted and replaced with an *Xho*I linker (White et al. 1993, Jauert et al. 2002). The TATA box was left intact, but the transcription factor binding sites and the meiotic DSB sites have been removed (White et al. 1993). Strains bearing the *his4*-Δ*52* allele exhibit a loss of *HIS4* transcription and significantly reduced levels of meiotic recombination as measured by *HIS4* aberrant segregation levels (Jauert et al. 2002, White et al. 1993).

The Kirkpatrick lab inserted the *HRAS1-A1* minisatellite allele into the deleted region of the *his4*-Δ*52* allele, replacing the deleted promoter sequences (Jauert et al. 2002). This novel allele of *HIS4* was designated *his4-A1* (Jauert et al. 2002). Using the *his4-A1* yeast system, the Kirkpatrick lab demonstrated that the minisatellite insert exhibited the same phenotypes in yeast that it exhibits in a mammalian system: i) the length of the minisatellite insert is stable during mitotic growth but alters at a high frequency during meiosis, ii) both expansions and contractions in minisatellite length occur, and iii) the minisatellite restored transcription to the neighboring *HIS4* gene. Additionally, the minisatellite restored meiotic recombination hotspot activity; it was determined that meiotic DSBs formed in the regions flanking the minisatellite insert (Jauert et al. 2002).

Further analysis revealed that minisatellite length alterations occurred specifically in units of 28 bp (same length as the repeat unit) and are dependent on the meiotic recombination initiating DSB endonuclease *SPO11* (Jauert et al. 2002), demonstrating that meiotic recombination is necessary for minisatellite alterations. Finally, our lab

determined that the *RAD1*-dependent LLR pathway controlled the expansions, but not the contractions, of the common *HRAS1-A1* minisatellite allele, and thereby plays a direct role in the meiotic stability of the *HRAS1* minisatellite (Jauert et al. 2002).

Recently our lab identified a new gene, *CSM3*, with a role in the stability of the *HRAS1* minisatellite in yeast during stationary phase (Alver, Kelly and Kirkpatrick *submitted*). *CSM3* (chromosome segregation in meiosis) was first identified in a screen for genes that are necessary for wild-type meiosis in *S. cerevisiae* (Rabitsch et al. 2001). The loss of *CSM3* resulted in a "mild chromosome missegregation" phenotype and a loss of spore viability, but the functional role of *CSM3* during meiosis remains poorly understood. Since then research has focused on the role of *CSM3* during S phase in mitotically dividing cells. Studies have shown that the products of the *CSM3*, *MRC1*, and *TOF1* genes form a heterotrimeric complex that interacts directly with the replisome, specifically the MCM helicase, during S phase (Calzada et al. 2005, Nedelcheva et al. 2005, Bando et al. 2009, Osborn and Elledge 2003, Katou et al. 2003). The *CSM3/MRC1/TOF1* complex is not required for DNA synthesis, but instead serves as a mediator of replication fork progression. In the event of DNA damage or replicative stress, DNA synthesis pauses leading to the accumulation of RPA bound single-stranded DNA regions, the activation of the replication checkpoint, and phosphorylation of Mrc1p by Mec1 (Nedelcheva et al. 2005, Bando et al. 2009, Calzada et al. 2005, Osborn and Elledge 2003, Foss 2001). The Csm3/Mrc1/Tof1 complex stabilizes the MCM helicase and prevents further DNA unwinding, effectively keeping the replisome intact and stabilizing the replication fork (Nedelcheva et al. 2005, Calzada et al. 2005, Bando et al.

2009). Additionally, Mrc1 and Tof1, and presumably Csm3, have been shown to play a role in replication fork progression recovery (Tourriere et al. 2005). While *CSM3*, *MRC1*, and *TOF1* clearly have a role during DNA synthesis and have been shown to function in minisatellite stability during stationary phase (Alver et al. *submitted*), it remains to be shown whether *CSM3*, *MRC1*, or *TOF1* have a role in the stability of minisatellite DNA during meiosis.

Goals of this thesis project:

In this research we continue our analysis of minisatellite stability and recombination during meiosis using a derivative of the *A1* allele, the *his4-H10* allele, which contains 10.5 copies of the 28 bp repeat sequence (Jauert and Kirkpatrick 2005). We took a candidate gene approach, focusing on genes whose products are known to function during DNA recombination and repair. Our goals were to identify more factors involved in minisatellite stability during meiosis, to characterize these factors within the known context of the meiotic *RAD1*-dependent LLR pathway, and to ultimately elucidate a better understanding of the mechanism that drives minisatellite alterations during meiotic recombination.

In this study we analyzed several candidate genes, including *CSM3* and its interacting partners *MRC1* and *TOF1*, for a role in meiotic minisatellite stability. We also characterized the role of *CSM3* in large loop repair by analyzing the loss of *CSM3* in strains heterozygous for the *his4-lopd* allele and compared the results to a *RAD1* mutant. Finally, we analyzed *CSM3 RAD1* double mutants in a heterozygous *his4-lopd* diploid to determine whether they are in the same LLR pathway, or if *CSM3* is the first gene to be identified that is part of the *RAD1*-independent LLR pathway. In agreement with our goals, the results obtained from this research identified more factors involved in minisatellite stability and large loop repair during meiosis. This data will be the focus of Chapter 2.

During the course of this research, we uncovered a novel recombination phenotype associated with the *HRAS1* minisatellite. In the absence of crossover

promoting genes *MSH4*, *MSH5, MER3*, and *SPO16*, crossover levels were maintained at wild-type levels in the minisatellite-spanning *HIS4-LEU2* interval. We further characterized this recombination phenotype by analyzing aberrant segregation levels at the minisatellite-containing *HIS4* locus and comparing this data to other loci throughout the yeast genome. Finally, we inserted the *H10* allele upstream of a second marker, *ARG4*, and characterized the recombination phenotypes at this locus in a *MSH5* mutant. In agreement with our goals, the results obtained from this study further characterized factors that influence meiotic recombination activity at minisatellite DNA, which has broader implications for genomic stability of repetitive DNA in eukaryotic genomes. These data will be the focus of Chapter 3.

Figure 1

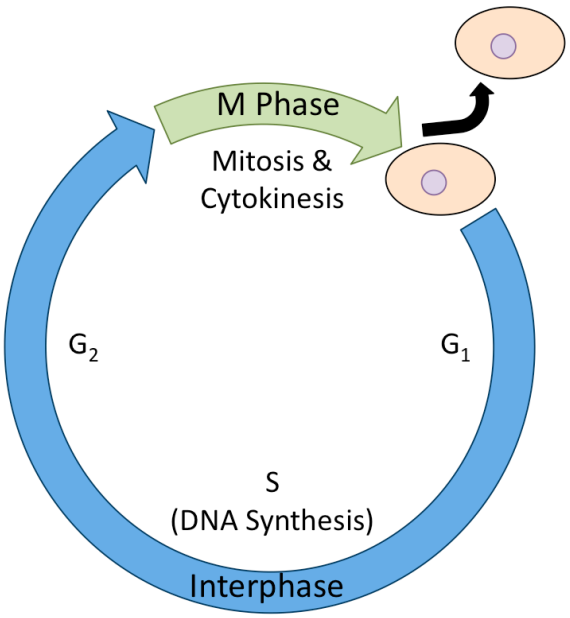

Figure 1. Overview of the cell cycle. Growing cells alternate between Interphase and M phase. Interphase consists of two periods of growth (G_1 and G_2), and a period of DNA synthesis (S) during which cells replicate their entire genome, in preparation for cell division. M phase consists of two stages: Mitosis is the division of the nucleus and its replicated genomic contents into two new nuclei, and cytokinesis is the division of the cytoplasm and its contents. Completion of M phase produces two new daughter cells that are genetically identical.

Figure 2

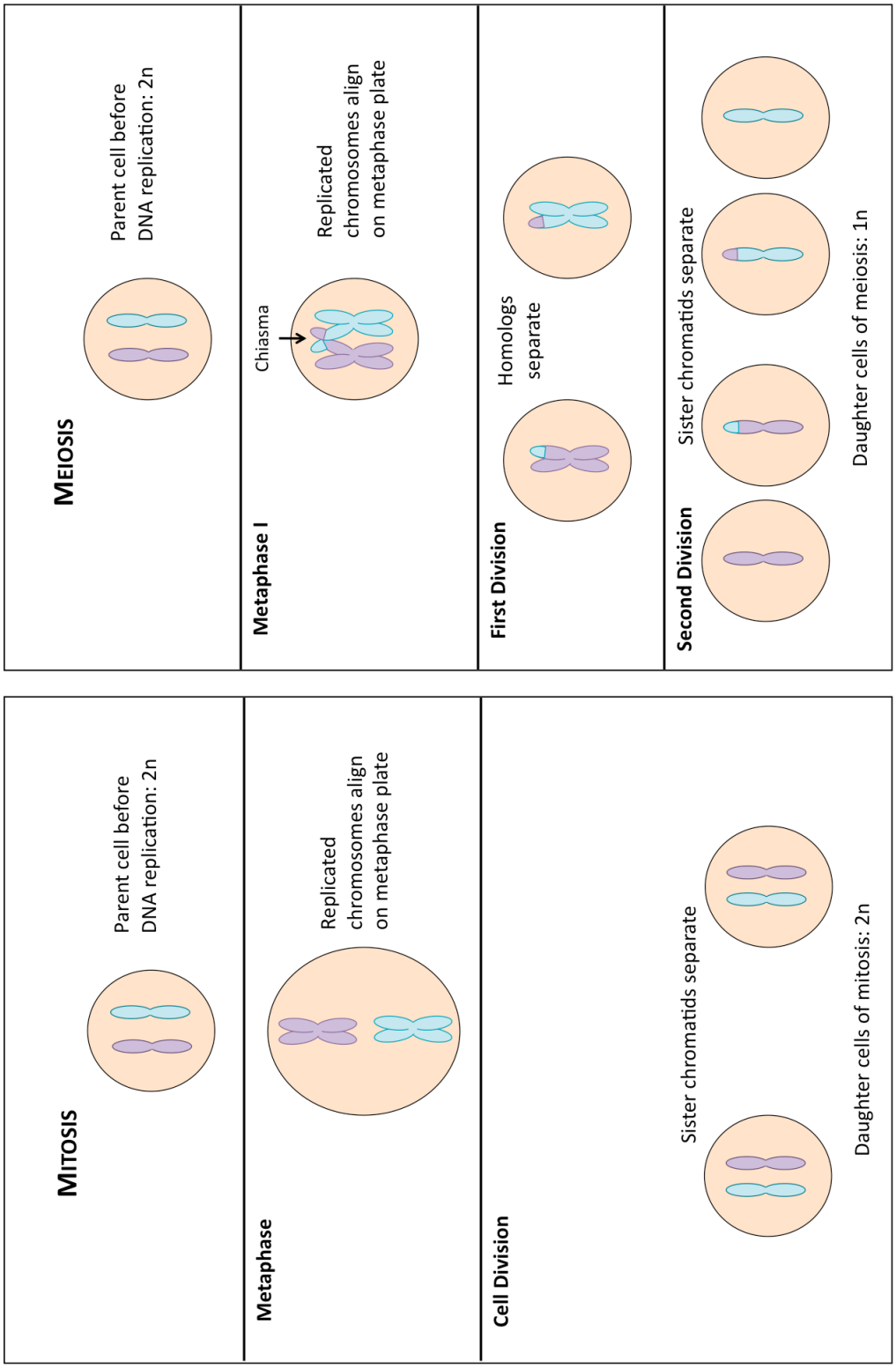
MEIOSIS
Parent cell before DNA replication: 2n
Metaphase I
Chiasma
Replicated chromosomes align on metaphase plate
First Division
Homologs separate
Second Division
Sister chromatids separate
Daughter cells of meiosis: 1n
MITOSIS
Parent cell before DNA replication: 2n
Metaphase
Replicated chromosomes align on metaphase plate
Cell Division
Sister chromatids separate
Daughter cells of mitosis: 2n

Figure 2. An overview of mitosis and meiosis. Shown here is a diploid cell with a single homologous pair of chromosomes. Prior to division, cells replicate their genome and each chromosome consists of two identical sister chromatids that remain attached. During mitosis, chromosomes align independently on the metaphase plate, sister chromatids are separated and segregated to opposite poles. After cytokinesis, two new daughter cells exist that are identical in genomic content to each other and to their progenitor cell. During meiosis, homologous chromosomes exchange DNA and form a physical bridge, chiasma, that holds the homologs together as they align as a pair on the metaphase I plate. The homologs are separated and segregated to opposite poles, and cytokinesis completes the first division. A second division follows, which separates and segregates the sister chromatids to opposite poles. After cytokinesis, four new daughter cells exist that contain half the genetic content of their progenitor cell.

Figure 3

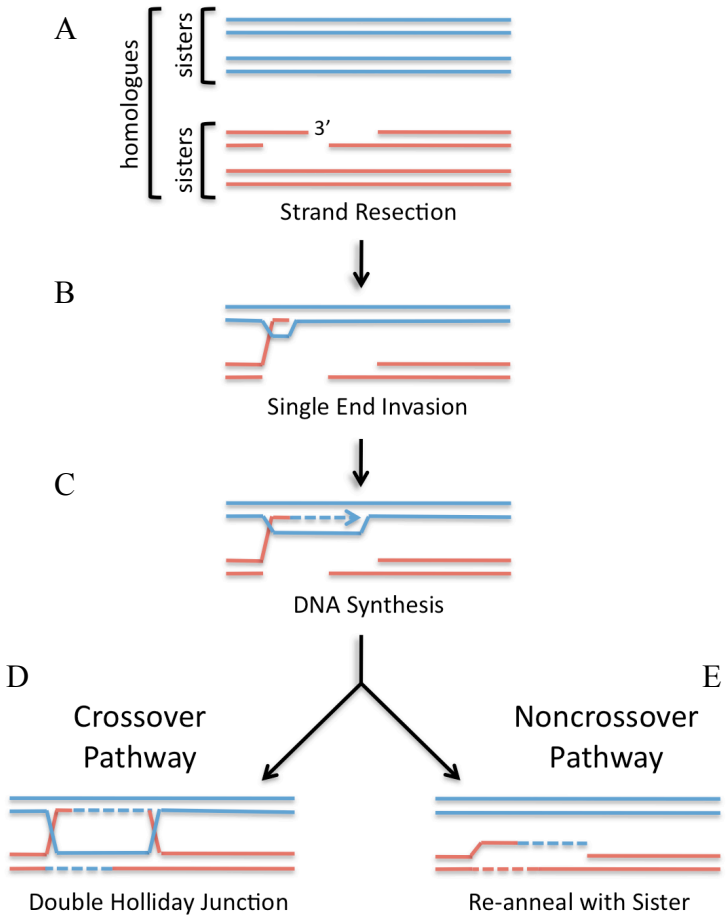

Figure 3. An overview of meiotic recombination. The crossover and the noncrossover pathways share similar precursor intermediates. (A) Recombination is initiated by a double-strand break and processed by 5' strand resection. (B) The overhanging 3' single-strand tail invades the duplex DNA of the homolog, forming a heteroduplex DNA region. (C) The 3' end functions as a primer for DNA synthesis, which further drives strand invasion. (D) The second end is captured, generating a double-Holliday Junction structure that can be resolved as a crossover. (E) The invading strand is released with enough DNA synthesis to repair the initial DSB and reanneals with its partner.

Figure 4

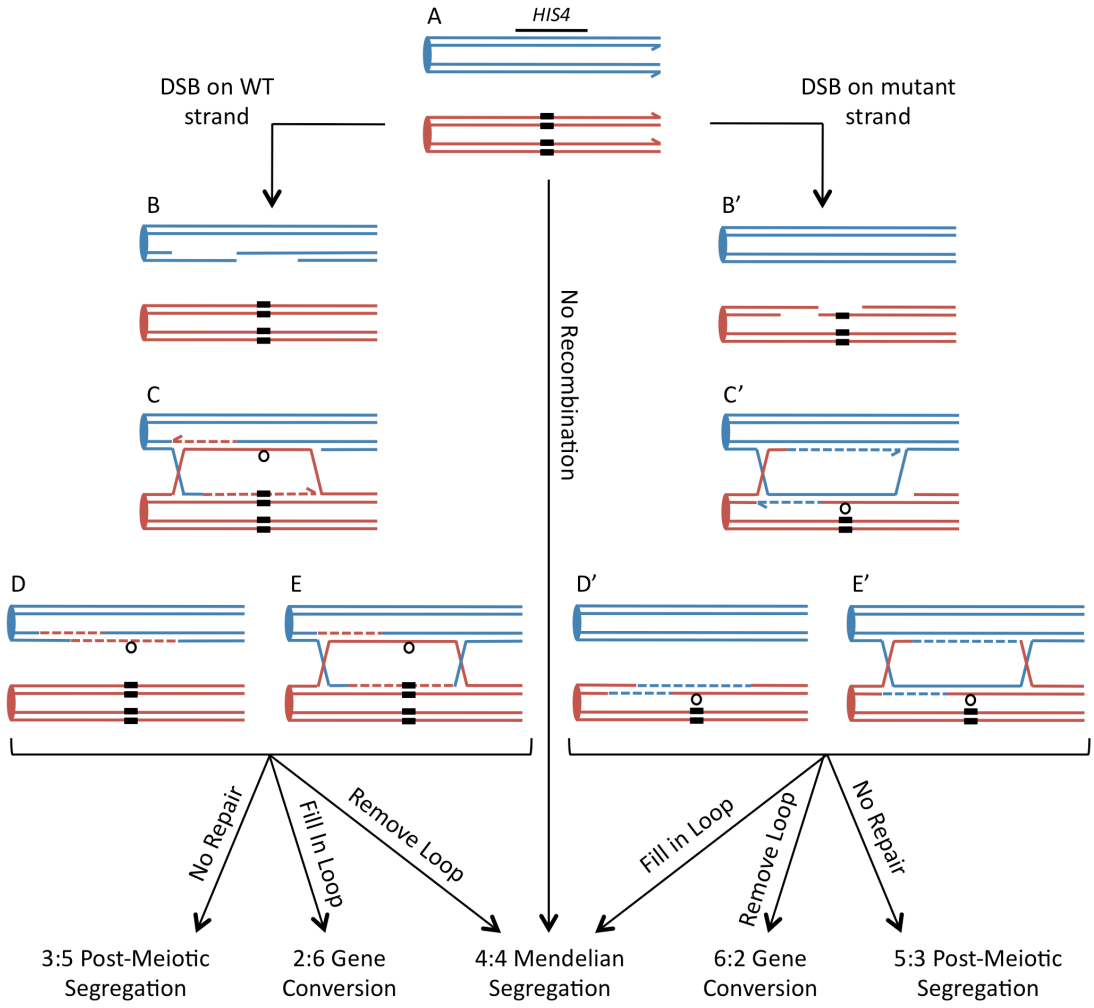

Figure 4. Large loop formation and repair during meiotic recombination. (A) Shown here is a pair of homologous chromosomes (one blue, one red) that have undergone DNA replication and consist of two sister chromatids each. The region spanning the *HIS4* gene is indicated (thin black bar). One homolog contains the wild-type *HIS4* gene (blue chromosome) while the other contains either the *his4-lopd* or *his4-lopc* allele (red chromosome), which has a 26 bp insertion +470 bp into the coding region of *HIS4* (thick

black bar). During meiotic recombination, meiotic DSBs form in the 5' region adjacent to *HIS4* on either the WT (B) or the mutant (B') strand. Following 5' strand resection and 3' strand invasion, a heteroduplex DNA forms that spans the *lopd/lopc* insert (C and C'). Because there is no sequence homology between the insert and the WT strand, the insert loops out of the heteroduplex (black loop). This large loop is substrate for repair, and will form regardless of if the intermediate is processed as a noncrossover (D and D') or a crossover (E and E'). Repair of the loop by the LLR pathway generates either a gene conversion (2:6 or 6:2) or leads to the restoration of Mendelian segregation. Lack of repair generates a post-meiotic segregation (3:5 or 5:3).

Figure 5

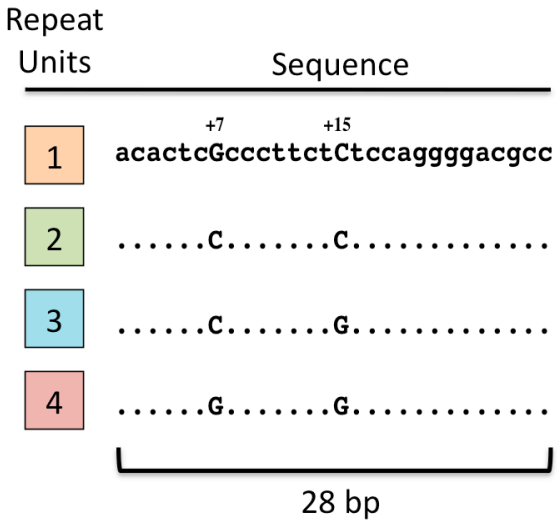

Figure 5. *HRAS1* repeat units. The *HRAS1* minisatellite is composed of a 28 bp consensus sequence that is repeated in direct tandem arrays. There are four versions of the consensus sequence each differing at the 7th or the 15th position. Either position can be a cytosine or a guanine.

Chapter 2

The Role of *CSM3*, *MRC1*, and *TOF1* in Minisatellite Stability and Large Loop DNA Repair During Meiosis in Yeast

Double-stranded break (DSB) repair during meiotic recombination in yeast *Saccharomyces cerevisiae* leads to the formation of heteroduplex DNA, a hybrid DNA molecule composed of single strands from two homologous chromosomes. If a difference in sequence exists between the strands within the heteroduplex DNA, a mismatch or a large unpaired loop will form that is a substrate for repair. At least two pathways function to repair large loops that form within heteroduplex DNA: the *RAD1*-dependent large loop repair (LLR) pathway and another as yet uncharacterized *RAD1*-independent LLR pathway. Repair of large loops during meiotic recombination is especially important for the genomic stability of the repetitive minisatellite sequences. Minisatellite DNA is generally stable during mitotic growth but frequently alters in length during meiosis. Using a yeast minisatellite system in which the human minisatellite associated with the *HRAS1* proto-oncogene has been inserted into the recombination hotspot region upstream of *HIS4* in *S. cerevisiae*, our lab previously showed that the *RAD1*-dependent LLR pathway controls minisatellite length expansions, but not contractions. Here we show that minisatellite length expansions are also controlled by the products of the *CSM3* and *TOF1* genes, while contractions are controlled by *MRC1*. Analysis of yeast strains heterozygous for the *his4-lopd* insert confirmed that deleting *CSM3* caused a loss of fill-in-loop repair similar to that of a *RAD1* mutant, and that loss of fill-in-loop repair is greater in a *RAD1 CSM3* double mutant but this effect is not addition suggesting some overlap between the two genes.

Results

Loss of *CSM3, MRC1,* or *TOF1* affects minisatellite stability during meiosis: To identify genes that have a role in minisatellite stability during meiosis, we took a candidate gene approach focusing on genes whose products are known to play a role in some aspect of DNA repair and/or recombination during meiosis. We used a yeast minisatellite model system developed by our lab, in which an *HRAS1* minisatellite allele is inserted upstream of the *HIS4* gene on chromosome III (Figure 1) (Jauert et al. 2002). The primary minisatellite allele used in this study is the *his4-H10* allele, which contains ten and a half repeats derived from the most common human *HRAS1* allele *A1* (Jauert and Kirkpatrick 2005). All strains used in this study are diploids that are homozygous for the *his4-H10* insertion and a deletion of the candidate gene of interest (see Materials and Methods).

We measured minisatellite stability by performing a PCR across the minisatellite tract in a minimum of 200 four-viable spore tetrads of each strain. Using this assay, we were able to detect the total number of tetrads exhibiting a minisatellite that had undergone a meiotic alteration, as well as the type of alteration that had occurred (i.e. expansion or contraction). If a gene functions in the type of LLR that fills-in loops, deleting this gene will decrease the percent of minisatellite expansions. If a gene functions in the type of LLR that removes loops, deleting this gene will decrease the percent of minisatellite contractions. It is possible that a gene may function in both types of repair, in which case we expect to observe decreases in both expansions and contractions.

In the wild-type *his4-H10* strain, the most common minisatellite alteration we observed were in tetrads with a minisatellite length contraction in a single spore (16%), followed by tetrads with a minisatellite length expansion in a single spore (5%), while tetrads with two, three, or four spores with an altered minisatellite were observed at 0-1% (Table 1). The wild-type strain had a total meiotic alteration frequency of 22% (Table 1).

Four of the candidate genes we analyzed, *SLX1*, *SLX4*, *UBX7*, and *MLH3*, had no significant effect on the meiotic stability of the *his4-H10* minisatellite (Table 1). We included *SLX1, SLX4,* and *MLH3* in this study because they have each been previously determined to have a role in promoting meiotic crossing over in yeast and in humans (Wang, Kleckner and Hunter 1999, Santucci-Darmanin et al. 2002, Fekairi et al. 2009, Svendsen et al. 2009, Munoz et al. 2009), and in the case of *SLX1* and *SLX4*, also have a role in maintaining the stability of the repetitive ribosomal DNA (rDNA) loci in *S. cerevisiae* and *S. pombe* (Mullen et al. 2001, Fricke and Brill 2003, Coulon et al. 2004). While *UBX7* has no role in meiotic crossing over, it has been implicated in minisatellite stability during stationary phase in yeast (Alver et al. *submitted*). Loss of these candidate genes had no significant effect on the pattern or the total percent of minisatellite length alterations (Table 1).

Our lab has previously shown that *RAD1* plays a direct role in the meiotic stability of the larger *HRAS1-A1* allele (Jauert et al. 2002). Here we wanted to determine if the loss of *RAD1* also had an effect on the shorter *A1*-derived *H10* allele. In a *RAD1* mutant, the total percent of tetrads with an altered minisatellite significantly decreased from 22% to 14% ($p = 0.021$, Table 1). Specifically, we observed a significant decrease in the

percent of tetrads with a minisatellite length expansion (from 5% to 1%, p = 0.021), and a small but not significant decrease in tetrads with a length contraction (from 16% to 11%, p = 0.17), while the percent of tetrads with minisatellite alterations in two, three, or four spores remained at 1% or less (Table 1). These data demonstrate that *RAD1* functions in the meiotic stability of the *his4-H10* allele, primarily in the type of fill-in-loop repair that generates expansions and matches previously published data (Jauert et al. 2002, Kirkpatrick and Petes 1997).

Our lab recently identified *CSM3* in a forward screen for genes that have a significant effect on minisatellite stability during stationary phase in *S. cerevisiae* (Alver et al. *submitted*). We wanted to determine if *CSM3* also functioned in minisatellite stability during meiosis. In a *CSM3* mutant, the total percent of tetrads with an altered minisatellite significantly decreased from 22% to 13% (p = 0.008, Table 1). Similar to the *RAD1* mutant, we observed a significant decrease in the percent of tetrads with a length expansion (to 1%, p = 0.044), a small but not significant decrease in length contractions (to 11%, p = 0.12), while the percent of tetrads with two, three or four altered spores remained at 1% or less (Table 1).

This result prompted us to analyze *his4-H10* stability in strains bearing deletions in the *CSM3* interacting partners *MRC1* and *TOF1*. The *his4-H10 mrc1*Δ and *tof1*Δ strains also exhibited significant decreases in the total percent of minisatellite alterations, to 15% each (p = 0.038 and p = 0.046, respectively, Table 1). Similar to *CSM3*, a *TOF1* mutation decreased the percent of tetrads with a minisatellite length expansion (to 2%, p = 0.19) and moderately decreased length contractions (to 11%, p = 0.15), although

neither of these changes was significant (Table 1). In contrast, the *MRC1* mutant exhibited a significant loss of minisatellite length contractions (to 8%, p = 0.018), about half that of a wild-type strain, and very little change in length expansions (Table 1). These results demonstrate that *CSM3*, *MRC1*, and *TOF1* play a role in the meiotic stability of the *HRAS1* minisatellite in yeast; *CSM3* and *TOF1* mutants exhibited a loss of minisatellite expansions akin to loss of fill-in-loop LLR, similar to *RAD1*, while the *MRC1* mutant exhibited a loss of minisatellite contractions and likely functions in LLR activity that removes loops (Table 1).

Loss of *CSM3, MRC1,* or *TOF1* had no effect on *HIS4* segregation and crossovers: As part of our analysis on minisatellite stability during meiosis, we measured the level of meiotic recombination at the *HIS4* locus. Each diploid strain is heterozygous for the *HIS4* gene (Figure 1), containing one wild-type allele and a mutant *his4-lopc* allele that bears a 26 bp palindromic insertion within the *HIS4* coding region that forms a stem-loop structure when incorporated into heteroduplex DNA (Figure 3) (Nag et al. 1989). Repair of the loop can generate a gene conversion (GC) or restoration of Mendelian segregation; lack of repair generates a post-meiotic segregation (PMS) (Nag et al. 1989, Kirkpatrick and Petes 1997). Utilizing an insert that is not easily repaired gives a better indication of the level of recombination events initiating at the *HIS4* locus because it inhibits large loop repair that restores Mendelian segregation (Nag et al. 1989). Following the nomenclature of 8-spored fungi, a Mendelian segregation is scored as 4 His+ strands: 4 His- strands (4:4). Any deviation from Mendelian segregation is an aberrant segregation;

aberrant segregation indicates that recombination occurred at the *HIS4* locus. A high frequency of aberrant segregation indicates a high level of recombination. We measured the level of *HIS4* aberrant segregation in a minimum of 300 4-viable spore tetrads of each strain.

In a wild-type *his4-H10* strain, the majority of tetrads exhibited 4:4 Mendelian segregation (53%, Table 2). Of the tetrads with an aberrant segregation, most exhibited a 3:5 or 5:3 PMS event (14% and 16%, respectively), while a smaller percent exhibited a 2:6 or 6:2 GC event (4% and 5%, respectively), and even less exhibited an aberrant 4:4 event (3%) or another type of aberrant segregation (5%, Table 2). Deleting *RAD1, CSM3*, *MRC1*, or *TOF1* in *his4-H10* strains heterozygous for *his4-lopc* did not cause a significant deviation from the wild-type pattern of segregation, or in the overall percent of aberrant segregation (from 47% to 52%, 50%, 47%, and 48%, respectively, Table 2).

We measured the level of intergenic crossing over occurring in the *his4-H10* minisatellite-spanning interval by examining linkage between the *HIS4/his4-lopc* and *LEU2/leu2-3* alleles (Figure 1). A parental marker configuration indicated no crossover between *HIS4* and *LEU2*, a tetratype configuration indicated that a single crossover had occurred, and a nonparental configuration indicated a double crossover had occurred. Genetic distance (cM) was calculated by the Perkins Equation (see Materials and Methods). A wild-type *his4-H10* strain exhibited a crossover frequency of 32 cM (Table 2). Deleting *RAD1, CSM3*, *MRC1*, or *TOF1* did not significantly affect the level of crossovers for the *HIS4-LEU2* interval (to 34, 29, 35, and 33 cM, respectively, Table 2).

Effect of *CSM3* mutation on *his4-A1* minisatellite allele: Our lab has previously shown that *RAD1* plays a direct role in the meiotic stability of the *his4-A1* allele (Figure 1) (Jauert et al. 2002). Because we identified *CSM3* as having a role in the meiotic stability of the shorter *his4-H10* allele, we analyzed the effect of deleting *CSM3* on *his4-A1* stability. A wild-type *his4-A1* strain exhibited minisatellites alterations in 45% of all tetrads (Table 1). Nineteen percent of all tetrads exhibited a minisatellite length decrease and 9% exhibited a length increase (Table 1). Ten percent of all tetrads exhibited a meiotic minisatellite alteration in two spores, 6% had an alteration in three spores, and 0.5% had an alteration in four spores (Table 1).

The *his4-A1 csm3*Δ strain exhibited an overall minisatellite alteration in 43% of all tetrads (Table 1), which is not significantly different than the wild-type strain. We did not observe any deviation in the pattern of minisatellite alterations in the *CSM3* mutant strain as well (Table 1). This is in contrast to the *his4-A1 rad1*Δ strain, where although the total percent of tetrads with a minisatellite alteration did not significantly differ from the wild-type strain, there was a significant drop in the percent of tetrads that exhibited a minisatellite length expansion in a single spore (Jauert et al. 2002). Neither the *CSM3* or *RAD1* mutation affected the level of *his4-lopc* aberrant segregation or the level of intergenic recombination between *HIS4* and *LEU2* in the *his4-A1* strain (Table 2).

***CSM3* and *RAD1* mutations affect *his4-lopd* repair:** To further characterize the role of *CSM3* in large loop repair and compare it to the LLR activity of *RAD1*, we examined the meiotic segregation pattern of diploid strains heterozygous for the *his4-lopd* insertion.

The *his4-lopd* insert is a 26 bp non-palindromic insertion within the *HIS4* coding region that has been used extensively in examining large loop repair pathways during meiotic recombination (Kirkpatrick and Petes 1997, Kearney et al. 2001, Jauert et al. 2002, Jensen et al. 2005). When incorporated into heteroduplex DNA, the *his4-lopd* allele forms a large 26 bp loop that is easily repaired (Figure 3); easily repaired markers frequently exhibit a greater percent of GC events, indicating repair, than PMS events, indicating no repair (Kearney et al. 2001, Jensen et al. 2005).

A wild-type strain exhibited *his4-lopd* aberrant segregation in 28% of tetrads, comprised of 21% GC events and 7% PMS events (Table 3). Within the class of tetrads with aberrant segregation of *HIS4* alleles, 24% exhibited PMS (Table 3). These data indicate that the 26 bp loop formed by the *his4-lopd* insert is efficiently recognized and repaired when incorporated into heteroduplex DNA. Deleting either *CSM3* or *RAD1* did not significantly alter the total percent of *his4-lopd* aberrant segregation ($p = 0.75$ and $p = 0.5$, respectively), however, both mutations decreased the percent of GC events and nearly doubled the percent of PMS events (Table 3). The shift from GC to PMS events reflects a loss of repair of the 26 bp loop formed by the *his4-lopd* insert when incorporated into heteroduplex DNA (Figure 4 of Introduction). Both mutations increased the percent of 3:5 and 5:3 tetrads and reduced the percent of 2:6 tetrads, while the percent of 6:2 tetrads did not significantly change (Table 3). These data suggest that *CSM3* and *RAD1* are used primarily in the type of repair that fills-in loops when either the wild-type or *his4-lopd* strand initiates recombination (Figure 4 of Introduction). This matches

previous research on *RAD1* activity during LLR (Kirkpatrick and Petes 1997, Kearney et al. 2001, Jauert et al. 2002).

***CSM3 RAD1* double mutant analysis:** Components of the *RAD1*-dependent LLR pathway have previously been identified in a *his4-lopd* background, where studies have indicated the existence of at least a second meiotic LLR pathway that is independent of *RAD1*; large loop repair is still observed in strains when components of the *RAD1*-LLR pathway are deleted (Kirkpatrick and Petes 1997, Kearney et al. 2001). We analyzed *HIS4* segregation in a *csm3*Δ *rad1*Δ strain heterozygous for *his4-lopd* to determine if these genes function in the same meiotic LLR pathway.

A *csm3*Δ *rad1*Δ strain exhibited *his4-lopd* aberrant segregation in 34% of tetrads, which is slightly increased compared to a wild-type ($p = 0.09$) and single mutant strains ($p = 0.06$ and $p = 0.35$, Table 3). Compared to a wild-type strain, the percent of GC events decreased by almost half and the percent of PMS events nearly tripled (Table 3). These data reveal that the *CSM3 RAD1* double mutant has an even greater loss of large loop repair activity than either single mutant. Specifically, the change in the percent of 2:6, 6:2, and 3:5 tetrads is similar to either single mutant; the greatest difference is the increased percent of 5:3 tetrads, which is twice that of either single mutant and quadruple that observed in a wild-type strain (Table 3). This is reflected in the increased percent of aberrant segregation tetrads that exhibited a PMS (64%, Table 3), which is significantly higher than either single mutant. However, the increase seen in the double mutant is not a completely additive effect, as would be expected if *CSM3* and *RAD1* were in two

completely separable LLR pathways. These results suggest that *CSM3* and *RAD1* play an overlapping role in the type of LLR activity that fills-in loops.

When we measured the level of intergenic recombination between the *HIS4* and *LEU2* markers, we observed no statistically significant difference between the wild-type and the *CSM3* mutant ($p = 0.53$), *RAD1* mutant ($p = 0.9$), or the double mutant ($p = 0.25$, Table 3).

Figure 1

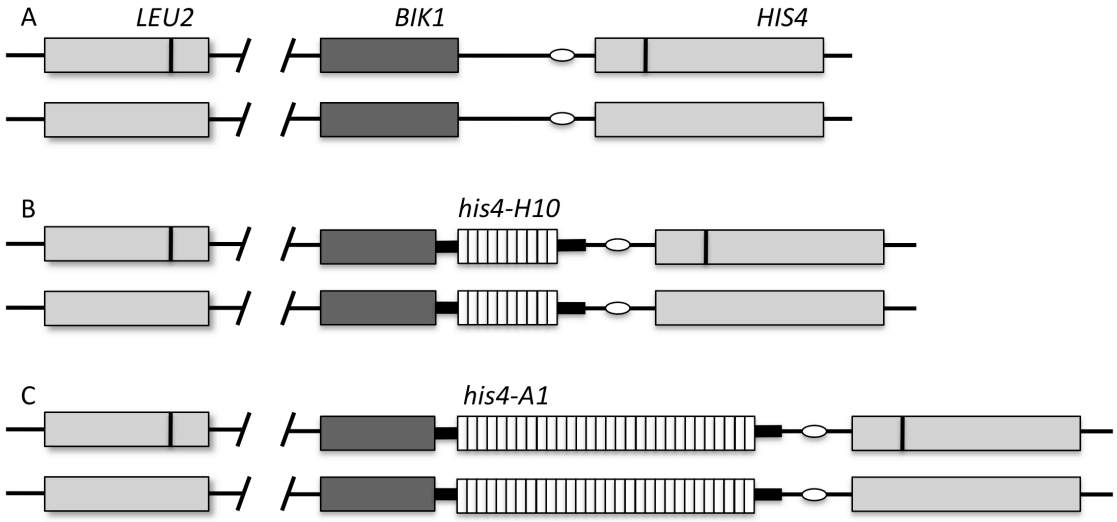

Figure 1. Diagram of chromosome III in diploid strains. A) A diploid strain bearing the wildtype *HIS4* promoter sequence and heterozygous for either the *his4-lopd* or *his4-lopc* insert (dark vertical bar) that disrupts the *HIS4* coding sequence. The *LEU2/leu2-3* alleles are upstream of the *his4-H10* insert and shown here in the parental marker configuration (*HIS4; LEU2/his4-lop; leu2-3*). B) A diploid strain isogenic to (A) but bearing the *his4-H10* minisatellite insert (white boxes) upstream of *HIS4* replacing endogenous promoter sequence. The TATA box (white circle) is left intact. C) A diploid strain bearing the *his4-A1* minisatellite insert (white boxes) upstream of *HIS4*, replacing the same endogenous promoter sequences as in (B).

Figure 2

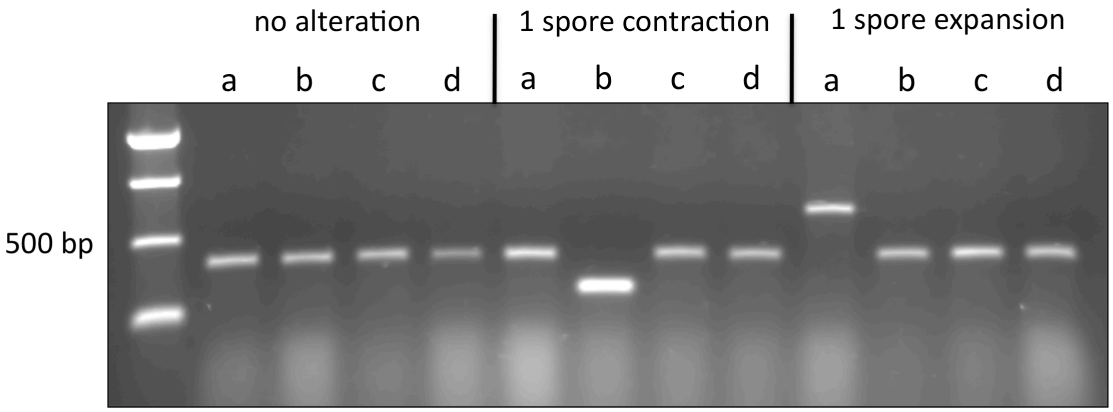

Figure 2. PCR analysis of minisatellite stability. PCR was performed across the minisatellite in 4-viable spore tetrads of each strain, using primers that anneal to unique sequences flanking the minisatellite insertion. The letters a, b, c, and d refer to the four spores of a single tetrad. Shown here are examples of a tetrad that had no minisatellite alteration, and tetrads with a single spore bearing a minisatellite length contraction and expansion.

Figure 3

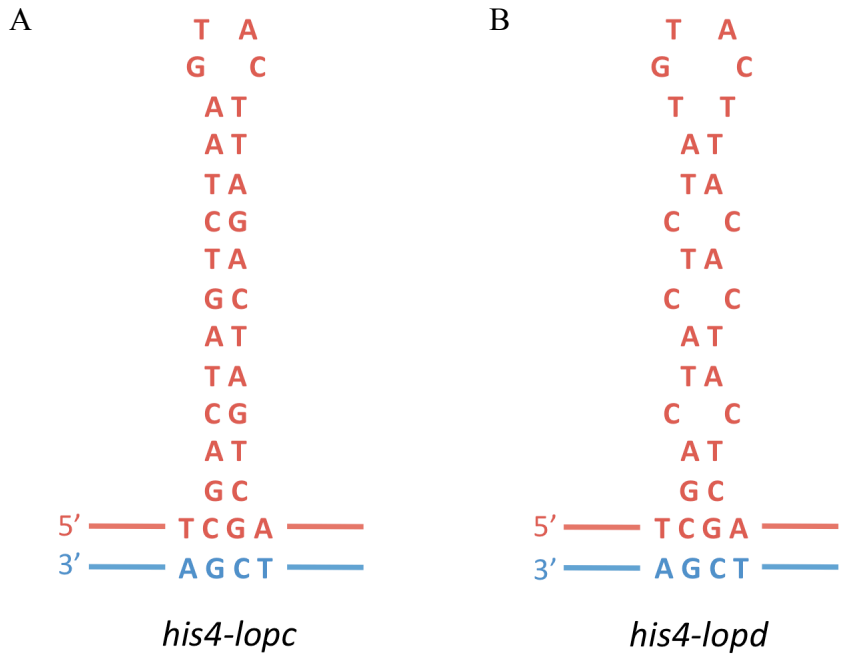

Figure 3. Diagram of *his4-lopc* and *his4-lopd* loop structures. Shown here is the region of heteroduplex DNA formed between a wild-type *HIS4* strand (in blue) and either the *his4-lopc* or *his4-lopd* insertion (in red). (A) The *his4-lopc* insertion is a palindromic sequence and forms a perfect stem loop structure when looped out of the heteroduplex, making this loop difficult to repair. (B) The *his4-lopd* insertion is not a perfect palindrome and forms a similar structure to the *lopc* allele, but is more easily repaired as the stem loop structure is not perfectly annealed.

Based on Nag, White and Petes (1989).

Table 1. Distribution of minisatellite length alterations in various strain backgrounds.

Strain	Relevant mutation	Total tetrads	% (No.) of tetrads with alteration						
			No alteration	Single spore expansion	Single spore contraction	Two spore alterations	Three spore alterations	Four spore alterations	Total alterations
his4-H10 strains									
DTK751	+	205	78 (159)	5 (10)	16 (32)	1 (2)	1 (2)	0 (0)	**22 (46)**
DTK802	*rad1*Δ	263	86 (226)	1 (3)*	11 (29)	1 (3)	0.4 (1)	0.4 (1)	**14 (37)***
DTK1459	*csm3*Δ	237	87 (207)	1 (3)*	11 (25)	0.4 (1)	0.4 (1)	0 (0)	**13 (30)***
DTK1684	*mrc1*Δ	255	85 (218)	4 (11)	8 (21)*	0.4 (1)	1 (2)	1 (2)	**15 (37)***
DTK1685	*tof1*Δ	224	85 (191)	2 (5)	11 (24)	1 (3)	0.4 (1)	0 (0)	**15 (33)***
DTK1460	*slx1*Δ	204	78 (159)	2 (4)	15 (31)	2 (4)	3 (6)	0 (0)	**22 (45)**
DTK1487	*slx4*Δ	222	83 (184)	2 (5)	13 (28)	1 (2)	1 (2)	0.5 (1)	**17 (38)**
DTK1480	*ubx7*Δ	222	84 (186)	2 (4)	11 (25)	2 (4)	1 (2)	0.5 (1)	**16 (36)**
DTK1567	*mlh3*Δ	220	77 (169)	2 (5)	17 (38)	2 (5)	1 (3)	0 (0)	**23 (51)**
his4-A1 strains									
DTK314[a]	+	213	55 (117)	9 (19)	19 (41)	10 (22)	6 (13)	0.5 (1)	**45 (95)**
DTK508[a]	*rad1*Δ	275	52 (142)	3 (9)	24 (67)	16 (44)	4 (11)	1 (2)	**48 (133)**
DTK1724	*csm3*Δ	206	57 (117)	8 (17)	22 (45)	8 (16)	4 (9)	1 (2)	**43 (89)**

Asterisks indicate statistically significant difference compared to wild-type strain (see Materials and Methods).
[a]Jauert et al. 2002.

Table 2. Meiotic segregation patterns and crossover frequencies of diploid strains heterozygous for *his4-lopc*.

Strain	Relevant mutation	Total tetrads	% Ab seg[b]	Percent (No.) of tetrads with *HIS4* segregaton pattern[a]							*HIS4-LEU2* distance (cM)[a]
				4:4	2:6	6:2	3:5	5:3	Ab 4:4	Other[d]	
his4-H10 strains											
DTK751	+	866	47	53 (455)	4 (38)	5 (47)	14 (121)	16 (137)	3 (30)	5 (46)	32
DTK802	*rad1*Δ	311	52	48 (150)	2 (6)	7 (22)	14 (43)	18 (56)	5 (16)	6 (18)	34
DTK1459	*csm3*Δ	318	50	50 (158)	5 (15)	3 (9)	16 (52)	19 (60)	3 (9)	5 (15)	29
DTK1684	*mrc1*Δ	361	47	53 (190)	4 (14)	6 (21)	11 (41)	15 (55)	1 (5)	10 (35)	35
DTK1685	*tof1*Δ	345	48	52 (178)	2 (8)	7 (25)	15 (51)	16 (55)	2 (8)	6 (20)	33
DTK1460	*slx1*Δ	389	55	45 (175)	3 (13)	4 (16)	19 (75)	19 (74)	4 (15)	5 (21)	34
DTK1487	*slx4*Δ	345	50	50 (173)	2 (8)	6 (20)	17 (59)	16 (54)	4 (13)	5 (18)	28
DTK1480	*ubx7*Δ	381	50	50 (189)	3 (10)	6 (21)	13 (50)	21 (79)	4 (17)	4 (15)	32
DTK1567	*mlh3*Δ	357	55	45 (161)	4 (14)	8 (27)	14 (51)	18 (64)	5 (18)	6 (22)	35
his4-A1 strains											
DTK314[c]	+	558	44	56 (310)	3 (16)	5 (29)	15 (85)	13 (75)	5 (25)	3 (18)	31
DTK508[c]	*rad1*Δ	487	43	57 (279)	5 (24)	6 (28)	13 (66)	12 (56)	5 (22)	2 (12)	25
DTK1724	*csm3*Δ	323	37	63 (205)	5 (15)	8 (26)	7 (24)	11 (37)	3 (10)	2 (6)	33

[a]See Materials and Methods. [b]Ab seg, aberrant segregation. [c]Jauert et al. 2002.
[d]Includes: aberrant 2:6, ab 6:2, deviant 3:5, dev 5:3, dev 4:4, 1:7, 7:1, 0:8, and 8:0.

Table 3. Meiotic segregation patterns and crossover frequencies of WT promoter strains heterozygous for *his4-lopd.*

Strain	Relevant mutation	Total tetrads	Percent (No.) of tetrads with *HIS4* segregaton pattern[a]							% Ab Seg	% GC	% PMS	% PMS/ Ab Seg	*HIS4-LEU2* distance (cM)[a]
			4:4	2:6	6:2	3:5	5:3	Ab 4:4	Other[b]					
DNY27	+	407	72 (293)	11 (45)	9 (35)	1 (6)	4 (17)	0.5 (2)	2 (9)	28	21	7	24	28
DTK1667	*csm3*Δ	357	73 (261)	6 (22)	8 (27)	3 (12)	8 (29)	0 (0)	2 (6)	27	15	12	44	30
DTK1731	*rad1*Δ	326	70 (227)	4 (14)	12 (38)	5 (15)	8 (26)	0.6 (2)	1 (4)	30	17	14	46	29
DTK1785	*csm3*Δ; *rad1*Δ	320	66 (211)	3 (10)	9 (28)	3 (10)	16 (52)	2 (5)	1 (4)	34	12	22	64	23

[a]See Materials and Methods. [b]Ab seg, aberrant segregation. [c]Jauert et al. 2002.
[d]Includes: aberrant 2:6, ab 6:2, deviant 3:5, dev 5:3, dev 4:4, 1:7, 7:1, 0:8, and 8:0.

Chapter 3

Minisatellite-Stimulated Meiotic Recombination in *MSH4* and *MSH5* Mutants in *Saccharomyces cerevisiae*

Crossover regulation is critical for proper chromosome alignment and segregation during the first meiotic division. Loss of crossover regulating genes leads to an increase in chromosome nondisjunction and gamete cell death. In this study, we analyzed the meiotic effects of a repetitive minisatellite DNA sequence in *Saccharomyces cerevisiae* strains bearing deletions in crossover-promoting genes *MSH4*, *MSH5*, *MER3*, and *SPO16*. We observed significant increases in the levels of aberrant segregation and wild-type crossover levels at the minisatellite locus – a surprising result given that loss of these genes leads to a significant decrease in crossovers at other loci. This effect is specific to the minisatellite-spanning region, as a genetically-marked interval neighboring the minisatellite exhibited a significant loss of crossovers. Deleting *MSH4* or *MSH5* significantly increased complex recombination events and overall aberrant segregation at the *HIS4* locus. Complementing this data, wild-type crossover levels were observed at a second minisatellite-spanning interval in a *MSH5* mutant when the minisatellite was inserted upstream of *ARG4*. Our data argue that the wild-type presence of these crossover-promoting genes is inhibiting a subset of meiotic recombination events occurring near the minisatellite. This inhibition is not at the level of initiation; analysis of meiotic double-strand break levels revealed no difference between *MSH5* and *msh5*Δ strains.

Results

Meiotic crossing over is maintained at the minisatellite locus in *msh4/5*Δ strains: Due to the crossover-promoting activities of *MSH4* and *MSH5,* we examined the level of intergenic crossing over for the minisatellite-spanning region between *HIS4* and *LEU2* by analyzing the segregation of the *his4-lopc/HIS4* and *leu2-3/LEU2* alleles in 4-viable spore tetrads of each strain (Figure 1). A parental marker configuration indicated that no crossover had occurred between the two markers, a tetratype indicated that a single crossover had occurred, and a nonparental segregation signified that a double crossover had occurred (Figure 2). The genetic distance (cM) between the two loci was calculated using the Perkins Equation (see Materials and Methods).

A strain with a wild-type promoter exhibited a high level of crossing over in the *HIS4-LEU2* interval (32 cM); deleting *MSH4* or *MSH5* significantly reduced the level of crossovers in this interval (20 and 18 cM, Table 1). A strain with the *his4-H10* minisatellite insert exhibited an equally high level of crossovers in the *HIS4-LEU2* interval (32 cM), however, deleting *MSH4* or *MSH5* did not reduce the level of crossovers (32 and 33 cM, Table 1). Three other intervals examined in these strains, *LEU2-CEN3, ARG4-CEN8,* and *TYR7-CEN16*, exhibited a significant reduction of crossing over in *MSH4/5* mutants (Table 1). These results argue that the wild-type level of crossovers in the *his4-H10 msh4*Δ or *msh5*Δ strain is specific to the *HIS4-LEU2* minisatellite-spanning interval.

We further analyzed minisatellite-interval specificity by constructing diploid strains heterozygous for a *URA3* insertion downstream of *HIS4* (Figure 3a). Both a wild-

type promoter and a *his4-H10* strain exhibited a crossover frequency of 11 cM in the *HIS4-URA3* interval and 31 cM in the *HIS4-LEU2* interval (Figure 3b). In a wild-type promoter *msh5*Δ strain, these levels significantly decreased to 5 and 20 cM, respectively. Intriguingly, in a *his4-H10 msh5*Δ strain the crossover levels decreased only in the non-minisatellite spanning *URA3-HIS4* interval and remained at a wild-type level in the minisatellite spanning *HIS4-LEU2* interval (Figure 3b). These results demonstrate that wild-type crossover levels are very specific to the interval spanning the minisatellite insert, as the interval immediately neighboring the minisatellite exhibited a significant decrease in crossover levels in a *MSH5* mutant.

To determine whether the crossover phenotype observed in *MSH4* and *MSH5* mutants was minisatellite specific, we analyzed two other repetitive DNA inserts. The *his4-202* insert contains 51 bp of telomere DNA (Figure 1), which has been shown to stimulate extremely high levels of meiotic recombination activity (White et al. 1993, Fan et al. 1995). The *his4-C48* microsatellite insert contains 48 copies of a semi-degenerate 5 nucleotide CCGnn sequence (Figure 1), and has been shown to exhibit extremely low levels of meiotic recombination activity (Kirkpatrick et al. 1999). The *his4-202* strain exhibited a high level of crossing over in the *HIS4-LEU2* interval (41 cM), and the *his4-C48* strain exhibited a low level of crossing over (8 cM, Table 1). Deleting *MSH4* or *MSH5* significantly decreased crossovers in all intervals examined of both strains, including *HIS4-LEU2* (Table 1). These data argue that the crossover phenotype is specific to minisatellite DNA.

Aberrant segregation increased in *his4-H10 msh4/5*Δ strains: As part of our recombination analysis of the minisatellite insert, we tallied the number of tetrads with a *HIS4* aberrant segregation event by scoring spore colony growth on media lacking histidine (see Materials and Methods). All of our diploid strains are heterozygous for the *his4-lopc* allele, a 26 bp palindromic sequence inserted +470 bp into the *HIS4* coding region (Figure 1) (Nag et al. 1989). Recombination at the *HIS4* locus causes the insert to loop out during strand invasion, as there is no homologous sequence in the wild-type allele, which can result in an aberrant segregation of the *HIS4/his4-lopc* alleles (Kirkpatrick and Petes 1997, Kearney et al. 2001, Jensen et al. 2005). A high level of *HIS4* aberrant segregation indicates a high level of recombination.

We observed high levels of *HIS4* aberrant segregation in strains with a wild-type promoter (44%) and a *his4-H10* promoter (48%, Table 2), characteristic of recombination hot spot activity (White and Petes 1994). Deleting *MSH4* or *MSH5* had no effect on *HIS4* aberrant segregation in strains with a wild-type promoter (Table 2), as expected based on prior research (Hollingsworth et al. 1995, Ross-Macdonald and Roeder 1994). In contrast, a *his4-H10 msh4*Δ or *msh5*Δ strain exhibited significantly elevated levels of *HIS4* aberrant segregation, with the biggest increase being in the complex meiotic recombination events represented in the "other aberrant segregation" column (Table 2). This signifies a shift towards more complex meiotic recombination events that include three or four sister chromatids of a homolog pair. In contrast to *HIS4*, aberrant segregation at the *LEU2*, *TRP1*, *ARG4*, and *TYR7* loci remained unchanged in both the

wild-type promoter and *his4-H10* strains upon deleting *MSH4* or *MSH5* (Figure 4); an increase in aberrant segregation is specific to the minisatellite-containing *HIS4* locus.

Analysis of *HIS4* aberrant segregation in strains bearing the *his4-202* insert (68%) and *his4-C48* insert (18%, Table 2) are similar to previously published data (White et al. 1993, Fan et al. 1995, Kirkpatrick et al. 1999). Deleting *MSH4* or *MSH5* did not alter the level of *HIS4* aberrant segregation in these strains (Table 2). These results argue that increased *HIS4* aberrant segregation is specific to minisatellite DNA.

***MER3* and *SPO16* mutants do not exhibit minisatellite specific increase in *HIS4* aberrant segregation:** Due to the very interesting recombination phenotypes we observed at the *HIS4* locus in *his4-H10 msh4/5*Δ strains, we analyzed strains bearing deletions in two other ZMM genes, *MER3* and *SPO16*. Previous research has shown that yeast strains bearing mutations in *MER3* or *SPO16* exhibit a significant reduction in crossing over and loss of spore viability due to increased meiosis I chromosome nondisjunction (Nakagawa and Ogawa 1999, Nakagawa and Kolodner 2002a, Lynn et al. 2007, Shinohara et al. 2008). Mer3p is a 3' to 5' helicase that promotes strand invasion during heteroduplex formation (Nakagawa and Ogawa 1999, Nakagawa, Flores-Rozas and Kolodner 2001, Nakagawa and Kolodner 2002b), while Spo16p has no assigned biochemical function.

Deleting *MER3* or *SPO16* in strains with a wild-type promoter reduced crossovers at all intervals examined, including the *HIS4-LEU2* interval (Table 1). In contrast, crossovers at the minisatellite spanning *HIS4-LEU2* interval were maintained at wild-type

levels in *his4-H10 mer3*Δ and *spo16*Δ strains; crossovers are maintained at the minisatellite-spanning interval in all four ZMM mutants (Table 1).

Deleting *MER3* or *SPO16* significantly increased *HIS4* aberrant segregation in both a wild-type promoter and *his4-H10* strain (Table 2). This is not surprising given that an increase in *HIS4* aberrant segregation was previously observed in a *SPO16* mutant, and characterized as an increase in noncrossover intermediates (Shinohara et al. 2008). Prior to this study the effect on *HIS4* aberrant segregation had not been analyzed in a *MER3* mutant. Our data suggest that a similar effect is occurring in the *MER3* mutant as in the *SPO16* mutant.

Crossover interference in the minisatellite region in *msh4/5*Δ strains: Because *MSH4* and *MSH5* have been implicated in crossover interference (Ross-Macdonald and Roeder 1994, Hollingsworth et al. 1995, Novak et al. 2001), we calculated the interference value for the *HIS4-LEU2* interval using the traditional Papazian equation (Papazian 1952). The Papazian equation uses the percent of single crossover events (seen as tetratypes, T) to determine an expected percent of double crossover events (seen as nonparental ditypes, NPD, Figure 2), assuming no interference. This value is listed as NPD expected (NPD_{exp}) in Table 3. The ratio of the percent of NPD observed (NPD_{obs}) to NPD_{exp} was determined, and subtracted from one to give the interference value (Interference = 1-NPD_{obs}/NPD_{exp}). If there is no interference, then NPD_{obs} should match NPD_{exp} and the interference value will be zero. If NPD_{obs} is less than NPD_{exp}, meaning there are less

double crossovers observed than expected, then interference is functioning and the interference value will be close to one.

Using the Papazian equation, we calculated an interference value of 0.33 for the *HIS4-LEU2* interval in the parental wild-type promoter strain (Table 3). The interference value does not decrease upon deletion of *MSH4* or *MSH5*. In fact, there is a slight increase in the interference value (to 0.60) in the *msh4*Δ strain, possibly due to an overall decrease in the number of single crossover events leading to an extremely low number of expected double crossovers. Similarly, interference in the strains bearing the *his4-202* allele increased upon deleting *MSH4* or *MSH5*. The *his4-C48* strains all exhibited very low numbers of single crossover events (Table 1), which greatly affected the interference calculations such that the NPD_{exp} values were nearly zero (Table 3). Therefore the presence of even a single NPD, such as that observed in the *his4-C48 msh4*Δ strain, lead to a negative interference value. Normally a negative interference value suggests that more double crossover events (NPDs) are occurring than expected, but in this particular strain the values of all numbers used were too low to be considered accurate. Regardless, the *his4-C48 msh4/5*Δ strains all exhibited a decrease in crossovers between *HIS4* and *LEU2* (Table 1), and the occurrence of a single NPD does not suggest a strong double crossover phenotype.

In contrast to the other parental strains, the parental *his4-H10* minisatellite strain exhibited no interference (-0.01, Table 3), meaning that double crossover events (NPDs) are occurring as expected. Intriguingly, the *his4-H10 msh4*Δ and *msh5*Δ strains had a negative interference value (-0.31 and -0.24, Table 3), implying that not only is crossover

interference not functioning in these strains, but that double crossover events are occurring more frequently than expected at the *HIS4* locus. This data complements our observation that the percent of complex aberrant segregation events, indicating strand invasion between multiple chromatids, increased at the *HIS4* locus in *his4-H10 MSH4/5* mutants (Table 2). Together, the interference data and the complex aberrant segregation data suggest recombination involving multiple strand exchanges is occurring at the *his4-H10* locus in *MSH4/5* mutants, which could account for the wild-type levels of crossovers forming at the *HIS4-LEU2* interval.

***MUS81* and *MMS4* mutants do not sporulate:** It is possible that in the absence of *MSH4/5* the minisatellite region is processed into crossovers by the non-interfering *MUS81/MMS4* pathway. Interestingly, *MMS4* mutants have been shown to exhibit stronger crossover reductions on smaller chromosomes than on larger chromosomes (de los Santos et al. 2003). Unfortunately, *mus81*Δ and *mms4*Δ strains did not sporulate in our AS4/AS13 strain background, which is not surprising given that these same mutations decrease sporulation by 95% to 100% in other strain backgrounds (de los Santos et al. 2001, de los Santos et al. 2003); we were unable to analyze the meiotic phenotypes of these strains.

Minisatellite DNA does not influence DSB formation in a *msh5*Δ strain: We previously demonstrated that an *HRAS1* minisatellite tract at the *HIS4* locus stimulated the formation of double-strand breaks (DSBs) in a *SPO11*-dependent manner (Jauert et

al. 2002). One possible explanation for the recombination phenotypes exhibited by *MSH4/5* mutants is a minisatellite-specific increase in recombination-initiating DSBs. Here we analyzed the level of DSBs in *rad50S* derivatives of the *his4-H10* and the *his4-H10 msh5*Δ strains. Cells were sporulated in liquid media and samples were taken at the zero and twenty-four hour time points. Using Southern blot analysis we determined that DSBs occurred at three different sites in the minisatellite region of both strains (Figure 5). Densitometry measurements revealed that fragments 1 and 2, corresponding to DSB sites flanking the minisatellite insert, were the most abundant while fragment 3, corresponding to the only DSB within the minisatellite insert, was the weakest band (Figure 5). We detected no significant change of DSB levels in the *his4-H10 msh5*Δ strain, as hypothesized. These results suggest that the recombination phenotypes at the minisatellite locus in *MSH4/5* mutants must be occurring by a mechanism other than increased meiotic DSB formation.

Minisatellite tract length is not significantly affected by *MSH4/5*: Given that we observed three DSB sites occurring in the minisatellite region (one specifically occurs within the insert, Figure 5) and an elevation of recombination events at the minisatellite locus in *MSH4*/*5* mutants (Tables 1 and 2), we determined the meiotic stability of the minisatellite insert in *his4-H10 MSH4/5* mutants by performing a PCR across the minisatellite tract in a minimum of 200 four-viable spore tetrads for each strain, using primers that anneal to unique regions of DNA flanking the minisatellite insert.

A wild-type *his4-H10* strain exhibited meiotic minisatellite length alterations in 22% of tetrads (46 of 205). Deleting *MSH4* or *MSH5* did not have a significant impact on meiotic minisatellite stability; length alterations were observed in 21% (49 of 230, p = 0.8) and 19% (41 of 214, p = 0.5) of tetrads, respectively. From these data we conclude that loss of *MSH4* or *MSH5* does not significantly affect the stability of the *his4-H10* minisatellite insert during meiosis, despite the increased levels of recombination observed in these mutants (Tables 1 and 2).

Minisatellite stimulated recombination restores proper chromosome III disjunction but does not rescue spore viability: A wild-type strain passed through meiosis with the majority of tetrads having four viable spores (73%) and a very high overall spore viability (90%, Table 4). Likewise, parental *his4-H10*, *his4-202*, and *his4-C48* strains underwent meiosis with a similar percent of tetrads having four viable spores and a high overall spore viability, compared to a wild-type *HIS4* promoter strain (Table 4).

Loss of crossover-promoting genes, such as *MSH4* and *MSH5*, impairs the formation of chiasmata and causes frequent chromosome nondisjunction during meiosis I (Roeder 1997, Page and Hawley 2003, Ross-Macdonald and Roeder 1994, Hollingsworth et al. 1995). Deleting *MSH4* or *MSH5* in a wild-type strain caused a decrease in overall spore viability and a distinct increase in the number of tetrads with 2- and 0-viable spores at the expense of tetrads with 4- or 3- viable spores (Table 4). This pattern indicates an increase in meiosis I nondisjunction events. The tetrads with two viable spores result when one or more pairs of homologs segregate to the same pole. The tetrads with zero

viable spores result when two or more pairs of homologs segregate to opposite poles. Similar spore viability patterns were observed in *msh4/5*Δ derivatives of *his4-202* and *his4-C48* strains. Although the *his4-C48 msh4/5*Δ strains did not exhibit a decrease in the percent of 3-viable spores, we still observed a greater percent of 2-viable spores compared to 3-viable spores (Table 4).

Deleting *MSH4* or *MSH5* in a *his4-H10* strain had a slightly different effect on spore viability pattern. These mutants exhibited a loss of 4-viable spores almost identical to that seen in mutants with a wild-type promoter, but did not exhibit a loss of tetrads with 3-viable spores or a greater percent of 2-viable spores than 3-viable spores (Table 4). This subtle effect suggests a partial rescue in chromosome disjunction and prompted us to analyze the meiosis I nondisjunction frequency of chromosome III, the minisatellite-containing chromosome, by analyzing the ability of 2-viable spore tetrads to mate (Novak et al. 2001). Improper chromosome III disjunction during meiosis I will generate spores that contain both a *MAT**a*** and a *MAT**α*** chromosome, which prevents them from mating. Upon deleting *MSH5*, we found that chromosome III nondisjunction events (as measured by failure to mate) increased from 0% (0/50 tetrads examined) to 6% (3/50 tetrads) in a strain with a wild-type promoter, but remained at 0% in a strain with the *his4-H10* insert. These subtle changes in spore viability pattern and chromosome III disjunction are consistent with the increase in crossovers in the *HIS4-LEU2* region of chromosome III in the *his4-H10 msh4/5*Δ strains.

Meiotic crossing over maintained in *msh5*Δ strains when *H10* inserted upstream of *ARG4*: We wanted to determine if the *his4-H10* minisatellite had a similar effect on recombination when inserted elsewhere in the yeast genome. We constructed diploid strains homozygous for an *URA3-H10* insertion upstream of the *ARG4* gene on chromosome VIII, called the *arg4-H10* allele, replacing endogenous wild-type promoter but leaving the TATA box intact (Figure 6, see Materials and Methods). Our diploid strains are heterozygous for the *arg4-17* allele, which has a T to A transversion +127 bp into the *ARG4* coding region (White et al. 1985). We examined the level of intergenic crossing over for a minisatellite-spanning interval by monitoring the segregation of the *ARG4/arg4-17* and *THR1/thr1*Δ::*NATMX* genes (DTK1798, Figure 6).

Both a wild-type promoter and an *arg4-H10* strain exhibited extremely high levels of intergenic crossing over of 121 and 138 cM, respectively, in the *ARG4-THR1* interval, and crossover levels of 14 and 18 cM in the neighboring *ARG4-CEN8* interval (Table 5). In a wild-type promoter *msh5*Δ strain, these levels significantly decreased to 32 and 7 cM, respectively. However, in an *arg4-H10 msh5*Δ strain the crossover levels decreased only in the non-minisatellite spanning *ARG4-CEN8* interval and remained at a wild-type level in the minisatellite spanning *ARG4-THR1* interval (Table 5). All other intervals examined in these strains exhibited significant decreases in crossover levels upon deleting *MSH5* (Table 5). As in the *his4-H10* strains, wild-type crossover levels are very specific to the interval spanning the minisatellite.

Because the level of crossovers was extremely high for the *ARG4-THR1* interval, we further investigated the accuracy of these data by constructing a diploid heterozygous

for *URA3*, essentially breaking the *ARG4-THR1* interval into two intervals (DTK1819, Figure 6). This was only constructed in the *arg4-H10* strain, as the wild-type promoter strain does not have a *URA3* insertion upstream of *ARG4* (see Materials and Methods). DTK1819 exhibited a crossover frequency of 7 cM in the non-minisatellite spanning *URA3-THR1* interval and 89 cM in the minisatellite-spanning *ARG4-URA3* interval (Table 5). In the *msh5*Δ derivative (DTK1858), the crossover levels remained at a wild-type level in the minisatellite spanning *ARG4-URA3* interval but significantly decreased at all other levels examined, including the neighboring *URA3-THR1* and *ARG4-CEN8* intervals (Table 5). PCR and sequence analysis confirmed that the *arg4-H10* region had not altered during construction of any of these strains (data not shown). These data argue that wild-type crossing over is specific to the minisatellite-spanning interval in a *MSH5* mutant, and further confirm the crossover phenotypes exhibited in the *his4-H10* strains.

We observed high levels of *ARG4* aberrant segregation in strains with a wild-type promoter (43%) and the *arg4-H10* promoter (40%, Table 6). Deleting *MSH5* caused *ARG4* aberrant segregation to significantly increase in the wild-type promoter, specifically in the percent of 2:6 and 6:2 gene conversion (GC) tetrads (Table 6). This is not surprising, given that a significant increase in *ARG4* aberrant segregation, specifically gene conversions, has been observed in *MSH4* and *MSH5* mutants in other studies (Ross-Macdonald and Roeder 1994, Hollingsworth et al. 1995). In contrast, the *arg4-H10 msh5*Δ strain exhibited a significant decrease in *ARG4* aberrant segregation, specifically in the percent of 2:6 GC tetrads (Table 6). A similar phenotype is observed when comparing DTK1819 and DTK1858 (Table 6). It should be noted that the percent of

complex aberrant segregation events is already high in the wild-type and parental *arg4-H10* strains (15% and 8%, respectively) and these percents remain elevated in a *msh5*Δ derivative (15% and 8%, respectively, Table 6). This suggests that in an *arg4-H10* strain, the already-high level of complex aberrant segregation events are being maintained in a *MSH5* mutant at the expense of an event involving a single strand exchange (2:6 GC tetrads).

Deleting *MSH5* did not affect stability of the *arg4-H10* minisatellite; length alterations were observed in 11% (29 of 258) and 12% (38 of 306, $p = 0.7$) of tetrads in DTK1798 and DTK1802, respectively.

Figure 1

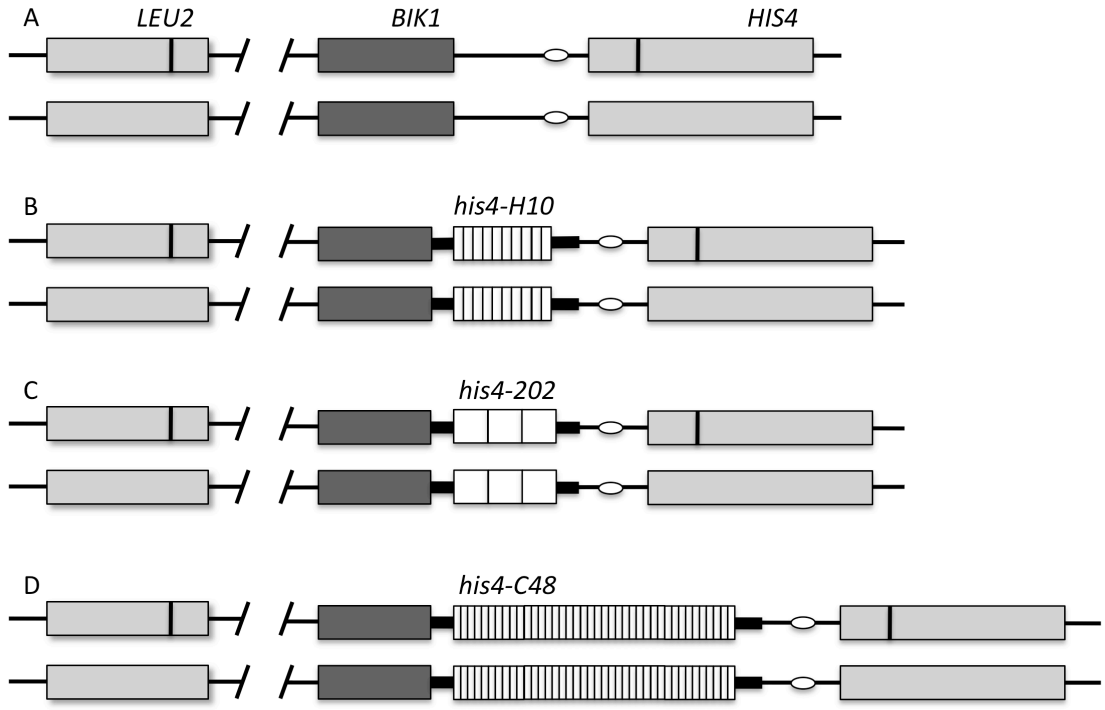

Figure 1. Diagram of chromosome III in diploid strains. A) A diploid strain bearing the wildtype *HIS4* promoter sequence and heterozygous for the *his4-lopc* insert (dark vertical bar) that disrupts the *HIS4* coding sequence. The *LEU2/leu2-3* alleles are upstream of the *his4-H10* insert and shown here in the parental marker configuration (*HIS4; LEU2/his4-lopc; leu2-3*). B) A diploid bearing the *his4-H10* minisatellite insert (white boxes) upstream of *HIS4* replacing endogenous promoter sequence. The TATA box (white circle) is left intact. C) A diploid strain bearing the *his4-202* insert, which is 51 bp of telomeric DNA (white boxes) consisting of three *RAP1* binding sites (White et al. 1993). D) A diploid strain bearing the *his4-C48* insert, which contains 48 copies of a degenerate CCGnn 5 bp repeat (Kirkpatrick et al. 1999). Strains shown in B, C, and D are otherwise isogenic to the strain shown in A.

Figure 2

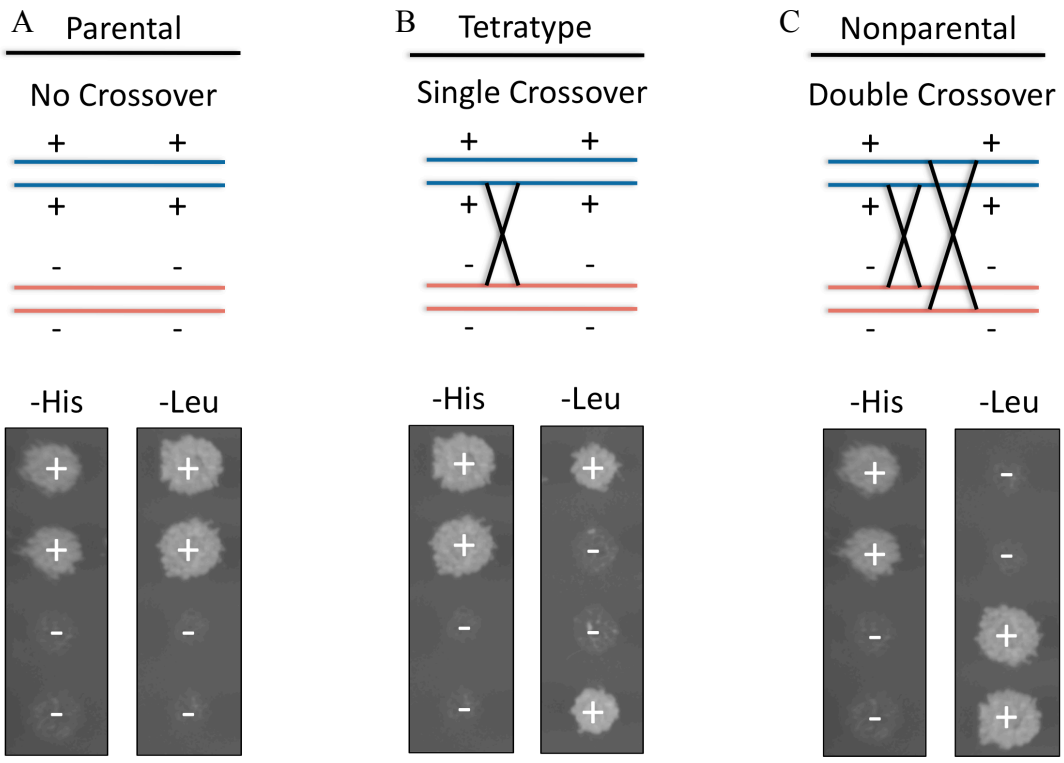

Figure 2. Diagram of the parental, tetratype, and nonparental marker segregation for the *HIS4-LEU2* interval. The *HIS4* and *LEU2* loci both reside on chromosome III. Shown here are chromosome III homologs, each consisting of two sister chromatids. The blue chromosome bears the wild-type alleles of both *HIS4* and *LEU2*, while the red chromosome bears the *his4-lopc* and *leu2-3* mutants. A) If there is no meiotic crossover between *HIS4* and *LEU2*, then the resulting four spores will display parental marker segregation when plated on –His and –Leu media. B) If there is a single crossover between *HIS4* and *LEU2*, then the resulting four spores will each display four different marker segregations. C) A double crossover will result in all four spores displaying nonparental marker configuration.

Figure 3

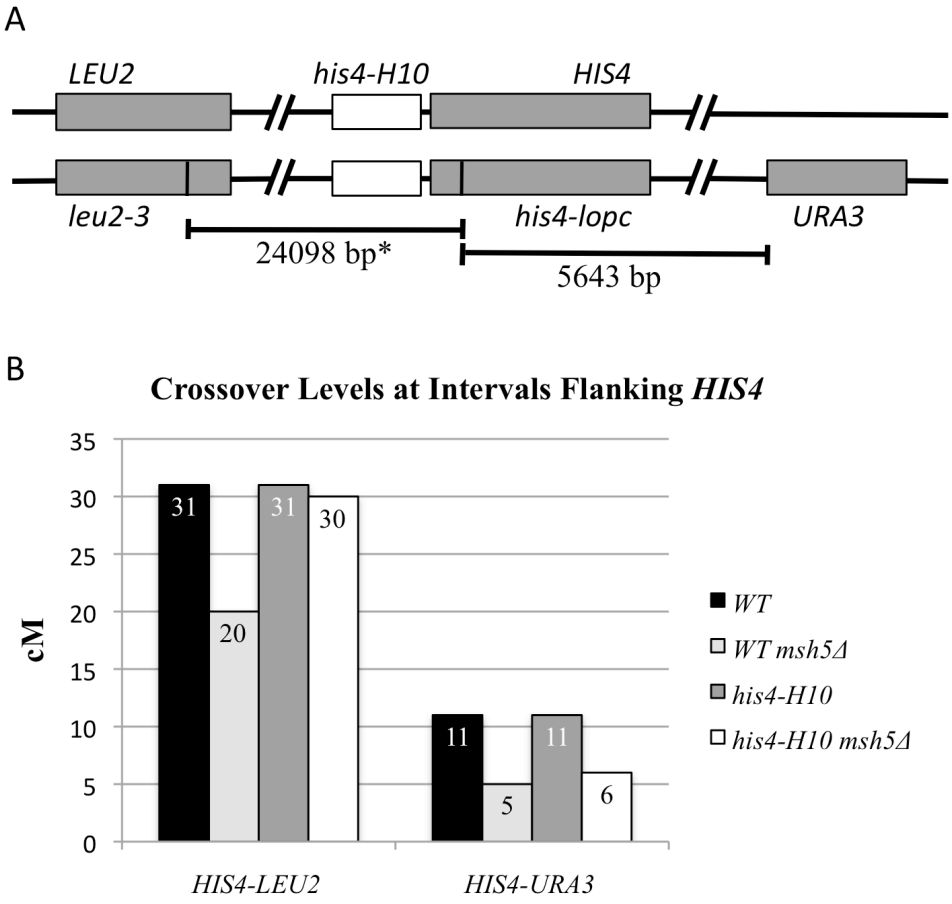

Figure 3. The minisatellite effect on crossover levels is specific to the minisatellite-spanning interval. (A) Diagram of chromosome III for strains with a *URA3* insertion. The asterisk indicates the distance between *his4-lopc* and *leu2-3* in a strain with the minisatellite insert, the distance for this interval is 23706 bp in a strain with a wild-type promoter. (B) Crossover analysis of the *HIS4-LEU2* and the *HIS4-URA3* intervals revealed a significant decrease in the *MSH5* mutants of all strains with the exception of the *HIS4-LEU2* minisatellite-spanning interval.

Figure 4

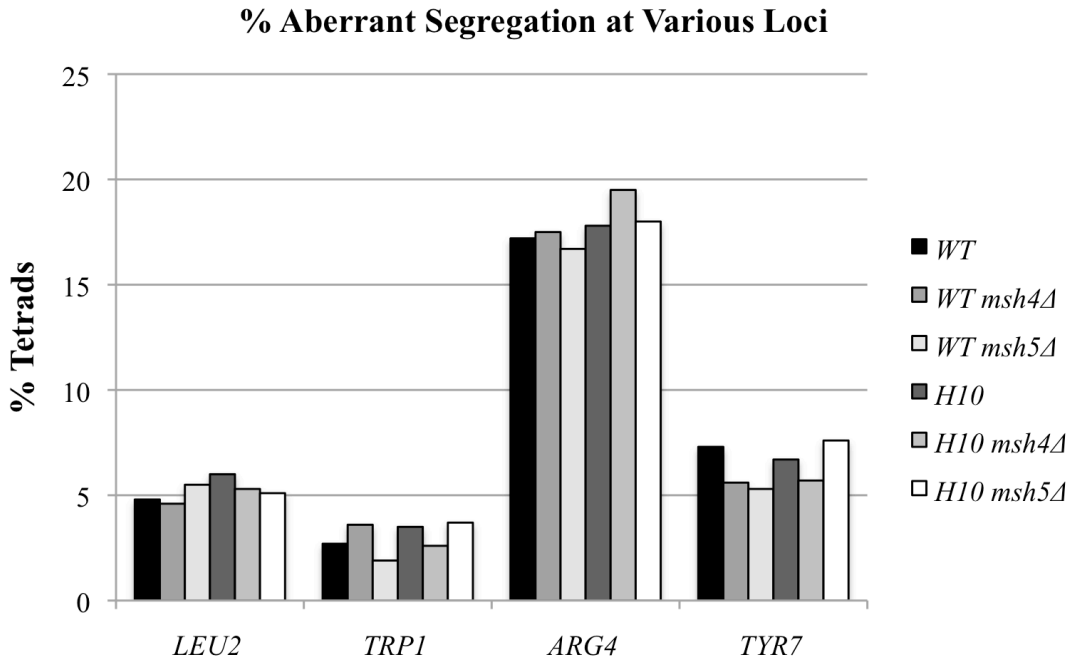

Figure 4. Aberrant segregation analysis of other loci. The percent of tetrads with an aberrant segregation were tallied at the *LEU2*, *TRP1*, *ARG4*, and *TYR7* locus in strains with either the wild-type or the *his4-H10* minisatellite promoter. We observed no significant change in aberrant segregation levels upon deletion of *MSH4* or *MSH5* at any of these four loci.

Figure 5

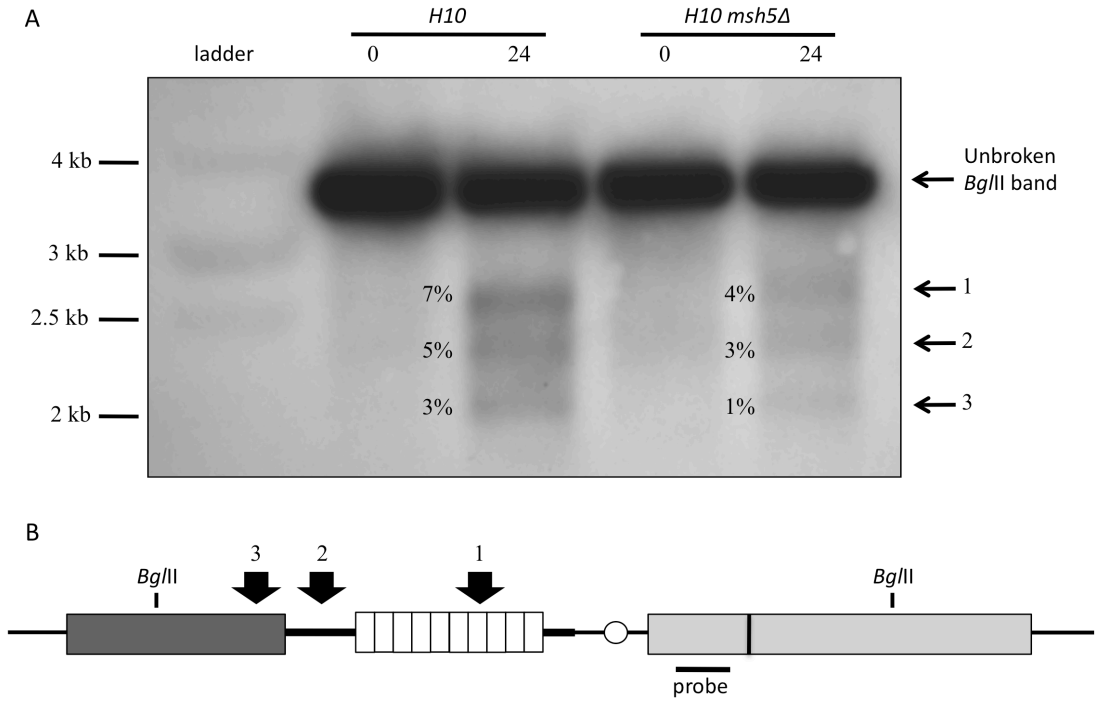

Figure 5. A meiotic DSB analysis of the *his4-H10* insert. (A) Southern blot analysis was performed on *Bgl*II-digested DNA isolated from DTK1339 (*his4-H10 rad50s*) and DTK1341 (*his4-H10 msh5*Δ *rad50s*) just prior to meiosis initiation (0 hr) and after 24 hours. The size and density of each indicated band was determined. The band sizes are approximately 2600 bp (band 1), 2300 bp (band 2), and 2050 bp (band 3). (B) Based on these measurements, we mapped the sites of meiotic DSB formation relative to the major features of the *HIS4* locus. The amount of each fragment, as measured by densitometry, was recorded as a percent of the unbroken fragment. The experiment was repeated on three independent samples with equivalent results.

Figure 6

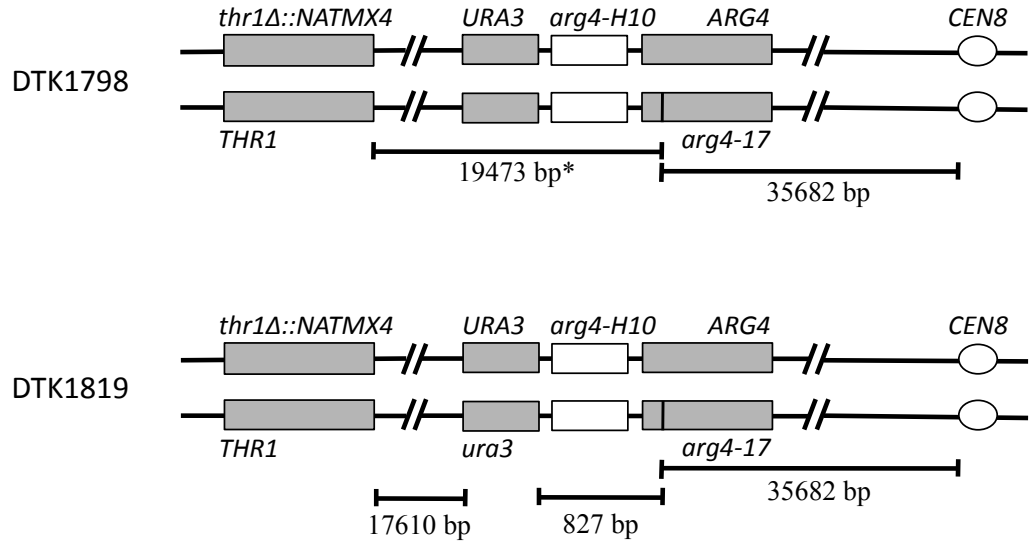

Figure 6. Diagram of chromosome VIII for strains with the *arg4-H10* insertion. DTK1798 is a diploid strain bearing the *URA3-H10* insertion upstream of *ARG4*, and heterozygous for the *arg4-17* allele that contains a T to A transversion (dark vertical bar) that disrupts the *ARG4* coding sequence (White et al. 1985). The *URA3-H10* insert replaced endogenous promoter sequences 316 and 180 bp upstream of *ARG4*, removing the endogenous site of meiotic DSB formation and leaving the TATA box intact. The asterisk indicates the distance between *arg4-17* and *THR1* in a strain with the *H10* minisatellite insert; the distance for this interval is 18053 bp in a strain with a wild-type promoter. DTK1819 is isogenic to DTK1798 but is heterozygous for *URA3*.

Table 1. The effect of ZMM deletions on meiotic crossing over

Strain	Relevant mutation	*HIS4-LEU2* interval				Other intervals (cM)		
		PD[a]	NPD	T	cM	*LEU2-CEN3*	*ARG4-CEN8*	*TYR7-CEN16*
HIS4 wild-type promoter								
DNY26	WT	182	10	166	32	8	9	27
DTK1152	*msh4*Δ	162	2	86	20*	4*	5*	12*
DTK1144	*msh5*Δ	310	4	134	18*	4*	5*	14*
DTK1607	*mer3*Δ	178	4	91	21*	6	7	18*
DTK1613	*spo16*Δ	151	2	96	22*	6	8	20*
his4-H10 minisatellite promoter								
DTK751	WT	374	25	306	32	8	16	28
DTK1086	*msh4*Δ	208	15	155	32	4*	6*	14*
DTK1075	*msh5*Δ	370	28	291	33	4*	6*	14*
DTK1296	*mer3*Δ	134	4	107	27	6	8*	26
DTK1297	*spo16*Δ	124	7	109	31	5*	7*	23*
his4-202 telomere promoter								
DTK1183	WT	96	11	126	41	5	12	28
DTK1223	*msh4*Δ	113	4	116	30*	4	3*	12*
DTK1707	*msh5*Δ	141	6	152	31*	5	5*	11*
his4-C48 microsatellite promoter								
DTK273	WT	266	0	53	8	9	9	28
DTK1576	*msh4*Δ	205	1	18	5	6*	3*	12*
DTK1578	*msh5*Δ	269	0	33	5	6*	6*	16*

[a]PD, parental ditype; NPD, nonparental ditype; T, tetratype. An asterisk indicates a statistically significant difference in crossovers where each mutant strain was compared to the otherwise isogenic wild-type strain (see Materials and Methods).

Table 2. The effect of ZMM deletions on *his4-lopc* segregation

Strain	Relevant mutation	4-viable spore tetrads	% (No.) of tetrads with indicated segregation patterns							**% Total *HIS4* Ab. Segregation**
			4:4	6:2	2:6	5:3	3:5	Aberrant 4:4	Other Ab. Segregation[a]	
HIS4 wild-type promoter										
DNY26	WT	437	56 (245)	6 (26)	5 (24)	14 (59)	14 (59)	2 (8)	4 (16)	**44**
DTK1152	*msh4*Δ	302	54 (164)	4 (13)	7 (20)	16 (48)	14 (42)	1 (4)	4 (11)	**46**
DTK1144	*msh5*Δ	509	53 (271)	3 (15)	3 (17)	17 (87)	16 (84)	4 (18)	3 (17)	**47**
DTK1607	*mer3*Δ	365	36 (133)	6 (23)	1 (4)	23 (83)	19 (68)	8 (29)	7 (25)	**64****
DTK1613	*spo16*Δ	319	37 (119)	5 (16)	2 (5)	20 (63)	20 (63)	10 (33)	6 (20)	**63****
his4-H10 minisatellite promoter										
DTK751	WT	866	53 (455)	5 (47)	4 (38)	16 (137)	14 (121)	3 (30)	4 (38)	**47**
DTK1086	*msh4*Δ	493	40 (199)	9 (42)	5 (24)	17 (86)	16 (77)	3 (17)	10 (48)	**60****
DTK1075	*msh5*Δ	840	41 (346)	3 (29)	3 (29)	18 (150)	21 (174)	4 (34)	9 (78)	**59****
DTK1296	*mer3*Δ	317	34 (113)	3 (11)	1 (2)	16 (51)	24 (76)	9 (27)	12 (37)	**64****
DTK1297	*spo16*Δ	307	37 (113)	7 (21)	3 (9)	19 (57)	18 (55)	4 (12)	13 (40)	**63****
his4-202 telomere promoter										
DTK1183	WT	331	32 (107)	8 (25)	5 (17)	20 (67)	14 (47)	8 (25)	13 (43)	**68**
DTK1223	*msh4*Δ	310	35 (107)	10 (31)	4 (13)	22 (69)	14 (44)	5 (14)	10 (32)	**65**
DTK1707	*msh5*Δ	367	36 (131)	4 (14)	1 (4)	19 (68)	21 (77)	8 (30)	12 (43)	**64**
his4-C48 microsatellite promoter										
DTK273	WT	337	82 (275)	3 (9)	0 (0)	11 (38)	3 (9)	0 (1)	1 (5)	**18**
DTK1576	*msh4*Δ	300	81 (242)	2 (5)	1 (2)	10 (30)	4 (12)	1 (2)	2 (7)	**19**
DTK1578	*msh5*Δ	328	82 (268)	2 (8)	0 (0)	9 (29)	5 (15)	1 (3)	2 (5)	**18**

[a]Ab. Segregation, aberrant segregation. An asterisk indicates a statistically significant difference in *HIS4* aberrant segregation where each mutant was compared to the otherwise isogenic wild-type strain (see Materials and Methods). A double asterisk indicates an extremely significant different ($p < 0.0001$).

Table 3

Table 3. The effect of *MSH4/5* deletions on crossover interference

Strain	Relevant mutation	NPD obs.	NPD exp.	Obs./exp.	Interference
HIS4 wild-type promoter					
DNY26	WT	10	15.0	.67	.33
DTK1152	*msh4*Δ	2	5.0	.40	.60
DTK1144	*msh5*Δ	4	6.4	.63	.37
his4-H10 minisatellite promoter					
DTK751	WT	25	24.8	1.01	-.01
DTK1086	*msh4*Δ	15	11.5	1.31	-.31
DTK1075	*msh5*Δ	28	22.6	1.24	-.24
his4-202 telomere promoter					
DTK1183	WT	11	15.1	.73	.27
DTK1223	*msh4*Δ	4	11.9	.34	.66
DTK1707	*msh5*Δ	6	19.9	.37	.63
his4-C48 microsatellite promoter					
DTK273	WT	0	1.2	0	1.0
DTK1576	*msh4*Δ	1	0.2	5.2	-4.2
DTK1578	*msh5*Δ	0	0.5	0	1.0

Table 4. The effect of ZMM deletions on spore viability

Strain	Relevant mutation	% of tetrads with indicated viable:inviable spore pattern					% overall viability
		4:0	3:1	2:2	1:3	0:4	
HIS4 wild-type promoter							
DNY26	WT	73	16	9	2	0.3	90
DTK1152	*msh4*Δ	60	10	16	3	12	76
DTK1144	*msh5*Δ	63	8	16	2	11	77
DTK1607	*mer3*Δ	43	19	17	8	13	66
DTK1613	*spo16*Δ	50	20	17	4	10	74
his4-H10 minisatellite promoter							
DTK751	WT	73	16	9	2	0.8	90
DTK1086	*msh4*Δ	60	16	13	3	8	79
DTK1075	*msh5*Δ	62	13	14	4	7	81
DTK1296	*mer3*Δ	41	24	18	7	10	70
DTK1297	*spo16*Δ	46	21	18	7	8	73
his4-202 telomere promoter							
DTK1183	WT	67	19	10	1	3	86
DTK1223	*msh4*Δ	58	10	17	4	11	75
DTK1707	*msh5*Δ	52	13	18	5	13	71
his4-C48 microsatellite promoter							
DTK273	WT	72	14	9	2	4	87
DTK1576	*msh4*Δ	54	13	16	5	11	73
DTK1578	*msh5*Δ	49	16	19	5	12	71

Table 5. The effect of deleting *MSH5* on meiotic crossing over between *ARG4* and *THR1*

Strain	Relevant mutation	Intervals measured in units of cM						
		ARG4-THR1	*ARG4-URA3*	*URA3-THR1*	*ARG4-CEN8*	*HIS4-LEU2*	*LEU2-CEN3*	*TYR7-CEN16*
ARG4 wild-type promoter								
DTK1835	WT	121	-	-	14	38	8	29
DTK1868	*msh5*Δ	32*	-	-	7*	22*	4*	14*
arg4-H10 minisatellite promoter								
DTK1798	WT	138	-	-	18	38	9	28
DTK1802	*msh5*Δ	157	-	-	7*	22*	5*	15*
DTK1819	5-FOA^R	121	89	7	15	35	7	31
DTK1858	5-FOA^R; *msh5*Δ	137	97	3*	8*	23*	4*	12*

An asterisk indicates a statistically significant difference in crossovers where each mutant strain was compared to the otherwise isogenic wild-type strain (see Materials and Methods).

Table 6. The effect of deleting *MSH5* on *arg4-17* segregation

Strain	Relevant mutation	4-viable spore tetrads	% (No.) of tetrads with indicated segregation patterns							**% Total *ARG4* Ab. Segregation**
			4:4	6:2	2:6	5:3	3:5	Aberrant 4:4	Other Ab. Segregation[a]	
ARG4 wild-type promoter										
DTK1835	WT	323	57 (184)	15 (50)	8 (26)	2 (6)	2 (8)	0 (0)	15 (49)	**43**
DTK1868	*msh5*Δ	343	43 (148)	21 (73)	19 (64)	2 (6)	0.6 (2)	0 (0)	15 (50)	**57***
arg4-H10 minisatellite promoter										
DTK1798	WT	359	60 (214)	17 (60)	11 (38)	2 (8)	2 (6)	0 (0)	9 (33)	**40**
DTK1802	*msh5*Δ	401	70 (281)	17 (67)	2 (10)	2 (8)	0.7 (3)	0 (0)	8 (32)	**30***
DTK1819	5-FOA^R	331	46 (153)	17 (55)	15 (49)	2 (5)	2 (7)	0 (0)	19 (62)	**54**
DTK1858	5-FOA^R; *msh5*Δ	342	57 (195)	12 (42)	8 (28)	1 (5)	0.6 (2)	0.3 (1)	20 (70)	**43***

[a]Ab. Segregation, aberrant segregation. An asterisk indicates a statistically significant difference in *ARG4* aberrant segregation where each mutant was compared to the otherwise isogenic wild-type strain (see Materials and Methods).

Chapter 4

Discussion and Future Directions

Discussion

In this study we analyzed several features of minisatellite DNA during meiosis using a yeast minisatellite model system developed by our lab, in which the minisatellite associated with the *HRAS1* proto-oncogene was inserted upstream of *HIS4* in *Saccharomyces cerevisiae* (Jauert et al. 2002, Jauert and Kirkpatrick 2005, LeClere, Jauert and Kirkpatrick *submitted,* LeClere et al. *unpublished*). Using this minisatellite model system, we were successfully able to identify three more genes whose products affect minisatellite stability and function in large loop repair (LLR) during meiosis (LeClere et al. *unpublished*), and uncovered a minisatellite-stimulated recombination phenotype associated with the *HRAS1* minisatellite (LeClere et al. *submitted*).

***RAD1*, *CSM3*, *TOF1*, and *MRC1* control minisatellite stability during meiosis:** At least two pathways exist that function to repair large loops that form within heteroduplex DNA during meiotic recombination: the *RAD1*-dependent large loop repair (LLR) pathway and an uncharacterized *RAD1*-independent LLR pathway (Kirkpatrick and Petes 1997, Kearney et al. 2001, Jauert et al. 2002). Our lab has previously shown that the *RAD1*-dependent LLR pathway controls the expansion, but not the contraction, of the *HRAS1-A1* allele when inserted upstream of the *HIS4* gene in yeast, and that these alterations are specific to meiosis (Jauert et al. 2002). In this study we identified three additional factors that control meiotic minisatellite stability: *CSM3*, *MRC1*, and *TOF1*. Deleting each of these genes significantly decreased the percent of meiotic minisatellite alterations. Specifically, *RAD1*, *CSM3*, and *TOF1* mutations significantly reduced the

percent of minisatellite length expansions, while a *MRC1* mutation significantly reduced the percent of length contractions. This matches previous research on the role of *RAD1* during LLR repair (Kirkpatrick and Petes 1997, Kearney et al. 2001, Jauert et al. 2002), and suggests that *CSM3* and *TOF1* have a similar function: to repair large loop formation by filling in the loop. These data also indicate that *MRC1* is functioning in the repair of large loops by the opposite mechanism of removing the loop. If *MRC1* does function in loop removal, then *MRC1* will be the first gene identified that functions in the loop removal LLR pathway.

Analysis of *CSM3* LLR activity in *his4-lopd* strains: When we deleted *CSM3* in strains heterozygous for the *his4-lopd* insert and compared it to a *RAD1* mutant, we observed a nearly identical shift from GC to PMS tetrads in both strains. Both mutants exhibited an increase in 3:5 and 5:3 tetrads and a decrease in 2:6 tetrads GC events, while the total percent of *HIS4* aberrant segregation remained unchanged. These data can be explained by a loss of a specific type of large loop repair that fills in the loop (which would be accomplished by nicking the strand opposite the loop and filling in the gap with DNA synthesis), rather than repair that initiates with loop removal. As shown in Figure 1 of the introduction, loss of fill-in loop repair would shift some of the 2:6 GC tetrads to 3:5 PMS tetrads when the DSB forms on the WT strand, and would shift the restored 4:4 tetrads to 5:3 tetrads when the DSB forms on the mutant strand. The expected result would be an increase in 3:5 and 5:3 tetrads, a loss of 2:6 tetrads, and no effect on 6:2 tetrads, which is exactly what was observed in the *RAD1* and *CSM3* mutants.

A double mutant analysis revealed that deleting both *CSM3* and *RAD1* exacerbated the phenotypes observed in either single mutant; the percent of PMS tetrads is almost doubled compared to either single mutant. This suggests that *CSM3*, and probably *TOF1*, does not completely fall within the known *RAD1*-dependent LLR pathway. Because the total percent of *HIS4* aberrant segregation is not significantly increased in a double mutant, it is possible that there may be some interaction between the *CSM3/TOF1* and *RAD1*-dependent LLR activities.

An expanded model for minisatellite alterations during meiosis: Our lab has previously proposed a model for meiotic minisatellite alterations that involved misalignment of repeat units during strand invasion (Jauert et al. 2002). In this model, a DSB forms adjacent to the minisatellite, and strand resection generates 3' single-stranded DNA, which then invades the homolog creating a region of heteroduplex DNA that includes the minisatellite. The repetitive minisatellite DNA can misalign, causing one or more of the repeat units to loop out of the heteroduplex region. Each repeat unit of the *HRAS1* minisatellite is 28bp in length, so a one-repeat misalignment would generate a 28bp loop. The size of this loop is well within the functional range of the *RAD1*-dependent LLR pathway (Jensen, Jauert and Kirkpatrick 2005).

The *RAD1*-dependent LLR pathway involves the *RAD1*, *RAD10*, *MSH2*, and *MSH3* genes (Kirkpatrick and Petes 1997, Kearney et al. 2001). Based on prior research and the known mitotic activities of each of these gene products, our lab favors a model where the *RAD1* and *RAD10* endonucleases generate a nick in the strand opposite of the loop, with the *MSH2* and *MSH3* proteins serving as loop-recognition factors (Jauert et al.

2002, Jensen et al. 2005). The cleaved DNA strand is filled in by DNA synthesis, generating a minisatellite length expansion (Jauert et al. 2002, Jensen et al. 2005).

This model can be expanded to incorporate the factors *CSM3*, *MRC1*, and *TOF1* (Figure 1). It is known that during mitotic growth, the products of the *CSM3*, *MRC1*, and *TOF1* genes form a heterotrimeric complex that interacts directly with the MCM helicase of the replisome, where it serves as a mediator of replication fork progression and transmits signaling for DNA repair (Calzada et al. 2005, Bando et al. 2009, Nedelcheva et al. 2005, Katou et al. 2003). During meiotic recombination, there is a stage of DNA synthesis necessary to repair the DSB using the homolog as template, and it has previously been shown to involve factors involved in DNA replication such as *POL3* (Maloisel, Bhargava and Roeder 2004, Stone et al. 2008). *CSM3*, *MRC1*, and *TOF1* have all been shown to genetically interact with *POL3* (Tong et al. 2004, Collins et al. 2007), as well as the MRX complex (*MRE11/RAD50/XRS2*), which is required for the formation and initial processing of meiotic DSBs (Borde 2007), and with *RAD51* which functions as a strand exchange factor in the early stages of meiotic recombination (Hunter 2006, Pan et al. 2006, Tong et al. 2004, Collins et al. 2007). These data along with our results suggest that the *CSM3/MRC1/TOF1* complex may form part of the DNA synthesis machinery involved in meiotic recombination, and is likely recruited to the heteroduplex intermediate.

Based on their known mitotic functions we propose that the *CSM3/TOF1/MRC1* complex localizes to heteroduplex DNA, and in the event of a minisatellite misalignment and large loop formation the complex functions as a central player that mediates how the loop is repaired (Figure 1). The type of repair that occurs appears to be different for

MRC1 than for *CSM3/TOF1*. The *CSM3* and *TOF1* gene products have been shown to co-depend on each other for proper localization (Bando et al. 2009), and is likely why both mutants exhibit similar loss of LLR activity. Our data argue that *CSM3/TOF1* are involved in the type of repair that fills-in loops and generates minisatellite length expansions, possibly by directly interacting with a helicase that opens the DNA duplex up around the region of the loop, allowing for easier access by an endonuclease such as *RAD1/10* to cleave the strand opposite the loop. Candidate helicases include *RAD3* and *RAD5*, which *CSM3* and *TOF1*, but not *MRC1*, have been shown to genetically interact with (Moriel-Carretero and Aguilera 2010, Pan et al. 2006, Tong et al. 2004). Intriguingly, our data argue that *MRC1* plays a role in the type of large loop repair that removes the loop and generates minisatellite length contractions. In the event of replication stress during mitotic growth, Mrc1p, but not Csm3p or Tof1p, is phosphorylated and recruits the sensor kinase Rad53p (Tanaka and Russell 2001, Osborn and Elledge 2003). It is possible that Mrc1p is also phosphorylated in the event of minisatellite misalignment and large loop formation, and transmits a signal that eventually recruits an as yet unidentified endonuclease to cleave the loop and generate a minisatellite length contraction (Figure 1). One candidate endonuclease is *MUS81*, which *MRC1*, but not *CSM3* or *TOF1*, has been shown to genetically interact with (Collins et al. 2007). Unfortunately, a *MUS81* mutant did not sporulate in our AS4/AS13 strain background, preventing us from determining the role of *MUS81* in minisatellite stability.

While several studies have shown that *MRC1*, *TOF1*, and *CSM3* have overlapping roles in DNA replication checkpoint activation (Nedelcheva et al. 2005, Bando et al. 2009, Calzada et al. 2005), our research is not the first to have observed a difference in

function between *MRC1* and *CSM3/TOF1*. Studies have shown that Mrc1p depends on Csm3p-Tof1p for proper localization while the reverse is not true (Bando et al. 2009), and that Csm3p-Tof1p but not Mrc1p is required for replication fork pausing at protein barriers (Calzada et al. 2005, Hodgson, Calzada and Labib 2007).

Crossovers maintained in minisatellite-spanning interval of *MSH4/5* mutants: Mutations in crossover promoting genes *MSH4* or *MSH5* usually cause a reduction of meiotic crossovers and have no significant effect on the level of aberrant segregation events at *HIS4* (Ross-Macdonald and Roeder 1994, Novak, Ross-Macdonald and Roeder 2001, Hollingsworth, Ponte and Halsey 1995). In this study we observed wild-type levels of crossing over and significant increases in aberrant segregation at the *HIS4* locus in *msh4/5*Δ yeast strains bearing the *his4-H10* minisatellite. These phenotypes were very specific to the minisatellite *HIS4* region, and were not observed in strains with a wild-type promoter or with other types of repetitive DNA. While it is possible that crossovers initiated in the vicinity of the minisatellite insert are not regulated by *MSH4* or *MSH5* and therefore not affected by mutations in these genes, we favor a model in which *MSH4* and *MSH5* inhibit recombination at the minisatellite insert as this also explains the significant increase in *HIS4* aberrant segregation we observed.

A model for minisatellite-stimulated meiotic recombination: To explain the significant increase of recombination events at the *HIS4* locus in *his4-H10 msh4/5*Δ strains, we propose a model in which *MSH4* and *MSH5* inhibit a subset of recombination events from becoming mature crossovers in the minisatellite region (Figure 2). We have

already determined that meiotic DSBs form at sites that are adjacent to or within the minisatellite insert. In our model, a meiotic DSB forms at one of these three sites on at least two of the sister chromatids. These DSBs are processed and invade the duplex DNA of the homolog, forming hetroduplex DNA. During meiosis in wild-type cells, the Msh4/5p heterodimer recognizes and binds to the Holliday junction, forming a clamp around the recombination intermediate (Pochart, Woltering and Hollingsworth 1997, Zalevsky et al. 1999, Snowden et al. 2004, Snowden et al. 2008). Msh4/5p activity stabilizes the intermediate and promotes crossover formation and also prevents processing of a neighboring DSB into a mature crossover product. Instead, the neighboring DSB is processed as a noncrossover with shorter heteroduplex formation that does not span the *his4-lopc* insert. The first DSB is processed as a crossover with much more extensive heteroduplex formation that includes the *his4-lopc* insert, which forms a large loop that is substrate for repair. The end result is a single mature crossover with one possible aberrant segregation event (Figure 2).

In a *his4-H10 MSH4* or *MSH5* mutant, the inhibition on the neighboring DSB is relieved and both strand invasion intermediates form extensive heteroduplex tracts that include the *his4-lopc* insert; there are two long heteroduplex tracts with large loops instead of one (Figure 2). Longer heteroduplex tracts increase the likelihood of both recombination intermediates being resolved as a crossover. The end result is two possible aberrant segregation events and two pro-crossover intermediates.

Having two pro-crossover intermediates form can easily explain the wild-type level of crossovers occurring at *HIS4-LEU2* in *his4-H10* mutants. Studies have shown that the loss of *MSH4/5* can cause crossover reductions of up to 50% (Ross-Macdonald

and Roeder 1994, Novak et al. 2001, Hollingsworth et al. 1995). If there are two potential crossover intermediates forming within the minisatellite-spanning interval, which is twice the normal amount, and only half of them become a mature crossover in the absence of *MSH4/5*, the result will be wild-type levels of crossovers. Following the logic of this model, we would expect to see an increase in *HIS4* aberrant segregation events, particularly in the percent of complex aberrant segregation events that indicate strand exchanges between more than two chromatids, and a wild-type level of crossovers at *HIS4-LEU2*. These predicted phenotypes are exactly what we observed in our *his4-H10 msh4/5*Δ strains. *MER3* and *SPO16* most likely function in the *MSH4/5* crossover-promoting pathway, as indicated in previous studies (Lynn, Soucek and Borner 2007, Shinohara et al. 2008, Nakagawa and Ogawa 1999, Nakagawa and Kolodner 2002), and by our recombination data.

Multiple strand exchanges occur in *arg4-H10 msh5*Δ strain: Analysis of the *arg4-H10* allele demonstrates that the crossover phenotype associated with the minisatellite in a *MSH5* mutant is not specific to the *HIS4* locus, but occurs elsewhere in the genome, despite there being a decrease in the level of *ARG4* aberrant segregation. This would not be the first difference in recombination observed between *ARG4* and *HIS4*; previous research has shown that deleting *MSH4* or *MSH5* increased *ARG4* aberrant segregation but had no effect on *HIS4* aberrant segregation (Hollingsworth et al. 1995, Ross-Macdonald and Roeder 1994), which is exactly what we observed in our wild-type promoter strains. In an *arg4-H10 msh5*Δ strain, the decrease in *ARG4* aberrant segregation is primarily due to a loss of 2:6 tetrads, representing a loss of events

involving a single strand exchange where the wild-type strand initiates recombination, while the percent of complex aberrant segregation events, which represent multiple strand exchange events, remained very high. This data is in agreement with our model; multiple strand exchanges are occurring more frequently than single strand exchanges at the *H10* insertion in *MSH5* mutants (Figure 2). In this particular case, the *ARG4* locus already exhibited high levels of multiple strand exchanges and the frequency of these events appears to not increase upon deleting *MSH5*, but is instead maintained.

Our model is supported by a recent article by Stahl and Foss (Stahl and Foss 2010), which describes two crossover pathways: an *MSH4*-dependent disjunction pathway with short conversion tracts and positive interference, and a *MSH4*-independent pairing pathway with longer conversion tracts and no interference. The loss of *MSH4* eliminates the disjunction pathway, thereby increasing the likelihood that DSB repair occurs via the pairing pathway with longer conversion tracts.

Broader implications on minisatellite-stimulated recombination, minisatellite stability, and human disease: The goal of this research was to expand our knowledge of the mechanism behind meiotic recombination driven alterations to minisatellite DNA. Minisatellite alterations during meiosis generate novel minisatellite alleles that are often associated with various types of human disease, as demonstrated by the correlation between rare alleles of the human *HRAS1* minisatellite and cancer (Krontiris et al. 1985, Krontiris et al. 1993, Krontiris 1995, Trepicchio and Krontiris 1992, Tamimi et al. 2003, Zhang et al. 2011).

This research has identified three more genes that function in meiotic large loop repair and minisatellite stability. *CSM3* and *TOF1* function in the type of large loop repair that fills-in loops, similar to the already characterized *RAD1*-dependent LLR pathway (Kirkpatrick and Petes 1997, Kearney et al. 2001, Jensen et al. 2005). In contrast, *MRC1* appears to be the first factor identified to function in the type of large loop repair that remove loops. The identification of large loop repair components is important for our understanding of factors that play a role in minisatellite stability. Furthering our understanding of how large loops are recognized and repaired during meiotic recombination will allow us to better understand the predisposition and initiation of human diseases associated with minisatellite DNA. The identification of additional factors involved in meiotic LLR gives us a new platform on which to base future research.

This research also identified intriguing interactions between repetitive minisatellite DNA and *MSH4/5*. We have demonstrated that the frequency of crossovers near the *H10* minisatellite tract at the *HIS4* and *ARG4* loci is maintained when crossover-promoters *MSH4* and *MSH5* are deleted. This phenotype is most likely due to high levels of multiple strand exchange events between homologs at the minisatellite locus in *MSH4/5* mutants (Figure 2). Because meiotic recombination is the primary driving force behind minisatellite alterations, characterizing intrinsic minisatellite factors that influence recombination activity is crucial to our understanding of genomic stability at repetitive DNA. It is unlikely that these phenotypes are novel to the *HRAS1* minisatellite. Further analysis of minisatellite-stimulated recombination is necessary to elucidate how the minisatellite contributes to hotspot activity, if other minisatellite sequences exhibit

similar recombination phenotypes, and if minisatellite-stimulated recombination is transferable to other regions of the genome as well as to other eukaryotes.

Figure 1

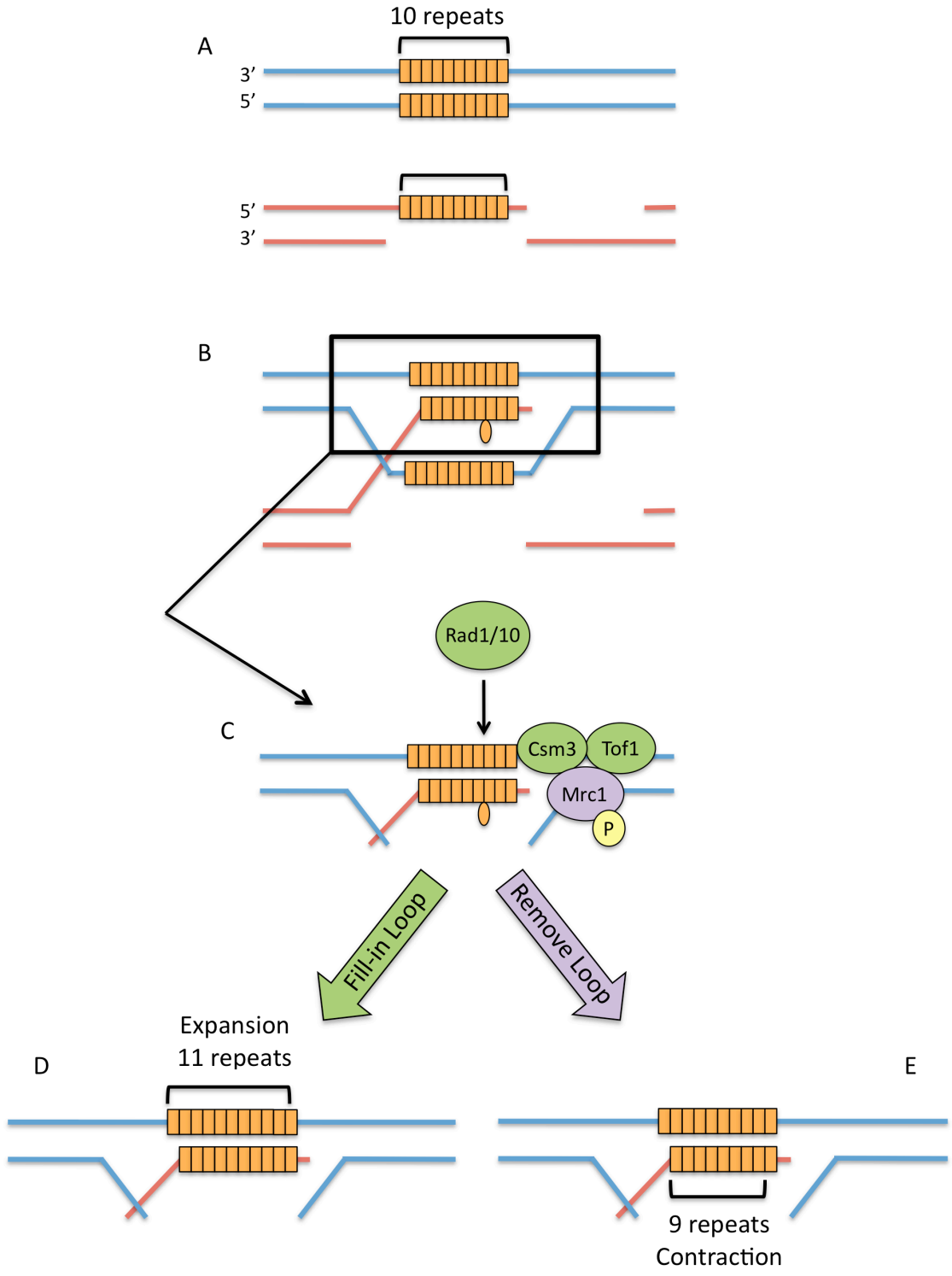
10 repeats
A
3’
5’
5’
3’
B
Rad1/10
C
Csm3
Tof1
Mrc1
P
Fill-in Loop
Remove Loop
Expansion
11 repeats
D
E
9 repeats
Contraction

Figure 1. A model for minisatellite alterations during meiosis. Shown here is a single sister chromatid of one chromosome III, in blue, and a single chromatid from the other chromosome III, in red. The *his4-H10* minisatellite is composed of 10.5 repeat units, represented here by 10 orange boxes. (A) During meiosis, a DSB forms in the region of the minisatellite, which is processed by 5' strand resection. (B) The overhanging 3' single-strand invades the duplex DNA of the homolog. Due to the repetitive nature of the minisatellite, a misalignment can occur causing one (or more) of the repeat units to form a loop. (C) The Csm3p/Tof1p/Mrc1p heterotrimeric complex localizes to the heteroduplex DNA region as part of the DNA synthesis machinery during meiotic recombination where, in the event of a minisatellite misalignment, they serve as mediators of repair. Csm3p/Tof1p function to fill-in the loop, possibly by interacting with a helicase that enables easier access for the Rad1/10 endonuclease. The endonuclease cleaves the DNA strand opposite the loop and the resulting gap is filled in, generating a minisatellite length expansion (D). In contrast, Mrc1p mediates remove loop repair. In the event of a misalignment, it is likely that Mrc1p is phosphorylated and signals the recruitment of an endonuclease to cleave the loop, generating a minisatellite length contraction (E).

Figure 2

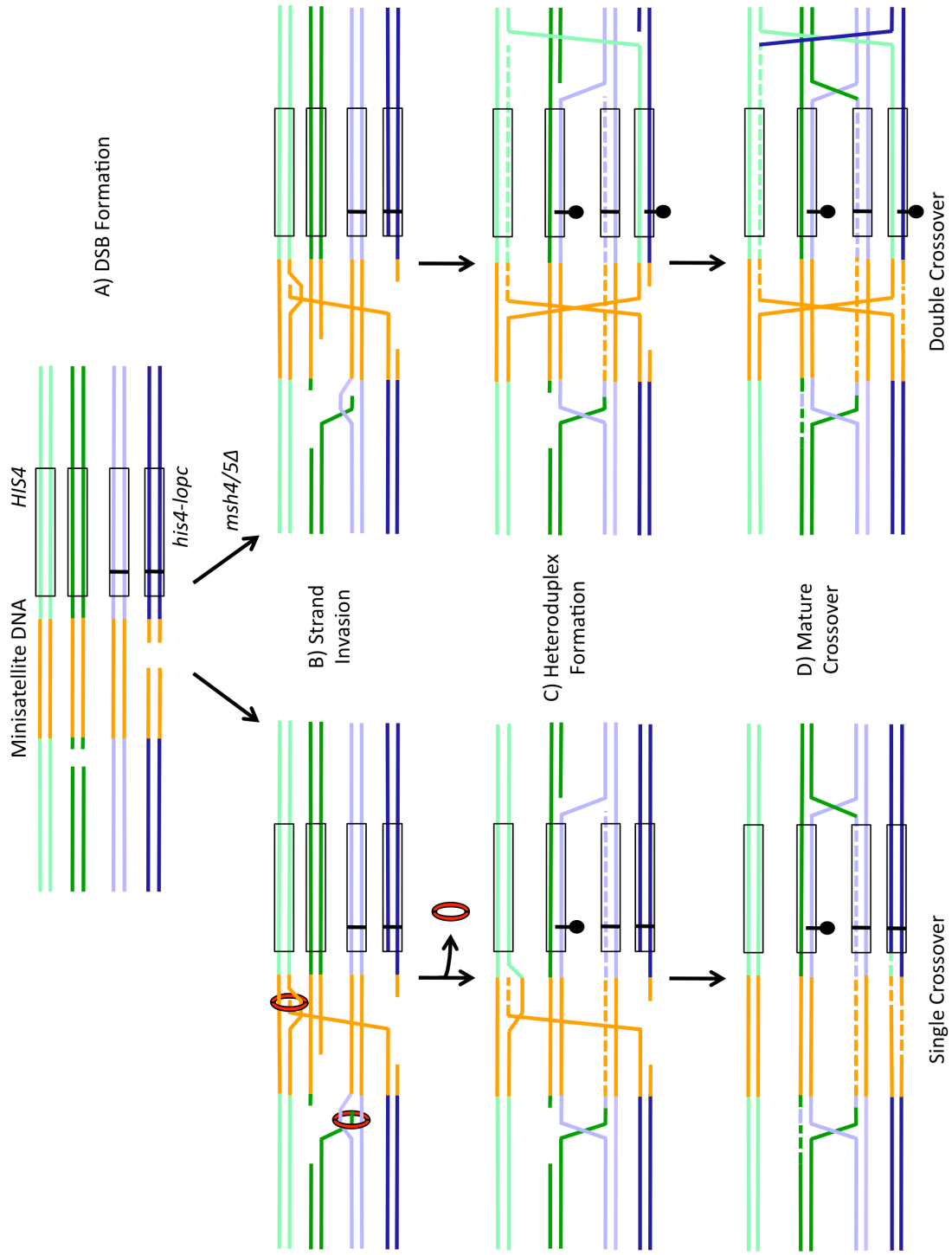
A) DSB Formation
Minisatellite DNA
HIS4
his4-lopc
msh4/5Δ
B) Strand Invasion
C) Heteroduplex Formation
D) Mature Crossover
Double Crossover
Single Crossover

Figure 2. A model for Msh4/5p inhibition of crossovers at minisatellite DNA. The *HIS4* locus in a diploid cell is shown, with paired sister chromatids in shades of green or blue. The homozygous minisatellite insertion is shown in orange. The coding region of the *HIS4* gene is indicated by the black box, and the vertical line in the blue chromatids shows the location of the *his4-lopc* insertion. (A) Double-strand breaks form adjacent to or within the minisatellite insertion. These breaks are then processed either with Msh4/5p, indicated by the red clamp (left-hand column), or without Msh4/5p (right-hand column). (B) The broken ends are processed and strand invasion occurs. (C) In the left column, one of the intermediates is processed to form a mature crossover. The presence of Msh4/5p prevents more than one intermediate from forming a crossover. In the right column, the absence of Msh4p/5p allows a second crossover intermediate to form. D) On the left, only a single mature crossover forms, as the inhibited crossover is dissolved after sufficient DNA synthesis (shown as a dashed line) to repair the initial DSB. One *his4-lopc* mismatch is formed in the heteroduplex region (as shown by the lollipop) – repair of this mismatch may lead to an aberrant segregation event (GC or PMS). On the right, both intermediates form extensive heteroduplex DNA that includes the *his4-lopc* mismatch. A mature crossover may form at either (or both) intermediate. The events normally inhibited by Msh4p/5p will be seen as an increase in aberrant segregation and the maintenance of crossover frequency.

Future Directions

The LLR pathway and minisatellite stability

LLR activity of TOF1 and MRC1: We identified *CSM3, TOF1,* and *MRC1* as three new genes that function during minisatellite stability during meiosis, and we further analyzed the role of the *CSM3* gene product in the large loop repair (LLR) pathway using strains heterozygous for *his4-lopd*. Future work should involve analyzing *his4-lopd* segregation and repair in a *MRC1* and *TOF1* mutant. Based on our observations on the effect of these mutants on minisatellite alterations, we predict that a *TOF1* mutant would exhibit the same loss of fill-in loop repair as seen in the *RAD1* or *CSM3 his4-lopd* mutants, while a *MRC1* mutant would exhibit loss of remove-loop repair.

Double mutant analysis: Analysis of a *csm3*Δ *rad1*Δ strain revealed that while both of these genes function in fill-in loop repair, *CSM3* does not fall within the known context of the *RAD1*-dependent LLR pathway. Likewise, both *MRC1* and *TOF1* mutants should be analyzed in a *rad1*Δ as well as a *csm3*Δ background to further define the pathways involved in large loop repair. Based on our minisatellite stability analysis, we predict that a *TOF1* mutant would exhibit the same loss of fill-in loop repair as seen in a *rad1*Δ or *csm3*Δ *his4-lopd* strain, and that a *csm3*Δ *tof1*Δ strain will have the same loss of large loop repair phenotypes as either single mutant, but not a *rad1*Δ *tof1*Δ strain. We predict that a *MRC1* mutant would exhibit loss of remove-loop repair, and that both a *rad1*Δ *mrc1*Δ and a *csm3*Δ *mrc1*Δ strain would exhibit significant loss of fill-in loop and remove-loop repair, distinguishing *MRC1* LLR activity from both *CSM3* and *RAD1*.

Does CSM3 based LLR repair involve helicase activity? The Csm3p/Tof1p/Mrc1p complex directly interacts with the MCM helicase during DNA replication (Calzada et al. 2005, Bando et al. 2009, Nedelcheva et al. 2005). In our model we proposed that Csm3p, and most likely Tof1p, interacts with a helicase during meiotic LLR and that this helicase opens the region of DNA around a large loop mismatch to allow easier access for the Rad1/10p endonuclease. Two possible candidates for this helicase include *RAD5* and *RAD3*, which have both been shown to genetically interact with *CSM3* and *TOF1*, but not *MRC1* (Moriel-Carretero and Aguilera 2010, Pan et al. 2006, Tong et al. 2004). Analysis of diploids bearing homozygous deletions of *RAD5* and *RAD3* will enable us to determine if these helicases are indeed involved in a meiotic LLR pathway.

Is Mrc1p phosphorylated during remove-loop LLR? MRC1 mutants exhibited loss of remove-loop repair, which distinguishes *MRC1* from all the other genes known to function in LLR (Kirkpatrick and Petes 1997, Kirkpatrick 1999). It is known that during DNA replication in S phase, in the event of replication stress Mrc1p is phosphorylated by Mec1p as part of the damage signaling process (Tanaka and Russell 2001, Osborn and Elledge 2003). In our model we hypothesized that in the event of misalignment and loop formation during meiosis, Mrc1p is phosphorylated as part of the series of events that ultimately lead to cleaving and removing the loop. To determine if Mrc1p phosphorylation is indeed required for remove-loop repair, analysis of a checkpoint-defecive *MRC1* allele should be performed. Mrc1p contains seventeen SQ and TQ motifs that are potential phosphorylation sites by Mec1p (Osborn and Elledge 2003, Kim et al. 1999); Osborn et al. constructed a *MRC1* allele, designated $mrc1^{AQ}$, where all seventeen SQ and TQ motifs have been transformed to AQ (Osborn and Elledge 2003). The $mrc1^{AQ}$

gene product has been shown to be checkpoint-defective, but can still localize and travel with the replisome (Osborn and Elledge 2003). Analysis of diploid strains homozygous for the *mrc1*^{AQ} allele will enable us to determine if phosphorylation of Mrc1p is necessary for the remove-loop LLR pathway.

Minisatellite-stimulated recombination

Does the HRAS1 minisatellite stimulate meiotic recombination at loci with low recombination activity? We have analyzed the *HRAS1* minisatellite in two different regions of the yeast genome, *HIS4* and *ARG4*. Both of these loci exhibit high endogenous levels of meiotic recombination activity, called recombination hotspots (Kirkpatrick and Petes 1997, Nicolas et al. 1989); deleting the promoter sequence significantly reduces recombination levels at both *HIS4* and *ARG4*. We have shown here that inserting the minisatellite sequence into deleted promoter regions restores recombination activity to *HIS4* and *ARG4*, and that crossover levels are maintained at the minisatellite-spanning interval in *msh4/5*Δ derivatives. To fully characterize the recombination phenotypes associated with the minisatellite, diploid strains bearing homozygous *H10* insertions at non-hotspot regions of the genome should be analyzed in parental and *msh4/5*Δ strains. Both the *LEU2* and *TRP1* genes exhibited low aberrant segregation levels throughout this study and thus make these loci excellent candidates for studying minisatellite-stimulated recombination at an area of the genome with low recombination activity.

Do other human minisatellite sequences stimulate recombination in MSH4/5 mutants? In this study we uncovered novel recombination phenotypes associated with the *HRAS1* minisatellite in *MSH4/5* mutants: 1) crossovers are maintained at wild-type levels in

HRAS1 minisatellite spanning intervals, and 2) complex aberrant segregation events, which indicate multiple strand exchanges, are either significantly increased (*HIS4* locus) or maintained at already high levels (*ARG4* locus). We also determined that these phenotypes are specific to the *HRAS1* minisatellite DNA; these phenotypes were not observed in strains bearing the *his4-202* telomere insert or the *his4-C48* microsatellite insert. It would be interesting to expand this analysis to include other types of minisatellite sequences. The insulin-linked polymorphic region (ILPR) is another highly polymorphic human minisatellite that is located 365 bp upstream of the human insulin (*INS*) gene (Bell, Selby and Rutter 1982). The ILPR minisatellite is composed of tandemly repeated arrays of a 14 bp consensus sequence, and shorter ILPR alleles have been associated with the development of human type 1 diabetes (Bell et al. 1982, Bennett et al. 1995, Kennedy, German and Rutter 1995, Adamson et al. 2007). The minisatellite found within exon III of the human Dopamine D4 Receptor Gene (*DRD4*) is composed of tandemly repeated arrays of a 48 bp consensus sequence and has been highly correlated with the development and persistence of ADHD (Smalley et al. 1998, Faraone et al. 2001, Li et al. 2006, Langley et al. 2009). Including these minisatellites in our study would enable us to determine if the recombination phenotypes associated with the *HRAS1* minisatellite are a general feature of minisatellite DNA, or if there are variations in recombination-stimulation based on different features between minisatellites, such as the size of the consensus repeat sequence. It would also allow us to determine if there are recombination-stimulation differences between minisatellites that are endogenously located outside of their associated human gene, such the *HRAS1* and ILPR minisatellites, or located within the coding region of their gene, such as the *DRD4* minisatellite.

Analyzing these minisatellites within our yeast minisatellite model system would enable us to further characterize several aspects of minisatellite-stimulated recombination.

Analysis of the recombination phenotypes associated with his4-H10 in msh4-R676W msh5-D539A mutants: Msh4p and Msh5p form a heterodimer that has pro-crossover activity by binding to Holliday junctions and stabilizing strand invasion intermediates (Snowden et al. 2004, Snowden et al. 2008). A complete null deletion of either gene, such as the mutants used in this study, leads to a loss of meiotic crossovers as well as loss of crossover interference in otherwise wild-type strains (Ross-Macdonald and Roeder 1994, Novak et al. 2001, Hollingsworth et al. 1995). Recent research from the Alani lab has characterized novel *MSH4* and *MSH5* alleles bearing non-null mutations (Nishant et al. 2010). Two of the alleles identified in this study, *msh4-R676W* and *msh5-D539A*, are capable of forming stable Msh4p-Msh5p complexes and binding to chromatin; intriguingly, strains bearing these alleles exhibited wild-type spore viability and crossover interference despite a loss of crossovers on all chromosomes examined (Nishant et al. 2010). In our model on minisatellite-stimulated recombination, we proposed that multiple strand exchanges occur at the minisatellite region in *msh4/5*Δ strains. Our model can be tested using the *msh4-R676W* and *msh5-D539A* mutants. Because the gene products of these alleles are capable of implementing crossover interference, then multiple strand exchanges should not occur in their presence. According to our model, we predict that strains bearing homozygous *msh4-R676W msh5-D539A* mutants in the *his4-H10* background will exhibit a loss of crossovers at the minisatellite-spanning interval because multiple strand exchanges cannot occur in these mutants and two pro-crossover intermediates will not form. It is quite possible that there

would only be a mild loss of crossovers at the *HIS4-LEU2* minisatellite-spanning interval, as the *msh4-R676W* and *msh5-D539A* mutations exhibited a weaker crossover loss on smaller chromosomes, and the *HIS4*-containing chromosome III is one of the smallest in the *S. cerevisiae* genome. If this is the case, analysis of *HIS4* aberrant segregation and of *msh4-R676W msh5-D539A* mutations in the *arg4-H10* background can be performed since the *ARG4*-containing chromosome VIII is larger than chromosome III. In summary, analyzing these mutants in our minisatellite model system will enable us to test our model and determine if multiple strand exchanges occur and account for the wild-type levels of crossovers at the minisatellite locus in *MSH4/5* mutants.

Materials and Methods

Strain Construction: All strains are isogenic derivatives of either AS4 or AS13. See Table 1 for the complete list of all haploid strains used. See Table 2 for the complete list of primers used during strain construction.

The *his4-H10* minisatellite allele (Jauert and Kirkpatrick 2005) was derived from DTK314 (Jauert et al. 2002) (which contains the 30-repeat *his4-A1* allele of the *HRAS1* human minisatellite tract) as a naturally occurring tract reduction during meiosis that was cloned by PCR from the original spore colony. The *his4-202* allele is a 51 bp sequence of telomeric DNA containing three copies of the *RAP1* protein binding site (White, Dominska and Petes 1993). The *his4-C48* and *his4-C12* alleles consist of 48 and 12 copies, respectively, of a 5 bp degenerate repeat with the first three nucleotides consisting of two cytosines followed by a guanine, while the last two nucleotides are random (Kirkpatrick et al. 1999). The *his4-H10, his4-202*, *his4-C48*, and *his4-C12* sequences were inserted into *his4-*Δ*52* strains at the site of the deleted promoter sequences upstream of *HIS4* (White et al. 1993, Kirkpatrick et al. 1999, Jauert and Kirkpatrick 2005). The *his4-lopc* and *his4-lopd* alleles were inserted into the AS13-derived haploids (Jauert et al. 2002).

Unless otherwise specified, all strains carrying gene deletions were constructed by one-step transformations using PCR products with 5' and 3' sequence homology flanking the target gene and an internal sequence of the *KANMX4* cassette encoding geneticin resistance; transformants were selected on YPD+G418 media (Jauert, Jensen and Kirkpatrick 2005). Strain construction was confirmed by PCR analysis using primers

external to the *KANMX4* insertion. The *rad50S* derivatives were constructed by one-step transformations using an *Eco*RI and *Bam*HI treated pNKY349 fragment (Fan, Xu and Petes 1995); transformants were selected on SD-Ura media, analyzed for MMS sensitivity on 0.02% MMS YPD media, and verified by sequencing. *URA3-H10-HIS4* strains were constructed by inserting *URA3* at a *Spe*1 site 3693bp downstream of *HIS4* by one-step transformation using PCR products that included the *URA3* gene +400bp flanking DNA from template pMW33 (White and Petes 1994) using primers lsb5+158F and lsb5+825R; transformants were selected on SD-Ura media and verified by PCR.

Construction of the *arg4-H10* locus in DTK1787 was accomplished by linking the *H10* minisatellite allele to the *URA3* marker (Figure 1). *URA3* was amplified from pRS316 using forward primer arg4-374F pRS-F and reverse primer Ras 5'RC pRS-R. The *H10* minisatellite allele was amplified from purified DTK750a DNA using forward primer pRS-R-RC Ras 5' and reverse primer arg4-130-RC Ras 3'. The *URA3* and *H10* PCR products were gel purified, and a PCR was performed to link the two fragments using forward primer arg4-375F and reverse primer arg4-135R. The *URA3-H10* construct was inserted into the promoter region of *ARG4* by one-step transformation, replacing the promoter sequence between 315 and 180bp upstream of *ARG4*, leaving the TATA box intact; transformants were selected on SD-Ura media and verified by PCR (Figure 2) and sequence analysis. DTK1796 was constructed by one-step transformation using an *URA3-H10* fragment that was PCR amplified from DTK1787 using primers arg4-517F and arg4-85R; transformants were selected on SD-Ura media and verified by PCR (Figure M2) and sequence analysis.

DTK1797 was constructed by deleting *THR1* in DTK1787 by one-step

transformation using PCR products with 5' and 3' sequence homology flanking the *THR1* locus and an internal sequence of the *NATMX* gene encoding nourseothricin resistance (Goldstein and McCusker 1999), using p4339 as a template (Tong et al. 2001) and primers thr1:NAT F and thr1:NAT R; transformants were selected on YPD+NAT media and verified by PCR. DTK1816 was constructed by spotting overnight cultures of DTK1796 onto 5-FOA media and isolating independent 5-FOA^R colonies. Isolates were confirmed by analyzing growth on SD-Ura and 5-FOA media, and PCR reactions B and C (Figure 2) were performed to ensure the *H10* allele had not altered during transformation. DTK1867 was constructed by one-step transformation using PCR products with 5' and 3' sequence homology flanking the *MSH5* locus and an internal sequence of the *URA3* gene that was amplified from pRS316 using primers msh5/prsF and msh5/prsR; transformants were selected on SD-URA media and verified by PCR.

Diploid strains generated: All haploid strains are listed in Table 1. All diploid strains used were constructed by the following crosses: DTK751 (DTK608 X DTK750), DTK1086 (DTK1083 X DTK1084), DTK1075 (DTK1063 X DTK1064), DTK1296 (DTK1284 X DTK1286), DTK1297 (DTK1285 X DTK1287), DNY26 (AS4 X DNY25), DTK1152 (DTK247 X DTK1139), DTK1144 (DTK1140 X DTK1141), DTK1607 (DTK1605 X DTK1606), DTK1613 (DTK1610 X DTK1611), DTK1183 (MW72 X MW73), DTK1223 (DTK1221 X DTK1222), DTK1707 (DTK1703 X DTK1704), DTK1339 (DTK1333 X DTK1334), DTK1341 (DTK1335 X DTK1336), DTK273 (DTK227 X DTK255), DTK1576 (DTK1568 X DTK1569), DTK1578 (DTK1570 X DTK1571), DTK1655 (AS4 X DTK1651), DTK1656 (DTK750 X DTK1652), DTK1669

(DTK1064 X DTK1653), DTK1670 (DTK1141 X DTK1654), DTK1798 (DTK1796 X DTK1797), DTK1802 (DTK1800 X DTK1800), DTK1819 (DTK1816 X DTK1797), DTK1835 (DTK1834 X AS4), DTK1858 (DTK1801 X DTK1857), DTK1868 (DTK1141 X DTK1867), DTK802 (DTK669 x DTK796), DTK1459 (DTK1451 x DTK1452), DTK1684 (DTK1679 x DTK1680), DTK1685 (DTK1681 x DTK1682), DTK1460 (DTK1454 x DTK1453), DTK1487 (DTK1462 x DTK1461), DTK1567 (DTK1566 x DTKDTK1565), DTK1480 (DTK1470 x DTK1469), DNY27k (DNY24 x AS4), DTK1667 (DTK1659 x DTK1660), DTK1731 (DTK221 x DTK225), DTK1785 (DTK1782 x DTK1783), DTK314 (DTK288 x DTK305), DTK508 (DTK506 x DTK507), and DTK1724 (DTK1661 x DTK1662).

Southern blot analysis of Chromosome VIII: Standard Southern analysis was performed using labeled digoxigenin PCR products as probes (Jauert et al. 2002). Labeling was done using PCR DIG Labeling Mix (Roche). Probe 1 was constructed using primers arg4+50F and arg4+322R, and probe 2 was constructed using primers thr1-725F and thr1-260R (Table 2). Strains were inoculated in overnight cultures of liquid YPD. DNA was purified, and 18μg of DNA was treated with *Mlu*1 and *Bgl*1. Nine micrograms of each sample were loaded into lanes 1 - 6 and the remaining 9μg were loaded into lanes 7 - 12 of a 0.8% agarose gel. The blot was cut in half. Lanes 1 - 6 were exposed to probe 1 and lanes 7 - 12 were exposed to probe 2.

Sporulation and tetrad dissection protocols: Standard sporulation (spo) media was used (Guthrie and Fink 1991, Jauert et al. 2002). To sporulate strains, a single diploid

colony was inoculated overnight in 5 mL of liquid YPD at 30 °C. The following morning the culture was pelleted, rinsed twice in 5 mL of sterile dH_20, and plated to spo media at 18°C for three days. *MER3* and *SPO16* mutants were incubated on spo media for 5 days due to low sporulation levels. To tetrad dissect, a sample of the culture was scraped from the spo media and incubated for 10 minutes at room temperature in 100 uL of tetrad dissecting solution (1 mL solution of 200 mM Tris/20 mM EDTA with 3.5 uL betamercaptoethanol added). Cells were pelleted and resuspended in a solution of 100 uL of sterile dH_20 with 6 uL of glusulase and incubated at room temperature for 10 minutes. Cells were spread across thin YPD plates and left for 20 minutes at room temperature. Tetrads were dissected using a Nikon ECLIPSE E400 microscope and placed at 30°C for 3-4 days to allow spore colony growth. Tetrad dissection of all diploids heterozygous for *THR1* required coating the thin YPD plates with 100 uL of sterile threonine solution (0.2g L-Threonine/3 mL of sterile dH_20).

Aberrant segregation analysis: Heterozygous marker segregation analysis was performed by replica plating the original tetrad dissection plate onto appropriate synthetic dropout media (Guthrie and Fink 1991, Jauert et al. 2002), and growing overnight at 30°C. For *THR1* heterozygous diploid strains, all replica plates were coated with 100 uL of threonine solution with the exception of SD-Arg and SD-Thr media. Marker segregation is described using the nomenclature of the eight-spored fungi where a tetrad exhibiting a Mendelian segregation event is described as 4 His^+: 4 His^- (or 4 Arg^+: 4 Arg^-), while deviations from Mendelian segregation (aberrant segregation) events include gene conversions (6:2 or 2:6) and post-meiotic segregation (PMS) events (5:3 and

3:5) among other aberrant segregations including: deviant 3:5, deviant 5:3, deviant 4:4, 1:7, 7:1, 0:8, and 8:0, which indicate a complex recombination event involving three or four sister chromatids. The overall aberrant segregation percent consists of the total number of tetrads exhibiting an aberrant segregation phenotype divided by the total number of tetrads. A minimum of 300 tetrads per strain was scored for segregation analysis.

Minisatellite tract-length analysis: Whole-cell PCR was performed on spore colonies to analyze the minisatellite tract length in four-spore tetrads. A sample was picked from each colony and suspended in 6 uL of sterile dH_20, boiled at 94°C for 6 minutes, and immediately placed at -80°C for a minimum of 5 minutes. The following 50 µl reaction was used to amplify the *his4-H10* allele: 5 µl 10X PCR buffer (Sigma P-2317), 7.5 µl 25 mM $MgCl_2$ (Sigma M-8787), 7.5 µl of 1.25 mM dNTPs, 1.25 µl each of 10 mM Ras 3' and 5' primers (Jauert et al. 2002), 2 µl *Taq* polymerase, and 19.5 µl of sterile dH_2O for a total of 44 µl, which was added to the 6 µl of H_2O containing DNA. Reagents were identical but the following volumes were changed for the *his4-A1* allele: 3.75 µl 25 mM $MgCl_2$, 8.3 µl of 1.25 mM dNTPs, and 22.45 µl of dH_2O. PCR was performed in a Hybaid PCR Express machine using the following parameters: 1 cycle of 94°C for 1 min; 30 cycles of 92°C for 1 min, 58°C for 45 s, and 72°C for 1 min for the *H10* allele or 2 min for the *A1* allele; 72°C for 10 min; and then held at 4°C. A minimum of 200 tetrads per strain was examined for tract-length alterations.

Southern blot analysis of meiotic DSBs: Strains were sporulated in liquid 1% potassium acetate at 26°C and samples taken at 0 and 24 hour time points (Fan et al. 1995). DNA was purified and 10 μg of DNA was treated with *Bgl*II and separated on a 0.8% agarose gel (Fan et al. 1995, Jauert et al. 2002). Standard Southern analysis was performed using a labeled digoxigenin PCR product as a probe. The probe was constructed using pDN42 as a template and primers his4+142F and his4+442R (Table 2). Labeling was done using PCR DIG Labeling Mix (Roche). Densitometry was determined using ImageJ software.

Mathematical analyses: Instat 1.12 (GraphPad) for Macintosh was used to calculate statistical significance. To compare aberrant segregation, the Fisher's Exact version of the χ^2 test was performed using the number of tetrads with an aberrant segregation and the number of tetrads with Mendelian segregation. To compare minisatellite tract-length alterations, a Fisher's Exact version of the χ^2 test was performed using the number of tetrads with a minisatellite alteration and the number of tetrads with no alteration. Results are considered statistically significant if $p \leq 0.05$.

Crossover frequencies were calculated using the Perkins equation (Perkins 1949). Interference was calculated using the Papazian equation (Papazian 1952), where the expected NPD frequency = ½ $[1\text{-fT-}(1\text{-}3\text{fT}/2)^{2/3}]$ and fT is the tetratype frequency.

To compare crossover frequencies for the *HIS4-LEU2, ARG4-CEN8, LEU2-CEN3,* and *TYR7-CEN16*, a contingency χ^2 test was performed using the number of nonrecombinant and recombinant tetrads. For the *HIS4-LEU2* interval, the number of nonrecombinants = PD – NPD + ½(T – 2NPD) and the number of recombinants = 4NPD + ½(T – 2NPD) (Chua and Roeder 1997). For the *ARG4-CEN8, LEU2-CEN3,* and *TYR7-*

CEN16 intervals, the number of recombinants = T and the number of nonrecombinants = PD + NPD.

To compare crossover frequencies for the *ARG4-THR1, ARG4-URA3,* and *URA3-THR1* intervals, the standard error of the variance between the mutant and wild-type strains was calculated. A change in crossover frequencies was considered significantly different if the absolute value of the difference between the intervals being compared was greater than twice the standard error (if $| X_1 - X_2 | > 2$*S.E.), where X_1 and X_2 are the intervals in Morgans. For each interval, X = (fT/2) + (3fN), where fT is the tetratype frequency and fN is the nonparental ditype frequency. The standard error (S.E.) of the variance between intervals was calculated by the following equations: S.E. = sqrt(Var[X_1-X_2]); Var[X_1-X_2] = Var[X_1] + Var[X_2]; Var[X] = 0.25*Var[fT] + 9*Var[fN] + 3*Cov[fT,fN]; Var[fT] = (fT)(1-fT)/n; Var[fN] = (fN)(1-fN)/n; Cov[fT,fN] = -(fT)(fN)/n, where n is the total number of tetrads. For a more streamlined calculation of these equations see the Stahl Lab Online Tools website (http://molbio.uoregon.edu/~fstahl). Analysis of the *HIS4-LEU2* interval was performed using these equations as a control.

Table 1

Table 1. Complete list of haploid strains

Strain	*HIS4* promoter	*HIS4* sequence	Introduced mutation	Parental strain	Source
Mata:					
AS4	WT[a]	WT	*trp1-1*; *tyr7-1*; *arg4-17*; *ade6*; *ura3*		Stapleton and Petes 1991
DTK247	WT	WT	*msh4Δ::KANMX4*	AS4	Kearney *et al.* 2001
DTK1141	WT	WT	*msh5Δ::KANMX4*	AS4	this study
DTK1605	WT	WT	*mer3Δ::KANMX4*	AS4	this study
DTK1611	WT	WT	*spo16Δ::KANMX4*	AS4	this study
DTK1640	WT	WT	*pch2Δ::KANMX4*	AS4	this study
DTK1746	WT	WT	*mus81Δ::KANMX4*	AS4	this study
DTK1758	WT	WT	*mms4Δ::KANMX4*	AS4	this study
DTK225	WT	WT	*rad1Δ*	AS4	Kirkpatrick and Petes 1997
DTK1659	WT	WT	*csm3Δ::KANMX4*	AS4	this study
DTK1783	WT	WT	*rad1Δ*; *csm3Δ::KANMX4*	DTK225	this study
PD63	*his4-Δ52*	WT	WT	AS4	Detloff, White and Petes 1992
DTK750	*his4-H10*	WT	WT	PD63	Jauert and Kirkpatrick 2005
DTK796	*his4-H10*	WT	*rad1Δ*	DTK750	Jauert and Kirkpatrick 2005
DTK1084*	*his4-H10*	WT	*msh4Δ::KANMX4*	DTK750	this study
DTK1064*	*his4-H10*	WT	*msh5Δ::KANMX4*	DTK750	this study
DTK1286	*his4-H10*	WT	*mer3Δ::KANMX4*	DTK750	this study
DTK1287	*his4-H10*	WT	*spo16Δ::KANMX4*	DTK750	this study
DTK1334	*his4-H10*	WT	*rad50S*	DTK750	this study
DTK1336	*his4-H10*	WT	*rad50s*; *msh5Δ::KANMX4*	DTK1064	this study
DTK1450	*his4-H10*	WT	*rdh54Δ::KANMX4*	DTK750	this study
DTK1452	*his4-H10*	WT	*csm3Δ::KANMX4*	DTK750	this study
DTK1454	*his4-H10*	WT	*slx1Δ::KANMX4*	DTK750	this study
DTK1462	*his4-H10*	WT	*slx4Δ::KANMX4*	DTK750	this study
DTK1470	*his4-H10*	WT	*ubx7Δ::KANMX4*	DTK750	this study
DTK1566	*his4-H10*	WT	*mlh3Δ::KANMX4*	DTK750	this study
DTK1638	*his4-H10*	WT	*pch2Δ::KANMX4*	DTK750	this study
DTK1680	*his4-H10*	WT	*mre1Δ::KANMX4*	DTK750	this study

Table 1 continued

DTK1682	*his4-H10*	WT	*tof1Δ::KANMX4*	DTK750	this study
DTK1745	*his4-H10*	WT	*mus81Δ::KANMX4*	DTK750	this study
DTK1757	*his4-H10*	WT	*mms4Δ::KANMX4*	DTK750	this study
MW73	*his4-202*	WT	WT	PD63	White *et al.* 1993
DTK1222	*his4-202*	WT	*msh4Δ::KANMX4*	MW73	this study
DTK1704	*his4-202*	WT	*msh5Δ::KANMX4*	MW73	this study
DTK227	*his4-C48*	WT	WT	PD63	Kirkpatrick *et al.*1999
DTK1568	*his4-C48*	WT	*msh4Δ::KANMX4*	DTK227	this study
DTK1570	*his4-C48*	WT	*msh5Δ::KANMX4*	DTK227	this study
DTK345	*his4-C12*	WT	WT	PD63	Kirkpatrick *et al.* 1999
DTK1573	*his4-C12*	WT	*msh4Δ::KANMX4*	DTK345	this study
DTK1575	*his4-C12*	WT	*msh5Δ::KANMX4*	DTK345	this study
DTK288	*his4-A1*	WT	WT	PD63	Jauert *et al.* 2002
DTK506	*his4-A1*	WT	*rad1Δ*	DTK288	Jauert *et al.* 2002
DTK1662	*his4-A1*	WT	*csm3Δ::KANMX4*	DTK288	this study
*Mat**a***:					
AS13	WT	WT	*leu2-3*; *ade6*; *ura3*; *rme1*		Stapleton and Petes 1991
DNY25	WT	*his4-lopc*	WT	AS13	Nag, White and Petes 1989
DTK1139	WT	*his4-lopc*	*msh4Δ::KANMX4*	DNY25	this study
DTK1140	WT	*his4-lopc*	*msh5Δ::KANMX4*	DNY25	this study
DTK1606	WT	*his4-lopc*	*mer3Δ::KANMX4*	DNY25	this study
DTK1610	WT	*his4-lopc*	*spo16Δ::KANMX4*	DNY25	this study
DTK1641	WT	*his4-lopc*	*pch2Δ::KANMX4*	DNY25	this study
DTK1747	WT	*his4-lopc*	*mus81Δ::KANMX4*	DNY25	this study
DTK1759	WT	*his4-lopc*	*mms4Δ::KANMX4*	DNY25	this study
DTK1651*	WT	*his4-lopc*	*URA3-H10-HIS4*	DNY25	this study
DTK1654*	WT	*his4-lopc*	*URA3-H10-HIS4*	DTK1140	this study
DNY24	WT	*his4-lopd*	WT	AS13	Nag, White and Petes 1989
DTK221	WT	*his4-lopd*	*rad1Δ*	DNY24	Kirkpatrick and Petes 1997
DTK1660	WT	*his4-lopd*	*csm3Δ::KANMX4*	DNY24	this study
DTK1782	WT	*his4-lopd*	*rad1Δ*; *csm3Δ::KANMX4*	DTK221	this study

Table 1 continued

PD57	*his4-Δ52*	WT	WT	AS13	Detloff, White and Petes 1992
PD80	*his4-Δ52*	*his4-lopc*	WT	AS13	Detloff, White and Petes 1992
DTK608	*his4-H10*	*his4-lopc*	WT	PD80	Jauert and Kirkpatrick 2005
DTK669	*his4-H10*	*his4-lopc*	*rad1Δ*	DTK608	Jauert and Kirkpatrick 2005
DTK1083*	*his4-H10*	*his4-lopc*	*msh4Δ::KANMX4*	DTK608	this study
DTK1063*	*his4-H10*	*his4-lopc*	*msh5Δ::KANMX4*	DTK608	this study
DTK1284	*his4-H10*	*his4-lopc*	*mer3Δ::KANMX4*	DTK608	this study
DTK1285	*his4-H10*	*his4-lopc*	*spo16Δ::KANMX4*	DTK608	this study
DTK1449	*his4-H10*	*his4-lopc*	*rdh54Δ::KANMX4*	DTK608	this study
DTK1639	*his4-H10*	*his4-lopc*	*pch2Δ::KANMX4*	DTK608	this study
DTK1652*	*his4-H10*	*his4-lopc*	*URA3-H10-HIS4*	DTK608	this study
DTK1333	*his4-H10*	*his4-lopc*	*rad50S*	DTK608	this study
DTK1335	*his4-H10*	*his4-lopc*	*rad50s; msh5Δ::KANMX4*	DTK1063	this study
DTK1653*	*his4-H10*	*his4-lopc*	*URA3-H10-HIS4*	DTK1063	this study
DTK1451	*his4-H10*	*his4-lopc*	*csm3Δ::KANMX4*	DTK608	this study
DTK1453	*his4-H10*	*his4-lopc*	*slx1Δ::KANMX4*	DTK608	this study
DTK1461	*his4-H10*	*his4-lopc*	*slx4Δ::KANMX4*	DTK608	this study
DTK1469	*his4-H10*	*his4-lopc*	*ubx7Δ::KANMX4*	DTK608	this study
DTK1565	*his4-H10*	*his4-lopc*	*mlh3Δ::KANMX4*	DTK608	this study
DTK1679	*his4-H10*	*his4-lopc*	*mrc1Δ::KANMX4*	DTK608	this study
DTK1681	*his4-H10*	*his4-lopc*	*tof1Δ::KANMX4*	DTK608	this study
DTK1744	*his4-H10*	*his4-lopc*	*mus81Δ::KANMX4*	DTK608	this study
DTK1756	*his4-H10*	*his4-lopc*	*mms4Δ::KANMX4*	DTK608	this study
MW68	*his4-202*	WT	WT	PD57	White *et al.* 1993
MW72	*his4-202*	*his4-lopc*	WT	MW68	White *et al.* 1993
DTK1221	*his4-202*	*his4-lopc*	*msh4Δ::KANMX4*	MW72	this study
DTK1703	*his4-202*	*his4-lopc*	*msh5Δ::KANMX4*	MW72	this study
DTK255	*his4-C48*	*his4-lopc*	WT	PD80	Kirkpatrick *et al.*1999
DTK1569	*his4-C48*	*his4-lopc*	*msh4Δ::KANMX4*	DTK255	this study
DTK1571	*his4-C48*	*his4-lopc*	*msh5Δ::KANMX4*	DTK255	this study
DTK344	*his4-C12*	*his4-lopc*	WT	PD80	Kirkpatrick *et al.*1999
DTK1572	*his4-C12*	*his4-lopc*	*msh4Δ::KANMX4*	DTK344	this study

Table 1 continued

DTK1574	*his4-C12*	*his4-lopc*	*msh5Δ::KANMX4*	DTK344	this study
DTK294	*his4-A1*	WT	WT	PD57	Jauert *et al.* 2002
DTK305	*his4-A1*	*his4-lopc*	WT	DTK294	Jauert *et al.* 2002
DTK507	*his4-A1*	*his4-lopc*	*rad1Δ*	DTK305	Jauert *et al.* 2002
DTK1661	*his4-A1*	*his4-lopc*	*csm3Δ::KANMX4*	DTK305	this study
Strain	*ARG4* promoter	*ARG4* sequence	Introduced mutation	Parental strain	Source
*Mat**a***:					
DTK1796	*arg4-H10*	*arg4-17*	WT	AS4	this study
DTK1800	*arg4-H10*	*arg4-17*	*msh5Δ::KANMX4*	DTK1796	this study
DTK1816	*arg4-H10*	*arg4-17*	5-FOA^{R}	DTK1796	this study
DTK1857	*arg4-H10*	*arg4-17*	*msh5Δ::KANMX4*	DTK1816	this study
*Mat**α***:					
DTK1834*	WT	WT	*thr1Δ::KANMX4*	DNY25	this study
DTK1867*	WT	WT	*msh5Δ::URA3*	DTK1834	this study
DTK1787	*arg4-H10*	WT	WT	DNY25	this study
DTK1797*	*arg4-H10*	WT	*thr1Δ::NATMX*	DTK1787	this study
DTK1801	*arg4-H10*	WT	*thr1Δ::NATMX*; *msh5Δ::KANMX4*	DTK1797	this study

*Constructed by Peter Jauert.

Table 2

Table 2. List of primers used		
Oligo	Sequence	Note
Ras 5’	CCCTGAGGTTGGGGGAGAGC	Used for *H10* and *A1* minisatellite length analysis
Ras 3’	GGGCTCCTGGCCTCGGGAAG	
KANMX4+17R	GTCTTTTCCTTACCCATG	Internal reverse primer of the *KANMX4* gene, used to verify gene deletions
msh4-140F	TCCCGAACGTACAGCTTTCA	Used to delete *MSH4* with *KANMX4*
msh4+2883R	ATGGGGCCAAGCAGTGATTAGA	
msh4-373F	GCGACTGTTAATCGCAAGATCGTG	Used to verify gene deletion
msh4+3289R	TTGGCTTGCCAACGAACGTACA	
msh5-270F	TCAGCTCGAGACATGGCA	Used to delete *MSH5* with *KANMX4*
msh5+2962R	ACTCAAGTCGGTTCGTGCAGTT	
msh5-499F	TCTGGGCCAAAATCAGTGGTCTCT	Used to verify gene deletion
msh5+3125R	GGGAAGGAAAATTGGCGGAATTGG	
mer3-155F	CATGTACCACGAATGGATGCAG	Used to delete *MER3* with *KANMX4*
mer3+3977R	GCTTATCGCGGTCATGTGACTA	
mer3-332F	ATCCAATTGAACCCCGACGTCATC	Used to verify gene deletion
mer3+3980R	ATCGCTTATCGCGGTCATGTGACT	
spo16-114F	GCTTACCCTGTTAACGCGTGAA	Used to delete *SPO16* with *KANMX4*
spo16+885R	GGCTGGTATCACCATGCTCATT	
spo16-310F	GCTGCTCAAACAGAACTCATGTGC	Used to verify gene deletion
spo16+1113R	CAATGAATCGGCGAAGACAGGAGA	
slx1-264F	TGCCAGTTTCCCTGATGCTGTA	Used to delete *SLX1* with *KANMX4*
slx1+1143R	ATGCCCCTCCAACAGCCAATTT	
slx1-460F	CATCCGCGATTTTCTCTCGTTCCA	Used to verify gene deletion
slx1+1279R	CCCGAGAATTTGACAGGCATTCAC	
slx4-84F	TGAATGGAACTCCGAACAAGCAAG	Used to delete *SLX4* with *KANMX4*
slx4+2500R	GACCGGCGTCTCAACTAAACTCAA	
slx4-359F	GAAACAGAGGCCAACATGCCTT	Used to verify gene deletion
slx4++2747R	GCCCTGTGTGAATTGGGAGAAACT	
mlh3-143F	TTATTTGCGAGCGCCACGAGAA	Used to delete *MLH3* with *KANMX4*
mlh3+2488R	CGCCCCATTTAGTTTGCCTAACCT	
mlh3+274F	GCGCAAATTCAACCCCATTGATAC	Used to verify gene deletion
mlh3+2720R	AGTCCAGCGCCCAGAAACTT	
ubx7-73F	TAAAAGGGAGCTGGGTTGAGGTTG	Used to delete *UBX7* with *KANMX4*
ubx7+1579R	TCTCACTCATTGCTCCTGTTTCGC	
ubx7-248F	TAAAGGTGACACCTGCGAGAGACT	Used to verify gene deletion
ubx7+1833R	ATCAGCCATGGGAACAAGCTTGTC	
csm3-296F	CGCCACGGCTAACTCCAAACATAA	Used to delete *CSM3* with *KANMX4*
csm3+1061R	ACACTCGAACCAGGCTCTTTCTAC	
csm3-401F	TGAGGCCGAAAGCAGAAGTGTT	Used to verify gene deletion
csm3+1190R	TGCTATTTGGCATCCGAGGGAA	
mrc1-121F	GCGTAAAACGCGTTTGCTTC	Used to delete *MRC1* with *KANMX4*
mrc1+3380R	CTAGACTCGGGTGCCATCTTTT	
mrc1-157F	CTTATCCTTCTTCGACGCGTCAT	Used to verify gene deletion
mrc1+3542R	TGCCTCCTTTACCTAACCTACTC	
tof1-46F	CTAGCTTGTGGGGTTTAGTG	Used to delete *TOF1* with *KANMX4*
tof1+3899R	GTCCTAATGGACATTTGAGTTCCT	

Table 2 continued

tof1-156F	TGACGCGTTTACTGCCGCATTA	Used to verify gene deletion
tof1+3987R	TAGCGGATTGCATGCGTCTTCA	
mms4-249F	CCTTTGCTGGTTGCTTGTGA	Used to delete *MMS4* with *KANMX4*
mms4+2153R	GGGGAAATAGAGCTGCAGTGAT	
mms4-381F	CCTACACAAGTTACGGCAAATC	Used to verify gene deletion
mms4+2368R	CGAGCCTCTAAAGGACAGACT	
mus81-131F	CTTGCTTTGCCTATTCGCGTCATC	Used to delete *MUS81* with *KANMX4*
mus81+2039R	GCGCGTTTCAGATATGCTTCTGGT	
mus81-175F	ATTAGATATCTGCCTTCCCCTGTA	Used to verify gene deletion
mus81+2140R	CTGGAAGAGGTTGGAAGGGTTT	
arg4-374F pRS-F	TATAACAATAAATGGTTGGCGCAGG CAATTAATTTTTCTTTACTCTTCCAA ACCCTCTGTgattgtactgagagtgcacc (upper case letters correspond to 375 to 315bp upstream of *ARG4*, lower case letters are the forward oligo to pRS316)	Used to amplify *URA3* from pRS316 during DTK1787 construction.
Ras 5'-RC pRS-R	GCTCTCCCCCAACCTCAGGGtctgtgcggt atttcacaccg (upper case letters are the reverse compliment of the Ras 5' oligo, lower case letters are the reverse oligo to pRS316)	
pRS-R-RC Ras 5'	CGGTGTGAAATACCGCACAGAccctga ggttgggggagagc (upper case letters are the reverse complement of the pRS316 reverse oligo, lower case letters are the Ras 5' oligo)	Used to amplify *H10* allele from DTK750a during DTK1787 construction
arg4-130-RC Ras3'	TTTTTTTCACATGTTTCAATTTGCGC CAGCTTATCCAAAAAGTGAGTCATgg gctcctggcctcgggaag (upper case letters correspond to 180 to 130bp upstream of *ARG4*, lower case letters are the Ras 3' oligo)	
arg4-375F	TATAACAATAAATGGTTGGCGCAGG CA	Linked the *URA3* and *H10* cassettes during DTK1787 construction
arg4-135R	TTCACATGTTTCAATTTGCGCCAG	
arg4-758F	ATCCGTCGACGTTTTGATGCCA	Used to verify *URA3-H10* insert
arg4+151R	CTGCAAGCCCGCTGTGTATACTTT	
arg4-517F	CGTTTCAGCGGTAGATGTAAGCCA	Used to amplify *URA3-H10* cassette from DTK1787 during DTK1796 construction
arg4-85R	TCTCAGAGTTCTGTGCTTCGCT	
his4+142F	GAAGTTCCATTGGTGCGTTTGTCC	Used to construct probe from pDN42 for DSB Southern blot
his4+442R	GACGGTCTGTACGTACTTCACCAA	
his4-687F	TGGTGCCAACGAAGATGTCGAA	Used to verify correct *HIS4* promoter sequences
his4+168R	CAAGGACAAACGCACCAATGGAAC	
pch2-81F	CGAAATGCGAGGCGGTTAAAAGAG	Used to delete *PCH2* with *KANMX4*
pch2+1890R	CGTTGGAATAGGGTTCGCGAAAGT	
pch2-237F	TGTTTGCCCCTCTCTTGAGTTG	Used to verify gene deletion
pch2+1966R	ACGTGTGGTTCACGATACACCTTG	
rdh54-195F	ACGCGCTGTTGGAGGTATCTCTAT	Used to delete *RDH54* with

Table 2 continued

rdh54+3056R	GCCCGCAGCGTATCGTTATCAAAT	*KANMX4*
rdh54+680R	AACAGCTGAGACAGAGGCATTTGG	Internal *RDH54* primer, used to verify gene deletion
thr1: NAT F	ACTTCTAACCTGCCTAATGGTTATAA CAGTAGCATAAAGTAGATATACGGA CTACAGAAACATGGAGGCCCAGAAT ACCC	Used to amplify *NATMX* cassette from p4339 during DTK1797 construction
thr1:NAT R	TACAGTATGTATATGGTCTACAATA GTATTTAACACAGTATACTAGGGGT AAAGGACATTCAGTATAGCGACCAG CATTCAC	
2796 (Berman lab)	GCTGCGCACGTCAAGACTGTCAAGG AGGG	Used with thr1:NAT F to verify *thr1*Δ::*NATMX* in DTK1797
3118 (Berman lab)	CCCAGATGCGAAGTTAAGTGCGCAG	Used with thr1:NAT R to verify *thr1*Δ::*NATMX* in DTK1797
thr1-580F	ACCCACATCCTGGTTGAACACA	Used to delete *THR1* with *KANMX4* for DTK1834
thr1+1615R	AGCCTACACAAAGGGCAATACC	
thr1-725F	CTGTGTGCAACAGCTCAGGTAA	Used to delete *THR1* with *KANMX4* for DTK1834
thr1+1677R	ACCGGCACCAATCATGGATGAA	
thr1-881F	ATGCCTTTTCGTGAGGAACACC	Used to verify *thr1*Δ::*KANMX4* in DTK1834
thr1+1188R	AGAAAAGACGGGTAACGGAAGA	
arg4+50F	CCGATCCTTTGATGCACC	Used to construct probe for Southern blot
arg4+322R	CTTTACCAGCAATATCGCGGC	
thr1-725F	CTGTGTGCAACAGCTCAGGTAA	Used to construct probe for Southern blot
thr1-260R	CAAAAGATGCTAAGGAACGGCG	
lsb5+158F	AAGCTGCGCGAGCACTTAGAAA	Used to amplify *URA3* from pMW33 for *URA3-H10-HIS4*
lsb5+825R	AGAAACTCACCCTCCGTGACCAAT	
lsb5-269F	AAGCATCGCAATCTGGAAACGC	Used to verify *URA3* insertion in *URA3-H10-HIS4* strains
lsb5+1174R	CAAGGACACCAGACACTGTGTGAA	
msh5/prsF	CATCAGTAATAAACATATGTAACTTT TTAACCTTAAAACATACTAATCTCCG TACTTTTTgattgtactgagagtgcacc (upper case letters correspond to 200 and 140bp upstream of *MSH5,* lower case letters are the forward oligo to pRS316)	Used to delete *MSH5* with *URA3* for DTK1867
msh5/prsR	AGAATTAAAAAAATTTACATATGTA GTATTTACCCAAGTAGTGGTGTCAA AATTTTTGTAtctgtgcggtatttcacaccg (upper case letters correspond to 95 and 154bp downstream of *MSH5*, lower case letters are the reverse oligo to pRS316)	

Figure 1

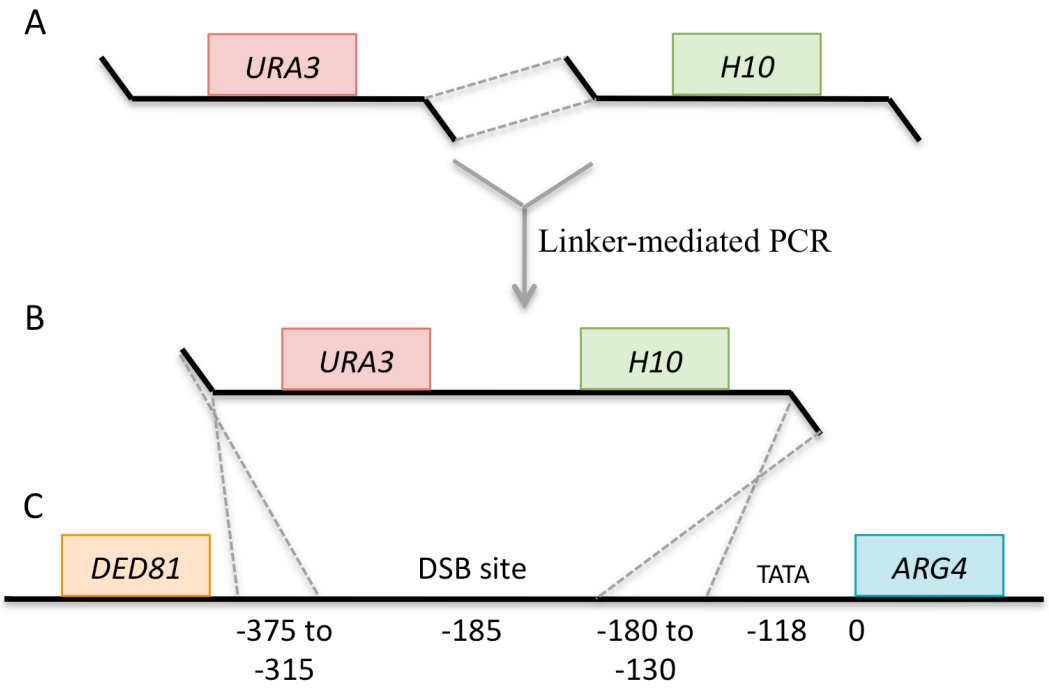

Figure 1. The construction of DTK1787. (A) Both the *URA3* gene and the *H10* minisatellite allele were PCR amplified using tagged primers that enabled the two products to be linked together (B). The final *URA-H10* product had 50-60 bp sequence homology to regions upstream of *ARG4* that enabled the construct to recombine into the yeast genome (C), relacing some of the endogenous *ARG4* promoter sequence that included the meiotic DSB site but leaving the TATA box intact.

Figure 2

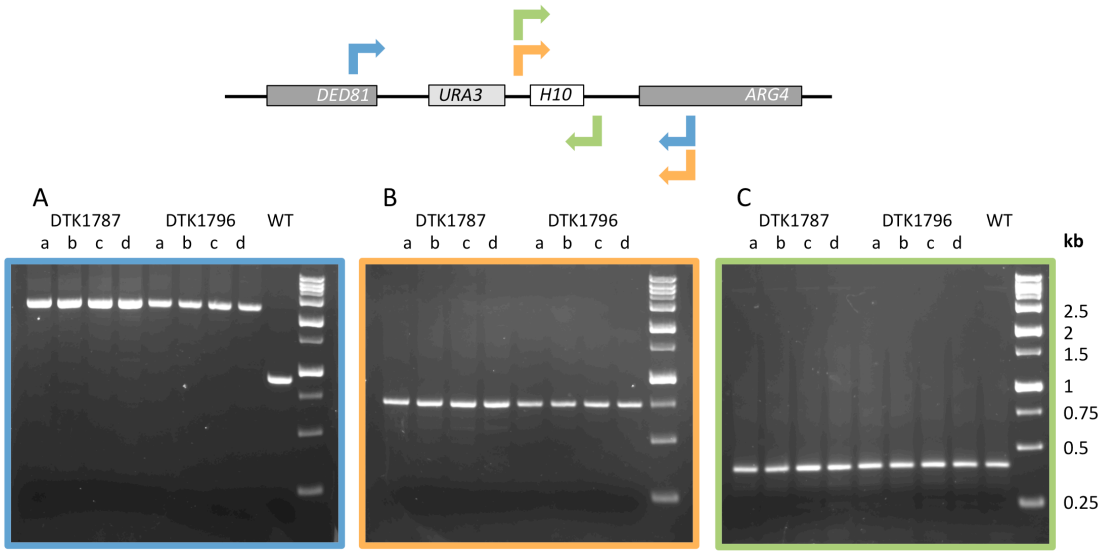

Figure 2. PCR verification of the *arg4-H10* allele. Using three different primer pairs, it was verified that the *URA3-H10* construct had properly inserted into the correct locus (A) and in the correct orientation (B) in the original *arg4-H10* haploid strains, and that the minisatellite had not altered in length during transformation (C). For both DTK1787 and DTK1796, a, b, c, and d are independent isolates. Each subsequent derivative of DTK1787 and DTK1796 was also checked. DTK750a was used as the wild-type control in both (A) and (C).

References

Adamson, K. A., T. D. Cheetham, P. Kendall-Taylor, J. R. Seckl & S. H. S. Pearce (2007) The role of the *IDDM2* locus in the susceptibility of UK APS1 subjects to type 1 diabetes mellitus. *Int. J. Immunogenet.,* 34**,** 17-21.

Alver, B., M. K. Kelly & D. T. Kirkpatrick (*submitted*) Novel Checkpoint Pathway Organization Promotes Genome Stability in Stationary Phase Yeast Cells. *Mol. Cell. Biol.*

Anderson, D. E., A. Losada, H. P. Erickson & T. Hirano (2002) Condensin and cohesin display different arm conformations with characteristic hinge angles. *J. Cell Biol.,* 156**,** 419-424.

Appelgren, H., H. Cederberg & U. Rannug (1997) Mutations at the human minisatellite MS32 integrated in yeast occur with high frequency in meiosis and involve complex recombination events. *Mol. Gen. Genet.,* 256**,** 7-17.

Appelgren, H., H. Cederberg & U. Rannug (1999) Meiotic interallelic conversion at the human minisatellite MS32 in yeast triggers recombination in several chromatids. *Gene,* 239**,** 29-38.

Ball Jr., A. R. & K. Yokomori (2001) The structural maintenance of chromosomes (SMC) family of proteins in mammals. *Chromosome Res.,* 9**,** 85-96.

Bando, M., Y. Katou, M. Komata, H. Tanaka, T. Itoh, T. Sutani & K. Shirahige (2009) Csm3, Tof1, and Mrc1 Form a Heterotrimeric Mediator Complex That Associates with DNA Replication Forks. *Journal of Biological Chemistry,* 284**,** 34355-34365.

Bastin-Shanower, S. A., W. M. Fricke, J. R. Mullen & S. J. Brill (2003) The Mechanism of Mus81-Mms4 Cleavage Site Selection Distinguishes It from the Homologous Endonuclease Rad1-Rad10. *Mol. Cell. Biol.,* 23**,** 3487-3496.

Bell, G. I., M. J. Selby & W. J. Rutter (1982) The highly polymorphic region near the human insulin gene is composed of simple tandemly repeating sequences. *Nature,* 295**,** 31-35.

Bennett, S. T., A. M. Lucassen, S. C. I. Gough, E. E. Powell, D. E. Undlien, L. E. Pritchard, M. E. Merriman, Y. Kawaguchi, M. J. Dronsfield, F. Pociot, J. Nerup, N. Bouzekri, A. Cambon-Thomsen, K. S. Ronningen, A. H. Barnett, S. C. Bain & J. A. Todd (1995) Susceptibility to human type 1 diabetes at *IDDM2* is determined by tandem repeat variation at the insulin gene minisatellite locus. *Nature Genetics,* 9**,** 284-292.

Berchowitz, L. E. & G. P. Copenhaver (2010) Genetic Interference: don't stand so close to me. *Current Genomics,* 11**,** 91-102.

Bishop, A. J. R., E. J. Louis & R. H. Borts (2000) Minisatellite Variants Generated in Yeast Meiosis Involve DNA Removal During Gene Conversion. *Genetics,* 156**,** 7-20.

Bishop, D. K., D. Park, L. Xu & N. Kleckner (1992) *DMC1*: A meiosis-specific yeast homolog of *E. coli recA* required for recombination, synaptonemal complex formation, and cell cycle progression. *Cell,* 69**,** 439-456.

Bishop, D. K. & D. Zickler (2004) Early Decision: Meiotic Crossover Interference prior to Stable Strand Exchange and Synapsis. *Cell,* 117**,** 9-15.

Blow, J. J. & T. U. Tanaka (2005) The chromosome cycle: coordinating replication and segregation. *EMBO Rep.,* 6**,** 1028-1034.

Bocker, T., A. Barusevicius, T. Snowden, D. Rasio, S. Guerrette, D. Robbins, C. Schmidt, J. Burczak, C. M. Croce, T. Copeland, A. J. Kovatich & R. Fishel (1999) hMSH5: A human MutS homolog that forms a novel heterodimer with hMSH4 and is expressed during spermatogenesis. *Cancer Res.,* 93**,** 816-822.

Boddy, M. N., P. H. Gaillard, W. H. McDonald, P. Shanahan, J. R. r. Yates & P. Russell (2001) Mus81-Eme1 are essential components of a Holliday junction resolvase. *Cell,* 107**,** 537-548.

Bois, P. R. J. (2003) Hypermutable minisatellites, a human affair? *Genomics,* 81**,** 349-355.

Borde, V. (2007) The multiple roles of the Mre11 complex for meiotic recombination. *Chromosome Research,* 15**,** 551-563.

Borde, V., W. Lin, E. Novikov, J. H. Petrini, M. Lichten & A. Nicolas (2004) Association of Mre11p with double-strand break sites during yeast meiosis. *Mol. Cell,* 13**,** 389-401.

Borner, G. V., N. Kleckner & N. Hunter (2004) Crossover/Noncrossover Differentiation, Synaptonemal Complex Formation, and Regulatory Surveillance at the Leptotene/Zygotene Transition of Meiosis. *Cell,* 117**,** 29-45.

Callender, T. L. & N. M. Hollingsworth (2010) Mek1 suppression of meiotic double strand break repair is specific to sister chromatids, chromosome autonomous and independent of rec8 cohesion complexes. *Genetics,* 185**,** 771-782.

Calzada, A., B. Hodgson, M. Kanemaki, A. Bueno & K. Labib (2005) Molecular anatomy and regulation of a stable replisome at a paused eukaryotic DNA replication fork. *Genes & Development,* 19**,** 1905-1919.

Campbell, S. L., R. Khosravi-Far, K. L. Rossman, G. J. Clark & C. J. Der (1998) Increasing complexity of Ras signaling. *Oncogene,* 17**,** 1395-1413.

Carballo, J. A., A. L. Johnson, S. G. Sedgwick & R. S. Cha (2008) Phosphorylation of the axial element protein Hop1 by Mec1/Tel1 ensures meiotic interhomolog recombination. *Cell,* 132**,** 758-770.

Chang, E. H., M. A. Gonda, R. W. Ellis, E. M. Scolnick & D. R. Lowy (1982) Human genome contains four genes homologus to transforming genes of Harvey and Kirsten murine sarcoma viruses. *Proc. Natl. Acad. Sci.,* 79**,** 4848-4852.

Chua, P. R. & G. S. Roeder (1997) Tam1, a telomere-associated meiotic protein, functions in chromosome synapsis and crossover interference. *Genes & Development,* 11**,** 1786-1800.

Ciccia, A., A. Constantinou & S. C. West (2003) Identification and characterization of the human mus81-eme1 endonuclease. *J. Biol. Chem.,* 278**,** 25172-25178.

Cohen, J. B., M. V. Walter & A. D. Levinson (1987) A Repetitive Sequence Element 3' of the human c-Ha-*ras*1 Gene Has Enhancer Activity. *J. Cell. Physiol. Suppl.,* 5**,** 75-81.

Collins, S. R., K. M. Miller, N. L. Maas, A. Roguev, J. Fillingham, C. S. Chu, M. Schuldiner, M. Gebbia, J. Recht, M. Shales, H. Ding, H. Xu, J. Han, K. Ingvarsdottir, B. Cheng, B. Andrews, C. Boone, S. L. Berger, P. Hieter, Z. Zhang, G. W. Brown, C. J. Ingles, A. Emili, C. D. Allis, D. P. Toczyski, J. S. Weissman, J. F. Greenblatt & N. J. Krogan (2007) Functional dissection of protein complexes involved in yeast chromosome biology using a genetic interaction map. *Nature,* 446**,** 806-810.

Conway, K., S. N. Edmiston, B. S. Hulka, P. A. Garrett & E. T. Liu (1996) Internal Sequence Variations in the Ha-*ras* Variable Number Tandem Repeat Rare and Common Alleles Identified by Minisatellite Variant Repeat Polymerase Chain Reaction. *Cancer Research,* 56**,** 4773-4777.

Cooper, D. N. & J. Schmidtke (1984) DNA restriction fragment length polymorphisms and heterozygosity in the human genome. *Human Genet.,* 66**,** 1-16.

Coulon, S., P.-H. L. Gaillard, C. Chahwan, W. H. McDonald, J. R. Yates III & P. Russell (2004) Slx1-Slx4 Are Subunits of a Structure-specific Endonuclease That Maintains Ribosomal DNA in Fission Yeast. *Molecular Biology of the Cell,* 15**,** 71-80.

de los Santos, T., N. Hunter, C. Lee, B. Larkin, J. Loidl & N. M. Hollingsworth (2003) The Mus81/Mms4 Endonuclease Acts Independently of Double-Holliday Junction Resolution to Promote a Distinct Subset of Crossovers During Meiosis in Budding Yeast. *Genetics,* 2003**,** 81-94.

de los Santos, T., J. Loidl, B. Larkin & N. M. Hollingsworth (2001) A Role for *MMS4* in the Processing of Recombination Intermediates During Meiosis in *Saccharomyces cerevisiae*. *Genetics,* 159**,** 1511-1525.

De Souza, C. P. C. & S. A. Osmani (2007) Mitosis, Not Just Open or Closed. *Eukaryotic Cell,* 6**,** 1521-1527.

de Vries, S. S., E. B. Baart, M. Dekker, A. Siezen, D. G. de Rooij, P. de Boer & H. te Riele (1999) Mouse MutS-like protein Msh5 is required for proper chromosome synapsis in male and female meiosis. *Genes & Dev.,* 13**,** 523-531.

Debrauwere, H., J. Buard, J. Tessier, D. Aubert, G. Vergnaud & A. Nicolas (1999) Meiotic instability of human minisatellite CEB1 in yeast requires DNA double-strand breaks. *Nat. Genet.,* 23**,** 367-371.

Detloff, P., J. Sieber & T. D. Petes (1991) Repair of specific base pair mismatches formed during meiotic recombination in the yeast *Saccharomyces cerevisiae*. *Molecular and Cellular Biology,* 11**,** 737-745.

Detloff, P., M. White & T. D. Petes (1992) Analysis of a gene conversion gradient at the *HIS4* locus in *Saccharomyces cerevisiae*. *Genetics,* 132**,** 113-123.

Diaz, R. L., A. D. Alcid, J. M. Berger & S. Keeney (2002) Identification of residues in yeast Spo11p critical for meiotic DNA double-strand break formation. *Mol. Cell. Biol.,* 22**,** 1106-1115.

Ding, S., G. P. Larson, K. Foldenauer, G. Zhang & T. G. Krontiris (1999) Distinct mutation patterns of breast cancer-associated alleles of the *HRAS1* minisatellite locus. *Human Molecular Genetics,* 8**,** 515-521.

Doe, C. L., J. S. Ahn, J. Dixon & M. C. Whitby (2002) Mus81-Eme1 and Rqh1 Involvement in Processing Stalled and Collapsed Replication Forks. *J. Biol. Chem.,* 277**,** 32753-32759.

Edelmann, W., P. E. Cohen, B. Kneitz, N. Winand, M. Lia, J. Heyer, R. Kolodner, J. W. Pollard & R. Kucheriapati (1999) Mammalian MutS homologue 5 is required for chromosome pairing in meiosis. *Nature Gen.,* 21**,** 123-127.

Ehmsen, K. T. & W.-D. Heyer (2008) *Saccharomyces cerevisiae* Mus81-Mms4 is a catalytic, DNA structure-selective endonuclease. *Nucleic Acids Res.,* 36**,** 2182-2195.

Fan, Q., F. Xu & T. D. Petes (1995) Meiosis-Specific Double-Strand DNA Breaks at the *HIS4* Recombination Hot Spot in the Yeast *Saccharomyces cerevisiae*: Control in *cis* and *trans*. *Molecular and Cellular Biology,* 15**,** 1679-1688.

Faraone, S. V., A. E. Doyle, E. Mick & J. Biederman (2001) Meta-analysis of the association between the 7-repeat allele of the dopamine D(4) receptor gene and attention deficit hyperactivity disorder. *Am. J. Psychiatry,* 158**,** 1052-1057.

Fekairi, S., S. Scaglione, C. Chahwan, E. R. Taylor, A. Tissier, S. Coulon, M.-Q. Dong, C. Ruse, J. R. Yates III, P. Russell, R. P. Fuchs, C. H. McGowan & P.-H. L. Gaillard (2009) Human SLX4 is a Holliday Junction Resolvase Subunit that Binds Multiple DNA Repair/Recombination Endonucleases. *Cell,* 138**,** 78-89.

Foss, E. J. (2001) Tof1p Regulates DNA Damage Responses During S Phase in *Saccharomyces cerevisiae*. *Genetics,* 157**,** 567-577.

Fricke, W. M. & S. J. Brill (2003) Slx1-Slx4 is a second structure-specific endonuclease functionally redundant with Sgs1-Top3. *Genes & Development,* 17**,** 1768-1778.

Gaillard, P. H., E. Noguchi, P. Shanahan & P. Russell (2003) The endonuclease Mus81-Eme1 complex resolves Holliday junctions by a nick and a counternick mechanism. *Mol. Cell,* 12**,** 747-759.

Garcia, V., S. E. Phelps, S. Gray & M. J. Neale (2011) Bidirectional resection of DNA double-strand breaks by Mre11 and Exo1. *Nature,* 479**,** 241-244.

Gaskell, L. J., F. Osman, R. J. C. Gilbert & M. C. Whitby (2007) Mus81 cleavage of Holliday junctions: a failsafe for processing meiotic recombination intermediates? *The EMBO Journal,* 26**,** 1891-1901.

Goldstein, A. L. & J. H. McCusker (1999) Three New Dominant Drug Resistance Cassettes for Gene Disruption in *Saccharomyces cerevisiae*. *Yeast,* 15**,** 1541-1553.

Green, M. & T. G. Krontiris (1993) Allelic Variation of Reporter Gene Activation by the *HRAS1* Minisatellite. *Genomics,* 17**,** 429-434.

Guo, X., R. G. Pace, J. R. Stonebraker, C. W. Commander, A. T. Dang, M. L. Drumm, A. Harris, F. Zou, D. M. Swallow, F. A. Wright, W. K. O'Neal & M. R. Knowles (2011) Mucin Variable Number Tandem Repeat Polymorphisms and Severity of Cystic Fibrosis Lung Disease: Significant Association with *MUC5AC*. *PLoS One,* 6**,** e25452.

Guthrie, C. & G. R. Fink (1991) Guide to yeast genetics and molecular biology. *Academic Press, Inc., San Diego, Calif.,* 194.

Haering, C. H., J. Lowe, A. Hochwagen & K. Nasmyth (2002) Molecular architecture of SMC proteins and the yeast cohesin complex. *Mol. Cell,* 9**,** 773-788.

Hassold, T., H. Hall & P. Hunt (2007) The origin of human aneuploidy: where we have been, where we are going. *Hum Mol Genet,* 16**,** R203-208.

He, Q., H. Cederberg & U. Rannug (2002) The Influence of Sequence Divergence between Alleles of the Human MS205 Minisatellite Incorporated into the Yeast Genome on Length-mutation Rates and Lethal Recombination Events During Meiosis. *J. Mol. Biol.,* 319**,** 315-327.

He, X., D. R. Rines, C. W. Espelin & P. K. Sorger (2001) Molecular analysis of kinetochore-microtubule attachment in budding yeast. *Cell,* 106**,** 195-206.

Hetzer, M. W. (2010) The nuclear envelope. *Cold Spring Harb. Perspect. Biol.,* 2**,** a000539.

Hiwasa, T., M. Hirono, M. Suzuki & T. Tanaka (1992) Expression and localization of epidermal growth factor receptors and ras oncogene products in gynecologic tumors. *Eur. J. Gynaecol. Oncol.,* 13**,** 241-245.

Hodgson, A., Y. Terentyev, R. A. Johnson, A. Bishop-Bailey, T. Angevin, A. Croucher & A. S. Goldman (2011) Mre11 and Exo1 contribute to the initiation and processivity of resection at meiotic double-strand breaks made independently of Spo11. *DNA Repair,* 10**,** 138-148.

Hodgson, B., A. Calzada & K. Labib (2007) Mrc1 and Tof1 Regulate DNA Replication Forks in Different Ways during Normal S Phase. *Molecular Biology of the Cell,* 18**,** 3894-3902.

Hollingsworth, N. M. (2010) Phosphorylation and the creation of interhomolog bias during meiosis in yeast. *Cell Cycle,* 9**,** 436-437.

Hollingsworth, N. M. & S. J. Brill (2004) The Mus81 solution to resolution: generating meiotic crossovers without Holliday junctions. *Genes & Development,* 18**,** 117-125.

Hollingsworth, N. M., L. Ponte & C. Halsey (1995) *MSH5*, a novel MutS homolog, facilitates meiotic reciprocal recombination between homologs in *Saccharomyces cerevisiae* but not mismatch repair. *Genes & Development,* 9**,** 1728-1739.

Hunter, N. (2006) Meiotic Recombination. *Topics in Current Genetics,* 17**,** 381-442.

Interthal, H. & W. D. Heyer (2000) MUS81 encodes a novel helix-hairpin-helix protein involved in the response to UV- and methylation-induced DNA damage in Saccharomyces cerevisiae. *Mol. Gen. Genet.,* 263**,** 812-827.

Iouk, T., O. Kerscher, R. J. Scott, M. A. Basrai & R. W. Wozniak (2002) The yeast nuclear pore complex functionally interacts with components of the spindle assembly checkpoint. *J. Cell Biol.,* 159**,** 807-819.

Jauert, P. A., S. N. Edmiston, K. Conway & D. T. Kirkpatrick (2002) *RAD1* Controls the Meiotic Expansion of the Human *HRAS1* Minisatellite in *Saccharomyces cerevisiae*. *Molecular and Cellular Biology,* 22**,** 953-964.

Jauert, P. A., L. E. Jensen & D. T. Kirkpatrick (2005) A novel yeast genomic DNA library on a geneticin-resistance vector. *Yeast,* 22**,** 653-657.

Jauert, P. A. & D. T. Kirkpatrick (2005) Length and Sequence Heterozygosity Differentially Affect *HRAS1* Minisatellite Stability During Meiosis in Yeast. *Genetics,* 170**,** 601-612.

Jeffreys, A. J., A. MacLeod, K. Tamaki, D. L. Neil & D. G. Monckton (1991) Minisatellite repeat coding as a digital approach to DNA typing. *Nature,* 354**,** 204-209.

Jeffreys, A. J., J. Murray & R. Neumann (1998a) High-resolution mapping of crossovers in human sperm defines a minisatellite-associated recombination hotspot. *Mol. Cell,* 2**,** 267-273.

Jeffreys, A. J., D. L. Neil & R. Neumann (1998b) Repeat instability at human minisatellites arising from meiotic recombination. *EMBO J.,* 17**,** 4147-4157.

Jeffreys, A. J., K. Tamaki, A. MacLeod, D. G. Monckton, D. L. Neil & J. A. Armour (1994) Complex gene conversion events in germline mutation at human minisatellites. *Nat. Genet.,* 6**,** 136-145.

Jeffreys, A. J., V. Wilson & S. L. Thein (1985) Individual-specific 'fingerprints' of human DNA. *Nature,* 316**,** 76-79.

Jensen, L. E., P. A. Jauert & D. T. Kirkpatrick (2005) The Large Loop Repair and Mismatch Repair Pathways of *Saccharomyces cerevisiae* Act on Distinct Substrates During Meiosis. *Genetics,* 170**,** 1033-1043.

Jeong, Y. H., M. C. Kim, E.-K. Ahn, S.-Y. Seol, E.-J. Do, H.-J. Choi, I.-S. Chu, W.-J. Kim, W. J. Kim, Y. Sunwoo & S.-H. Leem (2007) Rare Exonic Minisatellite Alleles in *MUC2* Influence Susceptibility to Gastric Carcinoma. *PLoS One,* 2**,** e1163.

Jiao, K., L. Salem & R. Malone (2003) Support for a meiotic recombination initiation complex: interactions among Rec102p, Rec104p, and Spo11p. *Mol. Cell. Biol.,* 23**,** 5928-5938.

Johzuka, K. & H. Ogawa (1995) Interaction of Mre11 and Rad50: Two Proteins Required for DNA Repair and Meiosis-Specific Double-Strand Break Formation in *Saccharomyces cerevisiae*. *Genetics,* 139**,** 1521-1532.

Kaback, D. B., D. Barber, J. Mahon, J. Lamb & J. You (1999) Chromosome Size-Dependent Control of Meiotic Reciprocal Recombination in *Saccharomyces cerevisiae*: The Role of Crossover Interference. *Genetics,* 152**,** 1475-1486.

Kadyk, L. C. & L. H. Hartwell (1992) Sister Chromatids Are Preferred Over Homologs as Subsrates for Recombinational Repair in *Saccharomyces cerevisiae*. *Genetics,* 132**,** 387-402.

Kagawa, W. & H. Kurumizaka (2010) From meiosis to postmeiotic events: uncovering the molecular roles of the meiosis-specific recombinase Dmc1. *FEBS J.,* 277**,** 590-598.

Kaliraman, V., J. R. Mullen, W. M. Fricke, S. A. Bastin-Shanower & S. J. Brill (2001) Functional overlap between Sgs1-Top3 and the Mms4-Mus81 endonuclease. *Genes Dev.,* 15**,** 2730-2740.

Kasperczyk, A., N. A. DiMartino & T. G. Krontiris (1990) Minisatellite Allele Diversification: The Origin of Rare Alleles at the HRAS1 Locus. *Am. J. Hum. Genet.,* 47**,** 854-859.

Katou, Y., Y. Kanoh, M. Bando, H. Noguchi, H. Tanaka, T. Ashikari, K. Sugimoto & K. Shirahige (2003) S-phase checkpoint proteins Tof1 and Mrc1 form a stable replication-pausing complex. *Nature,* 424**,** 1078-1083.

Kearney, H. M., D. T. Kirkpatrick, J. L. Gerton & T. D. Petes (2001) Meiotic Recombination Involving Heterozygous Large Insertions in *Saccharomyces cerevisiae*: Formation and Repair of Large, Unpaired DNA Loops. *Genetics,* 158**,** 1457-1476.

Keeney, S. (2001) Mechanism and control of meiotic recombination initiation. *Curr. Top. Dev. Biol.,* 52**,** 1-53.

Keeney, S., C. N. Giroux & N. Kleckner (1997) Meiosis-specific DNA double-strand breaks are catalyzed by Spo11, a member of a widely conserved protein family. *Cell,* 88**,** 375-84.

Kelly, K. O., A. F. Dernberg, G. M. Stanfield & A. M. Villeneuve (2000) *Caenorhabditis elegans* msh-5 is required for both normal and radiation-induced meiotic crossing over but not for completion of meiosis. *Genetics,* 156**,** 617-630.

Kennedy, G. C., M. S. German & W. J. Rutter (1995) The minisatellite in the diabetes susceptibility locus *IDDM2* regulates insulin transcription. *Nature Genetics,* 9**,** 293-298.

Kim, S.-T., D.-S. Lim, C. E. Canman & M. B. Kastan (1999) Substrate Specificities and Identification of Putative Substrates of ATM Kinase Family Members. *J. Biol. Chem.,* 274**,** 37538-37543.

Kirkbride, H. J., J. G. Bolscher, K. Nazmi, L. E. Vinall, M. W. Nash, F. M. Moss, D. M. Mitchell & D. M. Swallow (2001) Genetic poly morphism of *MUC7*: Allele frequencies and association with asthma. *Eur. J. Hum. Genet.,* 9**,** 347-354.

Kirkpatrick, D. T. (1999) Roles of the DNA mismatch repair and nucleotide excision repair proteins during meiosis. *Cell. Mol. Life Sci.,* 55**,** 437-449.

Kirkpatrick, D. T. & T. D. Petes (1997) Repair of DNA loops involves DNA-mismatch and nucleotide-excision repair proteins. *Nature,* 387**,** 929-931.

Kirkpatrick, D. T., Y.-H. Wang, M. Dominska, J. D. Griffith & T. D. Petes (1999) Control of Meiotic Recombination and Gene Expression in Yeast by a Simple Repetitive DNA Sequence That Excludes Nucleosomes. *Molecular and Cellular Biology,* 19**,** 7661-7671.

Kneitz, B., P. E. Cohen, E. Avdievich, L. Zhu, M. F. Kane, H. Hou Jr., R. D. Kolodner, R. Kucherlapati, J. W. Pollard & W. Edelmann (2000) MutS homolog 4 localization to meiotic chromosomes is required for chromosome pairing during meiosis in male and female mice. *Genes & Dev.,* 14**,** 1085-1097.

Krontiris, T. G. (1995) Minisatellites and Human Disease. *Science,* 269**,** 1682-1683.

Krontiris, T. G., B. Devlin, D. D. Karp, N. J. Robert & N. Risch (1993a) An Association between the Risk of Cancer and Mutations in the HRAS1 Minisatellite Locus. *N. Engl. J. Med.,* 329**,** 517-523.

Krontiris, T. G., B. Devlin, N. J. Robert, D. D. Karp & N. Risch (1993b) An association between cancer risk and mutations in the *HRAS1* minisatellite locus. *N. Engl. J. Med.,* 329**,** 517-523.

Krontiris, T. G., N. A. DiMartino, M. Colb & D. R. Parkinson (1985) Unique allelic restriction fragments of the human Ha-ras locus in leukocyte and tumour DNAs of cancer patients. *Nature,* 313**,** 369-374.

Krontiris, T. G., N. A. DiMartino, H. D. Mitcheson, J. A. Lonergan, C. Begg & D. R. Parkinson (1987) Human hypervariable sequences in risk assessment: rare Ha-ras alleles in cancer patients. *Environ. Health Perspect.,* 76**,** 147-153.

Krontiris, T. G., N.A. DiMartino, M. Colb, and D.R. Parkinson (1985) Unique allele restriction fragments of the human Ha-ras locus in leukocyte and tumour DNAs of cancer patients. *Nature,* 313**,** 369-374.

Kutay, U. & M. W. Hetzer (2008) Reorganization of the nuclear envelope during open mitosis. *Curr. Opin. Cell Biol.,* 20**,** 669-677.

Kwon, J.-A., S.-Y. Lee, E.-K. Ahn, S.-Y. Seol, M. C. Kim, S. J. Kim, S. I. Kim, I.-S. Chu & S.-H. Leem (2010) Short rare *MUC6* minisatellites-5 alleles influence susceptibility to gastric carcinoma by regulating gene. *Human Mutation,* 31**,** 942-949.

Lalioti, M. D., H. S. Scott, C. Buresi, C. Rossier, A. Bottani, M. A. Morris, A. Malafosse & S. E. Antonarakis (1997) Dodecamer repeat expansion in cystatin B gene in progressive myoclonus epilepsy. *Nature,* 386**,** 847-851.

Langley, K., T. A. Fowler, D. L. Grady, R. K. Moyzis, P. A. Holmans, M. B. M. van den Bree, M. J. Owen, M. C. O'Donovan & A. Thapar (2009) Molecular genetic contribution to the developmental course of attention-deficit hyperactivity disorder. *Eur. Child Adolesc. Psychiatry,* 18**,** 26-32.

Lao, J. P. & N. Hunter (2010) Trying to avoid your sister. *PLoS Biology,* 8**,** e1000519.

Larson, G. P., S. Ding, R. G. Lafreniere, G. A. Rouleau & T. G. Krontiris (1999) Instability of the EPM1 minisatellite. *Hum. Mol. Genet.,* 8**,** 1985-1988.

LeClere, A. R., P. A. Jauert & D. K. Kirkpatrick (*submitted*) Minisatellite-Stimulated Meiotic Recombination in *MSH4* and *MSH5* Mutants in *Saccharomyces cerevisiae*. *Genetics*.

LeClere, A. R., J. K. Yang, P. A. Jauert & D. T. Kirkpatrick (*unpublished*) The Role of *CSM3, MRC1,* and *TOF1* in Minisatellite Stability and Large Loop DNA Repair During Meiosis in Yeast.

Lee, M., J.-H. Ahn & K.-H. Eum (2009) The Difference in Biological Properties between Parental and v-Ha-*ras* Transformed NIH3T3 Cells. *Cancer Res. Treat.,* 41**,** 93-99.

Li, D., P. C. Sham, M. J. Owen & L. He (2006) Meta-analysis shows significant association between dopamine system genes and attention deficit hyperactivity disorder (ADHD). *Hum. Mol. Genet.,* 15**,** 2276-2284.

Lynn, A., R. Soucek & G. V. Borner (2007) ZMM proteins during meiosis: Crossover artists at work. *Chromosome Research,* 15**,** 591-605.

Maloisel, L., J. Bhargava & G. S. Roeder (2004) A Role for DNA Polymerase delta in Gene Conversion and Crossing Over During Meiosis in *Saccharomyces cerevisiae*. *Genetics,* 167**,** 1133-1142.

Mancera, E., R. Bourgon, A. Brozzi, W. Huber & L. M. Steinmetz (2008) High-resolution mapping of meiotic crossovers and non-crossovers in yeast. *Nature,* 454**,** 479-486.

Marinangeli, P., D. Angelozzi, M. Ciani, F. Clementi & I. Manazzu (2004) Minisatellites in *Saccharomycex cerevisiae* genes encoding cell wall proteins: a new way towards wine strain characterisation. *FEMS Yeast Research,* 4**,** 427-435.

Marston, A. L. & A. Amon (2004) Meiosis: Cell-Cycle Controls Shuffle and Deal. *Nat. Rev. Mol. Cell Biol.,* 5**,** 983-998.

Martinez-Perez, E. & M. P. Colaiacovo (2009) Distribution of meiotic recombination events: talking to your neighbors. *Current Opinion in Genetics & Development,* 19**,** 105-112.

Martini, E., R. L. Diaz, N. Hunter & S. Keeney (2006) Crossover Homeostasis in Yeast Meiosis. *Cell,* 126**,** 285-295.

McMahill, M. S., C. W. Sham & D. K. Bishop (2007) Synthesis-Dependent Strand Annealing in Meiosis. *PLOS Biology,* 5**,** 2589-2601.

McPherson, J. P., B. Lemmers, R. Chahwan, A. Pamidi, E. Migon, E. Matysiak-Zablock, M. E. Moynahan, J. Essers, K. Hanada, A. Poonepalli, O. Sanchez-Sweatman, R. Khokha, R. Kanaar, M. Jasin, M. P. Hande & R. Hakem (2004) Involvement of mammalian Mus81 in genome integrity and tumor suppression. *Science,* 304**,** 1822-1826.

Milman, N., E. Higuchi & G. R. Smith (2009) Meiotic DNA double-strand break repair requires two nucleases, MRN and Ctp1, to produce a single size class of Rec12 (Spo11)-oligonucleotide complexes. *Mol. Cell. Biol.,* 29**,** 5998-6005.

Moreau, S., J. R. Ferguson & L. S. Symington (1999) The nuclease activity of Mre11 is required for meiosis but not for mating type switching, end joining, or telomere maintenance. *Mol. Cell. Biol.,* 19**,** 556-566.

Moriel-Carretero, M. & A. Aguilera (2010) A Postincision-Deficient TFIIH Causes Replication Fork Breakage and Uncovers Alternative Rad51- or Pol32-Mediated Restart Mechanisms. *Molecular Cell,* 37**,** 690-701.

Mullen, J. R., V. Kaliraman, S. S. Ibrahim & S. J. Brill (2001) Requirement for three novel protein complexes in the absence of the Sgs1 DNA helicase in *Saccharomyces cerevisiae*. *Genetics,* 157**,** 103-118.

Munoz, I. M., K. Hain, A.-C. Declais, M. Gardiner, G. W. Toh, L. Sanchez-Pulido, J. M. Heuckmann, R. Toth, T. Macartney, B. Eppink, R. Kanaar, C. P. Ponting, D. M. J. Lilley & J. Rouse (2009) Coordination of Structure-Specific Nucleases by Human SLX4/BTBD12 is Required for DNA Repair. *Molecular Cell,* 35**,** 116-127.

Nag, D. K. & T. D. Petes (1993) Physical Detection of Heteroduplexes during Meiotic Recombination in the Yeast *Saccharomyces cerevisiae*. *Molecular and Cellular Biology,* 13**,** 2324-2331.

Nag, D. K., M. A. White & T. D. Petes (1989) Palindromic sequences in heteroduplex DNA inhibit mismatch repair in yeast. *Nature,* 340**,** 95-98.

Nakagawa, T., H. Flores-Rozas & R. D. Kolodner (2001) The MER3 Helicase Involved in Meiotic Crossing Over is Stimulated by Single-stranded DNA-binding Proteins and Unwinds DNA in the 3' to 5' Direction. *The Journal of Biological Chemistry,* 276**,** 31487-31493.

Nakagawa, T. & R. D. Kolodner (2002a) *Saccharomyces cerevisiae* Mer3 is a DNA Helicase Involved in Meiotic Crossing Over. *Molecular and Cellular Biology,* 22**,** 3281-3291.

Nakagawa, T. & R. D. Kolodner (2002b) The MER3 DNA Helicase Catalyzes the Unwinding of Holliday Junctions. *The Journal of Biological Chemistry,* 277**,** 28019-28024.

Nakagawa, T. & H. Ogawa (1999) The *Saccharomyces cerevisiae MER3* gene, encoding a novel helicase-like protein, is required for crossover control in meiosis. *EMBO,* 18**,** 5714-5723.

Neale, M. J. & S. Keeney (2006) Clarifying the mechanics of DNA strand exchange in meiotic recombination. *Nature,* 442**,** 153-158.

Nedelcheva, M. N., A. Roguev, L. B. Dolapchiev, A. Shevchenko, H. B. Taskov, A. Shevchenko, A. F. Stewart & S. S. Stoynov (2005) Uncoupling of Unwinding from DNA synthesis Implies Regulation of the MCM helicase by Tof1/Mrc1/Csm3 Checkpoint Complex. *Journal of Molecular Biology,* 347**,** 509-521.

Neyton, S., F. Lespinasse, P. B. Moens, R. Paul, P. Gaudray, V. Paquis-Flucklinger & S. Santucci-Darmanin (2004) Association between MSH4 (MutS homolog 4) and the DNA strand exchange proteins RAD51 and DMC1 during mammalian meiosis. *Mol Hum Reprod.,* 10**,** 917-924.

Nicolas, A., D. Treco, N. P. Schultes & J. W. Szostak (1989) An initiation site for meiotic gene conversion in the yeast *Saccharomyces cerevisiae*. *Nature,* 338**,** 35-39.

Nicolette, M. L., K. Lee, Z. Guo, M. Rani, J. M. Chow, S. E. Lee & T. T. Paull (2010) Mre11-Rad50-Xrs2 and Sae2 promote 5' strand resection of DNA double-strand breaks. *Nat. Struct. Mol. Biol.,* 17**,** 1478-1485.

Nishant, K. T., C. Chen, M. Shinohara, A. Shinohara & E. Alani (2010) Genetic Analysis of Baker's Yeast Msh4-Msh5 Reveals a Threshold Crossover Level for Meiotic Viability. *PLoS Genetics,* 6**,** e1001083.

Nishio, H., S. Nakamura, T. Horai, H. Ikegami & M. Matsuda (1992) Clinical and histopathologic evaluation of the expression of Ha-ras and fes oncogene products in lung cancer. *Cancer,* 69**,** 1130-1136.

Niu, H., X. Li, E. Job, C. Park, D. Moazed, S. Gygi & N. Hollingsworth (2007) Mek1 kinase is regulated to suppress double-strand break repair between sister chromatids during budding yeast meiosis. *Mol Cell Biol,* 27**,** 5456-67.

Niu, H., L. Wan, B. Baumgartner, D. Schaefer, J. Loidl & N. M. Hollingsworth (2005) Partner choice during meiosis is regulated by Hop1-promoted dimerization of Mek1. *Mol. Biol. Cell,* 16**,** 5804-5818.

Novak, J. E., P. B. Ross-Macdonald & G. S. Roeder (2001) The Budding Yeast Msh4 Protein Functions in Chromosome Synapsis and the Regulation of Crossover Distribution. *Genetics,* 158**,** 1013-1025.

Osborn, A. J. & S. J. Elledge (2003) Mrc1 is a replication fork component whose phosphorylation in response to DNA replication stress activates Rad53. *Genes Dev.,* 17**,** 1755-1767.

Osman, F., J. Dixon, C. L. Doe & M. C. Whitby (2003) Generating crossovers by resolution of nicked Holliday junctions: a role for Mus81-Eme1 in meiosis. *Mol. Cell,* 12**,** 761-774.

Osman, F. & M. C. Whitby (2007) Exploring the roles of Mus81-Eme1/Mms4 at perturbed replication forks. *DNA Repair,* 6**,** 1004-1017.

Page, S. L. & R. S. Hawley (2003) Chromosome Choreography: The Meiotic Ballet. *Science,* 301**,** 785-789.

Pan, X., P. Ye, D. S. Yuan, X. Wang, J. S. Bader & J. D. Boeke (2006) A DNA Integrity Network in the Yeast *Saccharomyces cerevisiae*. *Cell,* 124**,** 1069-1081.

Papazian, H. P. (1952) The analysis of tetrad data. *Genetics,* 37**,** 175-189.

Parikh, C., R. Subrahmanyam & R. Ren (2007) Oncogenic *NRAS, KRAS,* and *HRAS* Exhibit Different Leukemogenic Potentials in Mice. *Cancer Res.,* 67**,** 7139-7146.

Pearson, C. G., P. S. Maddox, E. D. Salmon & K. Bloom (2001) Budding yeast chromosome structure and dynamics during mitosis. 152**,** 1255-1266.

Pelaez, I. M., M. Kalogeropoulou, A. Ferraro, A. Voulgari, T. Pankotai, I. Boros & A. Pintzas (2010) Oncogenic RAS alters the global and gene-specific histone modification pattern during epithelial-mesenchymal transition in colorectal carcinoma cells. *The International Journal of Biochemistry & Cell Biology,* 42**,** 911-920.

Pereira, G. & E. Schiebel (2001) The role of the yeast spindle pole body and the mammalian centrosome in regulating late mitotic events. *Curr. Opin. Cell Biol.,* 13**,** 762-769.

Perkins, D. D. (1949) Biochemical mutants in the smut fungus *Ustilago maydis*. *Genetics,* 34**,** 607-626.

Peterson, J. B. & H. Ris (1976) Electron-Microscope study of the spindle and chromosome movement in the yeast *Saccharomyces cerevisiae*. *J. Cell Sci.,* 22**,** 219-242.

Pochart, P., D. Woltering & N. M. Hollingsworth (1997) Conserved Properties between Functionally Distinct MutS Homologs in Yeast. *The Journal of Biological Chemistry,* 272**,** 30345-30349.

Rabitsch, K. P., A. Toth, M. Galova, A. Schleiffer, G. Schaffner, E. Aigner, C. Rupp, A. M. Penkner, A. C. Moreno-Borchart, M. Primig, R. E. Esposito, F. Klein, M. Knop & K. Nasmyth (2001) A screen for genes required for meiosis and spore formation based on whole-genome expression. *Current Biology,* 11**,** 1001-1009.

Regairaz, M., Y. W. Zhang, H. Fu, K. K. Agama, N. Tata, S. Agrawal, M. I. Aladjem & Y. Pommier (2011) Mus81-mediated DNA cleavage resolves replication forks stalled by topoisomerase I-DNA complexes. *J. Cell Biol.,* 195**,** 739-749.

Richard, G.-F., A. Kerrest & B. Dujon (2008) Comparative Genomics and Molecular Dynamics of DNA Repeats in Eukaryotes. *Microbiology and Molecular Biology Reviews,* 72**,** 686-727.

Roeder, G. S. (1997) Meiotic chromosomes: it takes two to tango. *Genes & Development,* 11**,** 2600-2621.

Ross-Macdonald, P. & G. S. Roeder (1994) Mutation of a Meiosis-Specific MutS Homolog Decreases Crossing Over but Not Mismatch Correction. *Cell,* 79**,** 1069-1080.

Rossell, R., R. Calvo, J. J. Sanchez, J. Maurel, M. Guillot, M. Monzo, L. Nunez & A. Barnadas (1999) Genetic Susceptibility Associated with Rare *HRAS1* Variable Number of Tandem Repeats Alleles in Spanish Non-Small Cell Lung Cancer Patients. *Clin. Cancer Res.,* 5**,** 1849-1854.

Santucci-Darmanin, S., S. Neyton, F. Lespinasse, A. Saunieres, P. Gaudray & V. Paquis-Flucklinger (2002) The DNA mismatch-repair MLH3 protein interacts with MSH4 in meiotic cells, supporting a role for this MutL homolog in mammalian meiotic recombination. *Human Molecular Genetics,* 11**,** 1697-1706.

Schwacha, A. & N. Kleckner (1994) Identification of joint molecules that form frequently between homologs but rarely between sister chromatids during yeast meiosis. *Cell,* 76**,** 51-63.

Sehorn, M. G., S. Sigurdsson, W. Bussen, V. M. Unger & P. Sung (2004) Human meiotic recombinase Dmc1 promotes ATP-dependent homologous DNA strand exchange. *Nature*.

Sheridan, S. & D. Bishop (2006) Red-Hed regulation: recombinase Rad51, though capable of playing the leading role, may be relegated to supporting Dmc1 in budding yeast meiosis. *Genes Dev,* 20**,** 1685-91.

Shinohara, A., S. Gasior, T. Ogawa, N. Kleckner & D. K. Bishop (1997) Saccharomyces cerevisiae recA homologues RAD51 an DMC1 have both distinct and overlapping roles in meiotic recombination. *Genes Cells,* 2**,** 615-629.

Shinohara, A., H. Ogawa & T. Ogawa (1992) Rad51 protein involved in repair and recombination in *S. cerevisiae* is a RecA-like protein. *Cell,* 69**,** 457-470.

Shinohara, A. & M. Shinohara (2004) Roles of RecA homologues Rad51 and Dmc1 during meiotic recombination. *Cytogenet. Genome Res.,* 107**,** 201-207.

Shinohara, M., S. L. Gasior, D. K. Bishop & A. Shinohara (2000) Tid1/Rdh54 promotes colocalization of rad51 and dmc1 during meiotic recombination. *PNAS,* 97**,** 10814-10819.

Shinohara, M., S. D. Oh, N. Hunter & A. Shinohara (2008) Crossover assurance and crossover interference are distinctly regulated by the ZMM proteins during yeast meiosis. *Nature Genetics,* 40**,** 299-309.

Smalley, S. L., J. N. Bailey, C. G. Palmer, D. P. Cantwell, J. J. McGough, M. A. Del'Homme, J. R. Asarnow, J. A. Woodward, C. Ramsey & S. F. Nelson (1998) Evidence that the dopamine D4 receptor is a susceptibility gene in attention deficit hyperactivity disorder. *Mol. Psychiatry,* 3**,** 427-430.

Smith, G. P. (1976) Evolution of repeated DNA sequences by unequal crossover. *Science,* 191**,** 528-535.

Smith, G. R., M. N. Boddy, P. Shanahan & P. Russell (2003) Fission yeast Mus81*Eme1 Holliday junction resolvase is required for meiotic crossing over but not for gene conversions. *Genetics,* 165**,** 2289-2293.

Snowden, T., S. Acharya, C. Butz, M. Berardini & R. Fishel (2004) hMSH4-hMSH5 Recognizes Holliday Junctions and Forms a Meiosis-Specific Sliding Clamp that Embraces Homologous Chromosomes. *Molecular Cell,* 15**,** 437-451.

Snowden, T., K.-S. Shim, C. Schmutte, S. Acharya & R. Fishel (2008) hMSH4-hMSH5 Adenosine Nucleotide Processing and Interactions with Homologous Recombination Machinery. *The Journal of Biological Chemistry,* 283**,** 145-154.

Snyder, M. (1994) The spindle pole body of yeast. *Chromosoma,* 103**,** 369-380.

Stahl, F. W. & H. M. Foss (2010) A two-pathway analysis of meiotic crossing over and gene conversion in *Saccharomyces cerevisiae*. *Genetics,* 186**,** 515-536.

Stone, J. E., R. G. Ozbirn, T. D. Petes & S. Jinks-Robertson (2008) Role of Proliferating Cell Nuclear Antigen Interactions in the Mismatch Repair-Dependent Processing of Mitotic and Meiotic Recombination Intermediates in Yeast. *Genetics,* 178**,** 1221-1236.

Storlazzi, A., S. Gargano, G. Ruprich-Robert, M. Falque, M. David, N. Kleckner & D. Zickler (2010) Recombination proteins mediate meiotic spatial chromosome organization and pairing. *Cell,* 141**,** 94-106.

Svendsen, J. M., A. Smogorzewska, M. E. Sowa, B. C. O'Connell, S. P. Gygi, S. J. Elledge & J. W. Harper (2009) Mammalian BTBD12/SLX4 Assembles A Holliday Junction Resolvase and is Required for DNA Repair. *Cell,* 138**,** 63-77.

Szostak, J. W., T. L. Orr-Weaver, R. J. Rothstein & F. W. Stahl (1983) The double-strand-break repair model for recombination. *Cell,* 33**,** 25-35.

Tamimi, R. M., S. E. Hankinson, S. Ding, V. Gagalang, G. P. Larson, D. Spiegelman, G. A. Colditz, T. G. Krontiris & D. J. Hunter (2003) The *HRAS1* Variable Number of Tandem Repeats and Risk of Breast Cancer. *Cancer Epid. Biomark.,* 12**,** 1528-1530.

Tanaka, K. & P. Russell (2001) Mrc1 channels the DNA replication arrest signal to checkpoint kinase Cds1. *Nature Cell Biology,* 3**,** 966-972.

Tanaka, T., M. P. Cosma, K. Wirth & K. Nasmyth (1999) Identification of cohesin association sites at centromeres and along chromosome arms. *Cell,* 98**,** 847-858.

Tanaka, T., J. Fuchs, J. Loidl & K. Nasmyth (2000) Cohesin ensures bipolar attachment of microtubules to sister centromeres and resists their precocious separation. *Nat. Cell Biol.,* 2**,** 492-499.

Tong, A. H. Y., M. Evangelista, A. B. Parsons, H. Xu, G. D. Bader, N. Page, M. Robinson, S. Raghibizadeh, C. W. V. Hoge, H. Bussey, B. Andrews, M. Tyers & C. Boone (2001) Systematic Genetic Analysis with Ordered Arrays of Yeast Deletion Mutants. *Science,* 294**,** 2364-2368.

Tong, A. H. Y., G. Lesage, G. D. Bader, H. Ding, H. Xu, X. Xin, J. Young, G. F. Berriz, R. L. Brost, M. Chang, Y. Chen, X. Cheng, G. Chua, H. Friesen, D. S. Goldberg, J. Haynes, C. Humphries, G. He, S. Hussein, L. Ke, N. Krogan, Z. Li, J. N. Levinson, H. Lu, P. Menard, C. Munyana, A. B. Parsons, O. Ryan, R. Tonikian, T. Roberts, A.-M. Sdicu, J. Shapiro, B. Shiekh, B. Suter, S. L. Wong, L. V. Zhang, H. Zhu, C. G. Burd, S. Munro, C. Sander, J. Rine, J. Greenblatt, M. Peter, A. Bretscher, G. Bell, F. P. Roth, G. W. Brown, B. Andrews, H. Bussey & C.

Boone (2004) Global Mapping of the Yeast Genetic Interaction Network. *Science,* 303**,** 808-812.

Tourriere, H., G. Versini, V. Cordon-Preciado, C. Alabert & P. Pasero (2005) Mrc1 and Tof1 Promote Replication Fork Progression and Recovery Independently of Rad53. *Molecular Cell,* 19**,** 699-706.

Trepicchio, W. L. & T. G. Krontiris (1992) Members of the *rel*/NF-kB family of transcriptional regulatory proteins bind the *HRAS1* minisatellite DNA sequence. *Nucleic Acids Res.,* 20**,** 2427-2434.

Usui, T., H. Ogawa & J. H. Petrini (2001) A DNA damage response pathway controlled by Tel1 and the Mre11 complex. *Mol. Cell,* 7**,** 1255-1266.

Van Gils, C. H., K. Conway, Y. Li & J. A. Taylor (2002) *HRAS1* Variable Number of Tandem Repeats Polymorphism and Risk of Bladder Cancer. *Int. J. Cancer,* 100**,** 414-418.

Vega, A., M.J. Sobrido, C. Ruiz-Pointe, F. Barros, and A. Carracedo (2001) Rare HRAS1 alleles are a risk factor for the development of brain tumors. *Cancer,* 92**,** 2920-2926.

Virtaneva, K., E. D'Amato, J. Miao, M. Koskiniemi, R. Norio, G. Avanzini, S. Franceschetti, R. Michelucci, C. A. Tassinari, S. Omer, L. A. Pennacchio, R. M. Myers, J. Dieguez-Lucena, R. Krahe, A. de la Chapelle & A.-E. Lehesjoki (1997) Unstable minisatellite expansion causing recessively inherited myoclonus epilepsy, EPM1. *Nature Genetics,* 15**,** 393-396.

Wang, L., J.-C. Soria, Y.-S. Chang, H.-Y. Lee, O. Wei & L. Mao (2003) Association of a functional tandem repeats in the downstream of human telomerase gene and lung cancer. *Oncogene,* 22**,** 7123-7129.

Wang, T.-F., N. Kleckner & N. Hunter (1999) Functional specificity of MutL homologs in yeast: Evidence for three Mlh1-based heterocomplexes with distinct roles during meiosis in recombination and mismatch correction. *PNAS,* 96**,** 13914-13919.

Weitzel, J. N., S. Ding, G. P. Larson, R. A. Nelson, A. Goodman, E. C. Grendys, H. G. Ball & T. G. Krontiris (2000) The *HRAS1* Minisatellite Locus and Risk of Ovarian Cancer. *Cancer Res.,* 15**,** 259-261.

Weston, A. & J. H. Godbold (1997) Polymorphisms of H-*ras*-1 and *p53* in Breast Cancer and Lung Cancer: A Meta-analysis. *Environmental Health Perspectives,* 105**,** 919-926.

Whitby, M. C. (2005) Making crossovers during meiosis. *Biochemical Society Transactions,* 33**,** 1451-1455.

Whitby, M. C., F. Osman & J. Dixon (2003) Cleavage of model replication forks by yeast Mus81-Eme1 and budding yeast Mus81-Mms4. *J. Biol. Chem.,* 278**,** 6928-6935.

White, J. H., K. Lusnak & S. Fogel (1985) Mismatch-specific post-meiotic segregation frequency in yeast suggests a heteroduplex recombination intermediate. *Nature,* 315**,** 350-352.

White, M. A., M. Dominska & T. D. Petes (1993) Transcription factors are required for the meiotic recombination hotspot at the *HIS4* locus in *Saccharomyces cerevisiae*. *PNAS,* 90**,** 6621-6625.

White, M. A. & T. D. Petes (1994) Analysis of meiotic recombination events near a recombination hotspot in the yeast *Saccharomyces cerevisiae*. *Current Genetics,* 26**,** 21-30.

Wu, H. Y., H. C. Ho & S. M. Burgess (2010) Mek1 kinase governs outcomes of meiotic recombination and the checkpoint response. *Curr. Biol.,* 20**,** 1707-1716.

Wyman, A. R. & R. White (1980) A highly polymorphic locus in human DNA. *Proc. Natl. Acad. Sci.,* 77**,** 6754-6758.

Xu, L., B. M. Weiner & N. Kleckner (1997) Meiotic cells monitor the status of the interhomolog recombination complex. *Genes Dev.,* 11**,** 106-118.

Yanowitz, J. (2010) Meiosis: making a break for it. *Current Opinion in Cell Biology,* 22**,** 744-751.

Yeh, H.-H., R. Giri, T.-Y. Chang, C.-Y. Chou, S.-C. Su & H.-S. Liu (2009) Ha-*ras* Oncogene-Induced Stat3 Phosphorylation Enhances Oncogenicity of the Cell. *DNA and Cell Biology,* 28**,** 131-139.

Yoon, S.-L., D. C. Kim, S. H. Cho, S.-Y. Lee, I.-S. Chu, J. Heo & S.-H. Leem (2010) Susceptibility for breast cancer in young patients with short rare minisatellite alleles of BORIS. *BMB Rep.,* 43**,** 698-703.

Youds, J. L. & S. J. Boulton (2011) The choice in meiosis- defining the factors that influence crossover or non-crossover formation. *Cell Science,* 124**,** 501-513.

Zakharyevich, K., Y. Ma, S. Tang, P. Y.-H. Hwang, S. Boiteux & N. Hunter (2010) Temporally and Biochemically Distinct Activities of Exo1 during Meiosis: Double-Strand Break Resection and Resolution of Double Holliday Junctions. *Molecular Cell,* 40**,** 1001-1015.

Zalevsky, J., A. J. MacQueen, J. B. Duffy, K. J. Kemphues & A. M. Villeneuve (1999) Crossing over During *Caenorhabditis elegans* Meiosis Requires a Conserved MutS-Based Pathway That Is Partially Dispensable in Budding Yeast. *Genetics,* 153**,** 1271-1283.

Zhang, C., G.-Q. Lv, X.-M. Yu, Y.-L. Gu, J.-P. Li, L.-F. Du & P. Zhou (2011) Current evidence on the relationship between HRAS1 polymorphism and breast cancer risk: a meta-analysis. *Breast Cancer Research and Treatment,* 128**,** 467-472.